US010874304B2

(12) **United States Patent**
Islam

(10) **Patent No.: US 10,874,304 B2**
(45) **Date of Patent: *Dec. 29, 2020**

(54) **SEMICONDUCTOR SOURCE BASED NEAR INFRARED MEASUREMENT DEVICE WITH IMPROVED SIGNAL-TO-NOISE RATIO**

(71) Applicant: **Omni Medsci, Inc.**, Ann Arbor, MI (US)

(72) Inventor: **Mohammed N. Islam**, Ann Arbor, MI (US)

(73) Assignee: **OMNI MEDSCI, INC.**, Ann Arbor, MI (US)

(*) Notice: Subject to any disclaimer, the term of this patent is extended or adjusted under 35 U.S.C. 154(b) by 0 days.

This patent is subject to a terminal disclaimer.

(21) Appl. No.: **16/669,794**

(22) Filed: **Oct. 31, 2019**

(65) **Prior Publication Data**

US 2020/0077898 A1 Mar. 12, 2020

Related U.S. Application Data

(60) Continuation of application No. 16/284,514, filed on Feb. 25, 2019, now abandoned, which is a

(Continued)

(51) **Int. Cl.**
G01J 3/00 (2006.01)
A61B 5/00 (2006.01)

(Continued)

(52) **U.S. Cl.**
CPC ***A61B 5/0088*** (2013.01); ***A61B 5/0013*** (2013.01); ***A61B 5/0022*** (2013.01);

(Continued)

(58) **Field of Classification Search**
CPC G01J 3/02; G01J 3/28; G01J 3/42; G01N 21/31; G01N 21/552

(Continued)

(56) **References Cited**

U.S. PATENT DOCUMENTS

4,063,106 A 12/1977 Ashkin et al.
4,158,750 A 6/1979 Sakoe et al.

(Continued)

FOREIGN PATENT DOCUMENTS

CA 2458123 A1 9/2004
CN 101849821 A 10/2010

(Continued)

OTHER PUBLICATIONS

Inter Partes Review No. IPR2020-00175; Petition for Inter Partes Review of U.S. Pat. No. 10,188,299; *Apple Inc.* v. *Omni Medsci, Inc.*; pp. 1-91; dated Dec. 11, 2019.

(Continued)

Primary Examiner — Md M Rahman
(74) *Attorney, Agent, or Firm* — Brooks Kushman P.C.

(57) **ABSTRACT**

A measurement system is provided with a light source that is configured to increase signal-to-noise ratio by increasing a light intensity from at least one of a plurality of semiconductor sources. An apparatus to receive a portion of the output optical beam, and deliver an analysis output beam to a sample. A receiver to: receive and process at least a portion of the analysis output beam reflected or transmitted from the sample, generate an output signal, and synchronize to the light source. A smart phone or tablet to: receive and process at least a portion of the output signal, store and display the processed output signal, and transmit at least a portion of the processed output signal. A cloud to: receive an output status comprising the at least a portion of the processed output signal, process the received output status to generate processed data, and store the processed data.

27 Claims, 22 Drawing Sheets

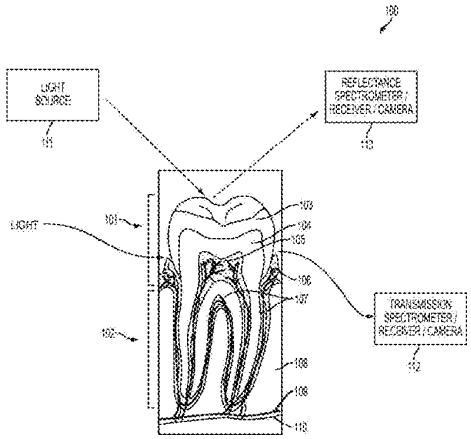

Related U.S. Application Data

continuation of application No. 16/016,649, filed on Jun. 24, 2018, now Pat. No. 10,213,113, which is a continuation of application No. 15/860,065, filed on Jan. 2, 2018, now Pat. No. 10,098,546, which is a continuation of application No. 15/686,198, filed on Aug. 25, 2017, now Pat. No. 9,861,286, which is a continuation of application No. 15/357,136, filed on Nov. 21, 2016, now Pat. No. 9,757,040, which is a continuation of application No. 14/651,367, filed as application No. PCT/US2013/075736 on Dec. 17, 2013, now Pat. No. 9,500,635, and application No. 16/669,794, which is a continuation of application No. 16/506,885, filed on Jul. 9, 2019, now Pat. No. 10,517,484, which is a continuation of application No. 16/272,069, filed on Feb. 11, 2019, now abandoned, which is a continuation of application No. 16/029,611, filed on Jul. 8, 2018, now Pat. No. 10,201,283, which is a continuation of application No. 15/888,052, filed on Feb. 4, 2018, now Pat. No. 10,136,819, which is a continuation of application No. 15/212,549, filed on Jul. 18, 2016, now Pat. No. 9,885,698, which is a continuation of application No. 14/650,897, filed as application No. PCT/US2013/075700 on Dec. 17, 2013, now Pat. No. 9,494,567, said application No. 16/506,885 is a continuation of application No. 16/004,359, filed on Jun. 9, 2018, which is a continuation of application No. 14/109,007, filed on Dec. 17, 2013, now Pat. No. 9,993,159, said application No. 16/506,885 is a continuation of application No. 16/188,194, filed on Nov. 12, 2018, now Pat. No. 10,386,230, which is a continuation of application No. 16/004,154, filed on Jun. 8, 2018, now Pat. No. 10,126,283, which is a continuation of application No. 15/855,201, filed on Dec. 27, 2017, now Pat. No. 9,995,722, which is a continuation of application No. 15/711,907, filed on Sep. 21, 2017, now Pat. No. 9,897,584, which is a division of application No. 15/357,225, filed on Nov. 21, 2016, now Pat. No. 9,797,876, which is a continuation of application No. 14/650,981, filed as application No. PCT/US2013/075767 on Dec. 17, 2013, now Pat. No. 9,500,634, said application No. 16/506,885 is a continuation of application No. 16/241,628, filed on Jan. 7, 2019, now Pat. No. 10,441,176, which is a continuation of application No. 16/015,737, filed on Jun. 22, 2018, now Pat. No. 10,172,523, which is a continuation of application No. 15/594,053, filed on May 12, 2017, now Pat. No. 10,188,299, which is a continuation of application No. 14/875,709, filed on Oct. 6, 2015, now Pat. No. 9,651,533, which is a continuation of application No. 14/108,986, filed on Dec. 17, 2013, now Pat. No. 9,164,032, said application No. 16/506,885 is a continuation of application No. 16/284,514, filed on Feb. 25, 2019, now abandoned, which is a continuation of application No. 16/016,649, filed on Jun. 24, 2018, now Pat. No. 10,213,113, which is a continuation of application No. 15/860,065, filed on Jan. 2, 2018, now Pat. No. 10,098,546, which is a continuation of application No. 15/686,198, filed on Aug. 25, 2017, now Pat. No. 9,861,286, which is a continuation of application No. 15/357,136, filed on Nov. 21, 2016, now Pat. No. 9,757,040, which is a continuation of application No. 14/651,367, filed as application No. PCT/US2013/075736 on Dec. 17, 2013, now Pat. No. 9,500,635.

(60) Provisional application No. 61/747,477, filed on Dec. 31, 2012, provisional application No. 61/754,698, filed on Jan. 12, 2013, provisional application No. 61/747,472, filed on Dec. 31, 2012, provisional application No. 61/747,553, filed on Dec. 31, 2012, provisional application No. 61/747,485, filed on Dec. 31, 2012, provisional application No. 61/747,487, filed on Dec. 31, 2012.

(51) **Int. Cl.**

A61C 19/04	(2006.01)
G16H 40/67	(2018.01)
A61B 5/145	(2006.01)
A61B 5/1455	(2006.01)
G01J 3/02	(2006.01)
G01J 3/10	(2006.01)
G01J 3/14	(2006.01)
G01J 3/28	(2006.01)
G01J 3/42	(2006.01)
G01J 3/453	(2006.01)
G01N 21/35	(2014.01)
G01N 21/3563	(2014.01)
G01N 21/359	(2014.01)
G01N 21/39	(2006.01)
G01N 21/88	(2006.01)
G01N 33/02	(2006.01)
G01N 33/15	(2006.01)
G01N 33/44	(2006.01)
G01N 33/49	(2006.01)
G06F 19/00	(2018.01)
H01S 3/067	(2006.01)
H01S 3/00	(2006.01)
A61C 1/00	(2006.01)
G01J 3/18	(2006.01)
G01J 3/12	(2006.01)
G01M 3/38	(2006.01)
G01N 21/85	(2006.01)
G01N 21/95	(2006.01)
H01S 3/30	(2006.01)

(52) **U.S. Cl.**

CPC ***A61B 5/0075*** (2013.01); ***A61B 5/0086*** (2013.01); ***A61B 5/1455*** (2013.01); ***A61B 5/14532*** (2013.01); ***A61B 5/14546*** (2013.01); ***A61B 5/4547*** (2013.01); ***A61B 5/6801*** (2013.01); ***A61B 5/7203*** (2013.01); ***A61B 5/7257*** (2013.01); ***A61B 5/742*** (2013.01); ***A61B 5/7405*** (2013.01); ***A61C 19/04*** (2013.01); ***G01J 3/0218*** (2013.01); ***G01J 3/108*** (2013.01); ***G01J 3/14*** (2013.01); ***G01J 3/28*** (2013.01); ***G01J 3/2823*** (2013.01); ***G01J 3/42*** (2013.01); ***G01J 3/453*** (2013.01); ***G01N 21/35*** (2013.01); ***G01N 21/359*** (2013.01); ***G01N 21/3563*** (2013.01); ***G01N 21/39*** (2013.01); ***G01N 21/88*** (2013.01); ***G01N 33/02*** (2013.01); ***G01N 33/025*** (2013.01); ***G01N 33/15*** (2013.01); ***G01N 33/442*** (2013.01); ***G01N 33/49*** (2013.01); ***G06F 19/00*** (2013.01); ***G16H 40/67*** (2018.01); *A61B 5/0024* (2013.01); *A61B 2562/0233* (2013.01); *A61B 2562/0238* (2013.01); *A61B 2562/146* (2013.01); *A61B 2576/02* (2013.01); *A61C 1/0046* (2013.01); *G01J 3/1838* (2013.01); *G01J 2003/104* (2013.01); *G01J 2003/1208*

(2013.01); *G01J 2003/2826* (2013.01); *G01M 3/38* (2013.01); *G01N 21/85* (2013.01); *G01N 21/9508* (2013.01); *G01N 2021/3595* (2013.01); *G01N 2021/399* (2013.01); *G01N 2201/061* (2013.01); *G01N 2201/062* (2013.01); *G01N 2201/06113* (2013.01); *G01N 2201/08* (2013.01); *G01N 2201/12* (2013.01); *G01N 2201/129* (2013.01); *H01S 3/0092* (2013.01); *H01S 3/06758* (2013.01); *H01S 3/302* (2013.01)

(58) **Field of Classification Search**
USPC 356/300
See application file for complete search history.

(56) **References Cited**

U.S. PATENT DOCUMENTS

4,221,997 A 9/1980 Flemming
4,275,266 A 6/1981 Lasar
4,374,618 A 2/1983 Howard
4,403,605 A 9/1983 Tanikawa
4,462,080 A 7/1984 Johnstone et al.
4,516,207 A 5/1985 Moriyama et al.
4,523,884 A 6/1985 Clement et al.
4,605,080 A 8/1986 Lemelson
4,641,292 A 2/1987 Tunnell et al.
4,704,696 A 11/1987 Reimer et al.
4,728,974 A 3/1988 Nio et al.
4,762,455 A 8/1988 Coughlan et al.
4,776,016 A 10/1988 Hansen
4,958,910 A 9/1990 Taylor et al.
4,989,253 A 1/1991 Liang et al.
5,078,140 A 1/1992 Kwoh
5,084,880 A 1/1992 Esterowitz et al.
5,086,401 A 2/1992 Glassman et al.
5,134,620 A 7/1992 Huber
5,142,930 A 9/1992 Allen et al.
5,180,378 A 1/1993 Kung et al.
5,191,628 A 3/1993 Byron
5,218,655 A 6/1993 Mizrahi
5,230,023 A 7/1993 Nakano
5,246,004 A 9/1993 Clarke et al.
5,267,152 A 11/1993 Yang et al.
5,267,256 A 11/1993 Saruwatari et al.
5,267,323 A 11/1993 Kimura
5,300,097 A 4/1994 Lemer et al.
5,303,148 A 4/1994 Mattson et al.
5,305,427 A 4/1994 Nagata
5,313,306 A 5/1994 Kuban et al.
5,323,404 A 6/1994 Grubb
5,345,538 A 9/1994 Narayannan et al.
5,368,224 A 11/1994 Richardson et al.
5,400,165 A 3/1995 Gnauck et al.
5,408,409 A 4/1995 Glassman et al.
5,458,122 A 10/1995 Hethuin
5,497,769 A 3/1996 Gratton et al.
5,544,654 A 8/1996 Murphy et al.
5,563,710 A 10/1996 Webb et al.
5,572,999 A 11/1996 Funda et al.
5,617,871 A 4/1997 Burrows
5,631,758 A 5/1997 Knox et al.
5,687,734 A 11/1997 Dempsey et al.
5,695,493 A 12/1997 Nakajima et al.
5,696,778 A 12/1997 MacPherson
5,704,351 A 1/1998 Mortara et al.
5,718,234 A 2/1998 Warden et al.
5,746,206 A 5/1998 Mannheimer
5,747,806 A 5/1998 Khalil et al.
5,748,103 A 5/1998 Flach et al.
5,774,213 A 6/1998 Trebino et al.
5,792,204 A 8/1998 Snell
5,795,300 A 8/1998 Bryars
5,812,978 A 9/1998 Nolan
5,855,550 A 1/1999 Lai et al.
5,862,803 A 1/1999 Besson et al.
5,867,305 A 2/1999 Waarts et al.
5,912,749 A 6/1999 Harstead et al.
5,919,134 A 7/1999 Diab
5,944,659 A 8/1999 Flach et al.
5,950,629 A 9/1999 Taylor et al.
5,957,854 A 9/1999 Besson et al.
5,970,457 A 10/1999 Brant et al.
6,014,249 A 1/2000 Fermann et al.
6,031,603 A 2/2000 Fine et al.
6,043,927 A 3/2000 Islam
6,044,283 A 3/2000 Fein et al.
6,078,833 A 6/2000 Hueber
6,115,673 A 9/2000 Malin et al.
6,181,414 B1 1/2001 Raz et al.
6,185,535 B1 2/2001 Hedin et al.
6,200,309 B1 3/2001 Rice et al.
6,212,310 B1 4/2001 Waarts et al.
6,224,542 B1 5/2001 Chang et al.
6,246,707 B1 6/2001 Yin et al.
6,246,896 B1 6/2001 Dumoulin et al.
6,273,858 B1 8/2001 Fox et al.
6,278,975 B1 8/2001 Brant et al.
6,281,471 B1 8/2001 Smart
6,285,897 B1 9/2001 Kilcoyne et al.
6,289,238 B1 9/2001 Besson et al.
6,301,271 B1 10/2001 Sanders et al.
6,301,273 B1 10/2001 Sanders et al.
6,325,978 B1 12/2001 Labuda et al.
6,333,803 B1 12/2001 Kurotori et al.
6,337,462 B1 1/2002 Smart
6,340,806 B1 1/2002 Smart et al.
6,350,261 B1 2/2002 Domankevitz et al.
6,364,834 B1 4/2002 Reuss et al.
6,374,006 B1 4/2002 Islam et al.
6,381,391 B1 4/2002 Islam et al.
6,402,691 B1 6/2002 Peddicord et al.
6,407,853 B1 6/2002 Samson et al.
6,436,107 B1 8/2002 Wang et al.
6,441,747 B1 8/2002 Khair et al.
6,442,430 B1 8/2002 Ferek-Petric
6,443,890 B1 9/2002 Schulze et al.
6,450,172 B1 9/2002 Hartlaub et al.
6,453,201 B1 9/2002 Daum et al.
6,454,705 B1 9/2002 Cosentino et al.
6,458,120 B1 10/2002 Shen et al.
6,462,500 B1 10/2002 L'Hegarat et al.
6,463,361 B1 10/2002 Wang et al.
6,480,656 B1 11/2002 Islam et al.
6,505,133 B1 1/2003 Hanna et al.
6,509,566 B1 1/2003 Wamsley et al.
6,512,936 B1 1/2003 Monfre et al.
6,534,012 B1 3/2003 Hazen et al.
6,549,702 B2 4/2003 Islam et al.
6,567,431 B2 5/2003 Tabirian et al.
6,587,702 B1 7/2003 Ruchti et al.
6,603,910 B2 8/2003 Islam et al.
6,605,080 B1 8/2003 Altshuler et al.
6,611,643 B2 8/2003 Birk et al.
6,619,835 B2 9/2003 Kita
6,625,180 B2 9/2003 Bufetov et al.
6,631,025 B2 10/2003 Islam et al.
6,640,117 B2 10/2003 Makarewicz et al.
6,659,947 B1 12/2003 Carter et al.
6,659,999 B1 12/2003 Anderson et al.
6,701,170 B2 3/2004 Stetson
6,708,048 B1 3/2004 Chance
6,731,967 B1 5/2004 Turcott
6,738,652 B2 5/2004 Mattu et al.
6,760,148 B2 7/2004 Islam
6,773,922 B2 8/2004 Jeng et al.
6,788,965 B2 9/2004 Ruchti et al.
6,802,811 B1 10/2004 Slepian
6,816,241 B2 11/2004 Grubisic
6,847,336 B1 1/2005 Lemelson et al.
6,864,978 B1 3/2005 Hazen et al.
6,885,498 B2 4/2005 Islam
6,885,683 B1 4/2005 Fermann et al.
6,898,451 B2 5/2005 Wuori
6,916,096 B2 7/2005 Eberl et al.

(56) **References Cited**

U.S. PATENT DOCUMENTS

6,943,936	B2	9/2005	Islam et al.
6,990,364	B2	1/2006	Ruchti et al.
7,010,336	B2	3/2006	Lorenz et al.
7,027,467	B2	4/2006	Baev et al.
7,060,061	B2	6/2006	Altshuler et al.
7,105,823	B2	9/2006	Abrahamsson et al.
7,133,710	B2	11/2006	Acosta et al.
7,167,300	B2	1/2007	Fermann et al.
7,184,148	B2	2/2007	Alphonse
7,209,657	B1	4/2007	Islam
7,233,816	B2	6/2007	Blank et al.
7,259,906	B1	8/2007	Islam
7,263,288	B1	8/2007	Islam
7,278,966	B2	10/2007	Hjelt et al.
7,294,105	B1	11/2007	Islam
7,299,080	B2	11/2007	Acosta et al.
7,317,938	B2	1/2008	Lorenz et al.
7,318,909	B2	1/2008	Lehmann et al.
7,332,784	B2	2/2008	Mills et al.
7,356,364	B1	4/2008	Bullock et al.
7,395,158	B2	7/2008	Monfre et al.
7,433,116	B1	10/2008	Islam
7,468,036	B1	12/2008	Rulkov et al.
7,519,253	B2	4/2009	Islam
7,519,406	B2	4/2009	Blank et al.
7,620,674	B2	11/2009	Ruchti et al.
7,648,463	B1	1/2010	Elhag et al.
7,697,966	B2	4/2010	Monfre et al.
7,771,320	B2	8/2010	Riley et al.
7,787,503	B2	8/2010	Wadsworth
7,787,924	B2	8/2010	Acosta et al.
7,800,818	B2	9/2010	Mattsson
7,807,718	B2	10/2010	Hashim et al.
7,847,234	B2	12/2010	Meyers et al.
7,848,605	B2	12/2010	Ridder et al.
7,890,158	B2	2/2011	Rowe et al.
8,000,574	B2	8/2011	Buchter et al.
8,145,286	B2	3/2012	Arai et al.
8,157,730	B2	4/2012	LeBoeuf et al.
8,158,175	B2	4/2012	Bourg, Jr.
8,158,493	B2	4/2012	Shah et al.
8,172,761	B1	5/2012	Rulkov et al.
8,180,422	B2	5/2012	Rebec
8,180,591	B2	5/2012	Yuen et al.
8,198,589	B2	6/2012	Tolton et al.
8,213,007	B2	7/2012	Wang et al.
8,310,336	B2	11/2012	Muhsin et al.
8,315,682	B2	11/2012	Such et al.
8,430,310	B1	4/2013	Ho et al.
8,463,576	B2	6/2013	Yuen et al.
8,472,108	B2	6/2013	Islam
8,475,367	B1	7/2013	Yuen et al.
8,509,882	B2	8/2013	Albert et al.
8,649,838	B2	2/2014	Chen et al.
RE44,875	E	4/2014	Kiani et al.
8,725,226	B2	5/2014	Isaacson
8,755,871	B2	6/2014	Weng et al.
8,767,190	B2	7/2014	Hall
8,788,002	B2	7/2014	LeBoeuf et al.
8,945,017	B2	2/2015	Venkatraman et al.
8,948,832	B2	2/2015	Hong et al.
8,954,135	B2	2/2015	Yuen et al.
9,142,117	B2	9/2015	Muhsin et al.
9,164,032	B2	10/2015	Islam
9,179,876	B2	11/2015	Ochs et al.
9,192,329	B2	11/2015	Al-Ali
9,207,121	B2	12/2015	Adler
9,241,676	B2	1/2016	Lisogurski et al.
9,326,712	B1	5/2016	Kiani
9,596,990	B2	3/2017	Park et al.
9,651,533	B2	5/2017	Islam
9,675,250	B2	6/2017	Tverskoy
9,723,993	B2	8/2017	Vermeulen
9,757,040	B2	9/2017	Islam
9,820,658	B2	11/2017	Tran
9,861,286	B1	1/2018	Islam
9,885,698	B2	2/2018	Islam
10,188,299	B2	1/2019	Islam
10,213,113	B2	2/2019	Islam
2002/0013518	A1	1/2002	West et al.
2002/0019584	A1	2/2002	Schulze et al.
2002/0032468	A1	3/2002	Hill et al.
2002/0082612	A1	6/2002	Moll et al.
2002/0109621	A1	8/2002	Khair et al.
2002/0115914	A1	8/2002	Russ
2002/0128846	A1	9/2002	Miller
2002/0178003	A1	11/2002	Gehrke et al.
2003/0022126	A1	1/2003	Buchalla et al.
2003/0107739	A1	6/2003	Lehmann et al.
2003/0109055	A1	6/2003	Lehmann et al.
2003/0152307	A1	8/2003	Von Drasek et al.
2004/0174914	A1	9/2004	Fukatsu
2004/0240037	A1	12/2004	Harter
2005/0049468	A1	3/2005	Carlson et al.
2005/0111500	A1	5/2005	Harter et al.
2005/0133691	A1	6/2005	Doppke et al.
2005/0209516	A1	9/2005	Fraden
2006/0058683	A1	3/2006	Chance
2006/0198397	A1	9/2006	Korolev et al.
2006/0223032	A1	10/2006	Fried et al.
2006/0245461	A1	11/2006	Islam
2006/0268393	A1	11/2006	Islam
2006/0281982	A1	12/2006	Grata et al.
2006/0283931	A1	12/2006	Polli et al.
2007/0021670	A1	1/2007	Mandelis et al.
2007/0078348	A1	4/2007	Holman
2008/0086318	A1	4/2008	Gilley et al.
2008/0105665	A1	5/2008	Kondo
2008/0240502	A1	10/2008	Freedman et al.
2009/0028193	A1	1/2009	Islam
2009/0105605	A1	4/2009	Abreu
2009/0156932	A1	6/2009	Zharov
2009/0185274	A1	7/2009	Shpunt
2009/0204110	A1	8/2009	Islam
2009/0244288	A1	10/2009	Fujimoto et al.
2009/0287067	A1	11/2009	Dorogusker et al.
2010/0007717	A1	1/2010	Spektor et al.
2010/0046067	A1	2/2010	Fermann et al.
2010/0118123	A1	5/2010	Freedman et al.
2010/0160794	A1	6/2010	Banet et al.
2010/0160798	A1	6/2010	Banet et al.
2010/0217099	A1	8/2010	LeBoeuf et al.
2010/0217102	A1	8/2010	LeBoeuf et al.
2010/0284082	A1	11/2010	Shpunt et al.
2010/0322490	A1	12/2010	Pan et al.
2010/0331637	A1	12/2010	Ting et al.
2011/0040197	A1	2/2011	Welch et al.
2011/0143364	A1	6/2011	Kim et al.
2011/0188054	A1	8/2011	Petronius et al.
2011/0208015	A1	8/2011	Welch et al.
2011/0237911	A1	9/2011	Lamego et al.
2011/0267688	A1	11/2011	Kleppe et al.
2011/0282167	A1	11/2011	Ridder et al.
2011/0292376	A1	12/2011	Kukushkin et al.
2012/0013722	A1	1/2012	Wong et al.
2012/0041767	A1	2/2012	Hoffman et al.
2012/0197093	A1	8/2012	LeBoeuf et al.
2012/0203077	A1	8/2012	He et al.
2012/0239013	A1	9/2012	Islam
2012/0245439	A1	9/2012	Andre et al.
2012/0310062	A1	12/2012	Li et al.
2012/0316455	A1	12/2012	Rahman et al.
2013/0274569	A1	10/2013	Islam
2013/0281795	A1	10/2013	Varadan
2013/0303921	A1	11/2013	Chu et al.
2013/0327966	A1	12/2013	Fidler et al.
2014/0078510	A1	3/2014	Rubio Guivernau et al.
2014/0081100	A1	3/2014	Muhsin et al.
2014/0236021	A1	8/2014	Islam
2014/0249427	A1	9/2014	Liu
2014/0275852	A1	9/2014	Hong et al.
2014/0275854	A1	9/2014	Venkatraman et al.
2015/0011851	A1	1/2015	Mehta et al.
2015/0338509	A1	11/2015	Lange

(56) **References Cited**

U.S. PATENT DOCUMENTS

2016/0045118	A1	2/2016	Kiani
2016/0327476	A1	11/2016	Islam
2018/0231373	A1	8/2018	Pesach et al.

FOREIGN PATENT DOCUMENTS

DE	102010012987	A1	10/2010
EP	1148666	A2	10/2001
JP	2005270544	A	10/2005
WO	1997015240	A1	5/1997
WO	1997049340	A1	12/1997
WO	2001050959	A1	7/2001
WO	2001089362	A2	11/2001
WO	2002027640	A2	4/2002
WO	2002028123	A2	4/2002
WO	2005013843	A2	2/2005
WO	2007061772	A1	5/2007
WO	2009130464	A1	10/2009
WO	2012135952	A1	10/2012
WO	2013012938	A1	1/2013
WO	2015084376	A1	6/2015

OTHER PUBLICATIONS

Inter Partes Review No. IPR2020-00209; Petition for Inter Partes Review of U.S. Pat. No. 10,213,113; *Apple Inc.* v. *Omni Medsci, Inc.*; pp. 1-91; dated Dec. 11, 2019.

File History for U.S. Pat. No. 10,213,113 issued Feb. 26, 2019, 686 pps.

Declaration of Brian W. Anthony , PhD, regarding U.S. Pat. No. 10,213,113 in IPR2020-00209, Dec. 11, 2019, 101 pps.

United States District Court Eastern District of Texas Marshall Division; *Omni Medsci, Inc.* vs. *Apple Inc.*; Civil Action No. 2:18-cv-00429; Second Amended Complaint; Feb. 26, 2019; 274 pps.

United States District Court Northern District of California Oakland Division;*Omni Medsci, Inc.* vs. *Apple Inc.*; Civil Action No. 19-cv-05673-YGR; Order staying the case; Nov. 20, 2019, 5 pps.

File History for U.S. Pat. No. 10,188,299 issued Jan. 29, 2019, 787 pps.

Declaration of Brian W. Anthony , PhD, regarding U.S. Pat. No. 10,188,299 in IPR2020-00175, Dec. 11, 2019, 119 pps.

United States District Court Eastern District of Texas Marshall Division; *Omni Medsci, Inc.* vs. *Apple Inc.*; Civil Action No. 2:18-cv-429; Amended Complaint; Jan. 28, 2019; 169 pps.

Aaviksoo, J., et al., "Observation of optical precursors at pulse propagation in GaAs", Physical Review A, vol. 44, No. 9, Nov. 1, 1991, pp. R5353-R5356.

Abeeluck, Akheelesh K., et al., "Continuous-wave pumping in the anomalous- and normal dispersion regimes of nonlinear fibers for supercontinuum generaffon", Optics Letters, vol. 30, No. 1, Jan. 1, 2005, pp. 61-63.

Absorption Coefficient and Penetration Depth, The Science of Solar, available at https://photon.libretexts.org/The_Science_of_Solar/Solar_Basics/C._Semico-nductors_and_Solar_Interactions/III._Absorption_of_Light_and_Generation/1.-Absorption_Coefficient_and_Penetration_Depth (Last Updated Nov. 3, 2018).

Akbari, H. K. Uto, Y. Kosugi, K. Kojima, N. Tanaka, "Cancer detection using infrared hyperspectral imaging," Cancer Science, vol. 102, No. 4, pp. 852-857 (Apr. 2011).

Amended Joint Claim Construction and Prehearing Statement filed in Case No. 2:18-cv-134-RWS (Jan. 11, 2019).

Analysis of Edible Oils Using FT-NIR Spectroscopy. Bruker Optics, www.azom.com/article.aspx?ArticleID=5981, Mar. 10, 2012.

Andreoli, G. B. Bulgarelli, B. Hosgood, D. Tarchi, "Hyperspectral analysis of oil and oil-impacted soils for remote sensing purposes," Institute for the Protection and Security of the Citizen, European Commission Joint Research Centre, EUR 22739 EN (Mar. 2007).

Apple Inc.'s Preliminary Claim Constructions and Extrinsic Evidence Pursuant to Patent Local Rule 4-2 served in Case No. 2:18-cv-134-RWS (Nov. 1, 2018).

Application Brief the role of infrared microprobe analysis in forensic drug analysis, www.smithsdetection.com, Jun. 27, 2005.

Aris, Ishak Bin, "An Internet-Based Blood Pressure Monitoring System for Patients"; Journal of Telemedicine and Telecare 2001; pp. 51-53.

Arnold, T., M. De Biasio, R. Leitner, "Near-Infrared Imaging Spectroscopy for Counterfeit Drug Detection," Next Generation Spectroscopic Technologies IV, edited by M. A. Druy, R.A. Crocombe, Proceedings of SPIE, vol. 8032, 80320Y-1 to 7, (2011).

Asada et al., Mobile Monitoring with Wearable Photoplethysmographic Biosensors, Technical and Clinical Aspects of a Ring Sensor for Ambulatory, Telemetric, Continuous Health Monitoring in the Field, in the Hospital, and in the Home, IEEE Engineering in Medicine and Biology Magazine, (May/Jun. 2003) 13 pages.

Asada et al., The MIT Ring: History, Technology, and Challenges of Wearable Health Monitoring, MIT Industrial Liaison Program (2010) R&D Conference, MA, 72 pages.

Asada; Charts 1-3: Asada-533; U.S. Pat. No. 9,651,533 vs. Asada; *Omni MedSci, Inc.* v. *Apple Inc.*, pp. 1-188; May 22, 2019.

Asare et al., Analysis of Multi-Spectral Photoplethysmograph Biosensors, Proc. SPIE 8801, Novel Biophotonic Techniques and Applications II, 880106 (Jun. 2013), European Conferences on Biomedical Optics, Munich, Germany, 7 pages.

Asobe, Masaki, "Nonlinear Optical Properties of Chalcogenide Glass Fibers and Their Application to All-Optical Switching", Optical Fiber Technology, vol. 3, Article No. OF970214, 1997, pp. 142-148.

Asobe, Masaki, et al., "Third-order nonlinear spectroscopy in As2S3 chalcogenide glass fibers", J. Appl. Phys. 77 (11), Jun. 1, 1995, pp. 5518-5523.

Avdokhin, A. V., et al, "Continuous-wave, high-power, Raman continuum generation in holey fibers", Optics Letters, vol. 28, No. 15, Aug. 1, 2003, pp. 1353-1355.

Ayvaz, Huseyin, et al. "Application of infrared microspectroscopy and chemometric analysis for screening the acrylamide content in potato chips." Analytical Methods 5.8 (2013): 2020-2027.

B. Rigas, P.T.T. Wong, "Human Colon Adenocarcinoma Cell Lines Display Infrared Spectroscopic Features," Cancer Research, Jan. 1, 1992, pp. 84-88.

Barolet, Daniel, Light-Emitting Diodes (LEDs) in Dermatology, Seminars in Cutaneous Medicine and Surgery 27:227-238 (2008).

Bashkatov, A., et al., Optical properties of human skin, subcutaneous and mucous tissues in the wavelength range from 400 to 2000 nm, Journal of Physics D: Applied Physics 38 (2005) 2543-2555.

Baum P., et al., Strategic Intelligence Monitor on Personal Health Systems, Phase 2: Market Developments—Remote Patient Monitoring and Treatment, Telecare, Fitness/Wellness and mHealth, JRC Scientific and Policy Reports of European Commission (2013).

Beck, Mattias, et al., "Continuous Wave Operation of a Mid-Infrared Semiconductor Laser at Room Temperature," Science vol. 295, www.sciencemag.org, Jan. 11, 2002, pp. 301-305.

Belikov, A.V., A.V. Skripnik, K.V. Shatilova, "Study of the dynamics of the absorption spectra of human tooth enamel and dentine under heating and ablation by submillisecond pulse radiation of an erbium laser with a generation wavelength of 2.79 um," Optics and Spectroscopy, vol. 109, No. 2, pp. 211-216 (2010).

Bellisola, G. C. Sorio, "Infrared spectroscopy and microscopy in cancer research and diagnosis," American Journal of Cancer Research, vol. 2, No. 1, pp. 1-21 (2012).

Bizheva, K, et al., "Compact, broad-bandwidth fiberlaserforsub-2-pm axial resolution optical coherence tomography in the 1300-nm wavelength region," Optics Letters, vol. 28, No. 9, May 1, 2003, pp. 707-709.

Blank, T.B., T.L. Ruchti, A.D. Lorenz, S.L. Monfre, M.R. Makarewicz, M. Mattu, K.H. Hazen, "Clinical results from a non-invasive blood glucose monitor," Optical Diagnostics and Sensing of Biological Fluids and Glucose and Cholesterol Monitoring II, A.V. Priezzhev and G.L. Cote, Editors, Proceedings of SPIE, vol. 4624, pp. 1019 (2002).

(56) **References Cited**

OTHER PUBLICATIONS

Boppart, Stephen A., et al., "Imaging developing neural morphology using optical coherence tomography", Journal of Neuroscience Methods 70, 1996, pp. 65-72.
Boppart, Stephen A., et al., "Noninvasive assessment of the developing Xenopus cardiovascular system using optical coherence tomography", Prec. Natl. Acad. Sci. USA, vol. 94, Apr. 1997, pp. 4256-4261.
Borlinghaus, R., "Colours Count: how the challenge of fluorescence was solved in confocal microscopy," in Modern Research and Educational Topics in Microscopy, A. Mendez-Vilas and J. Diaz, eds, pp. 890-899, Formatex (2007).
Borlinghaus, R., "The White Confocal: Continuous Spectral Tuning in Excitation and Emission," in Optical Fluorescence Microscopy, A. Diaspro (Ed), Chapter 2, pp. 37-54, ISBN 978-3-642-15174-3, Springer-Verlag, Berlin (2011).
Borlinghaus, R.T., L. Kuschel, "White Light Laser: The Ultimate Source for Confocal Microscopy," http://www.leica-microsystems.com/science-lab/white-light-laser (Jun. 27, 2012).
Borrelli, N. F., et al., "Resonant and non-resonant effects in photonic glasses", Journal of Non-Crystalline Solids 185, 1995, pp. 109-122.
Boult, Maggi, et aL, "Percutaneous Endoscopic Laser Discectomy", Systematic Review, Aust. N.Z.J. Surg., vol. 70, Apr. 7, 2000, pp. 475-479.
Boult, Maggi, et al., "Systematic Review of Percutaneous Endoscopic Laser Discectomy: Update and Re-appraisal", Australian Safety and Efficacy Register of New Interventional Procedures-Surgical Report No. 5, Feb. 2000, 49 pages.
Branche et al., Signal Quality and Power Consumption of a New Prototype Reflectance Pulse Oximeter Sensor, Proceedings of the IEEE 31st Annual Northeast Bioengineering Conference (2005), Hoboken, NJ, 2 pages.
Bronzino, Joseph D.; "The Biomedical Engineering Handbook", (1995).
Büning-Pfaue, Hans. "Analysis of water in food by near infrared spectroscopy." Food Chemistry 82.1 (2003): 107-115.
Burmen, M. P. Usenik, A. Fidler, F. Pernus, B. Likar, "A construction of standardized near infrared hyper-spectral teeth database—a first step in the development of reliable diagnostic tool for quantification and early detection of caries," Lasers in Dentistry XVII, edited by P. Rechmann, D. Fried, Proceedings of SPIE, vol. 7884, Paper 78840E (2011).
Busse, Lynda E., et al., "Design Parameters for Fluoride Multimode Fibers", Journal of Lightwave Technology, vol. 9, No. 7, Jul. 1991, pp. 828-831.
Buttussi, F., et al., MOPET: A context-aware and user-adaptive wearable system for fitness training, Artificial Intelligence in Medicine (2008) 42, 153-163.
Cai et al., Implementation of a Wireless Pulse Oximeter Based on Wrist Band Sensor, College of Biological Science and Medical Engineering Southeast University, (2010) 3rd International Conference on Biomedical Engineering and Informatics, Nanjing, China, 4 pages.
Camacho, Nancy P., et al., "FTIR Microscopic Imaging of Collagen and Proteoglycan in Bovine Cartilage," Biopolymers (Biospectroscopy), vol. 62, 2001, pp. 1-8.
Cardinal, T., et al., "Non-linear optical properties of chalcogenide glasses in the system As—S—Se", Journal of Non-Crystalline Solids 256 & 257, 1999, pp. 353-360.
Champert, Pierre-Alain, et al., "White-light supercontinuum generation in normally dispersive optical fiber using original multi-wavelength pumping system", Optics Express, vol. 12, No. 19, Sep. 20, 2004, pp. 4366-4371.
Choi, Joon Y., et al, "Thermal, Mechanical, Optical, and Morphologic Changes in Bovine Nucleus Pulposus Induced by Nd:YAG (λ=1.32 um) Laser Irradiation", Lasers in Surgery and Medicine, vol. 28, 2001, pp. 248-254.
Choi, Seung-Ho, et al., "Observation of Optical Precursors in Water", Physical Review Letters, vol. 92, No. 19, May 14, 2004, pp. 193903-1-193903-.3.
Chung, S., D. Fried, M. Staninec, C.L. Darling, "Multispectral near-IR reflectance and transillumination imaging of teeth," Biomedical Optics Express, vol. 2, No. 10, pp. 2804-2814.
Chung, S., D. Fried, M. Staninec, C.L. Darling, "Near infrared imaging of teeth at wavelengths between 1200 and 1600nm," Proceedings of the Society of Photo Optical Instrument Engineering, paper 7884 (2011).
Clark, R.N., J.M. Curchin, T. M. Hoefen, G.A. Swayze, "Reflectance Spectroscopy of organic compounds: 1. Alkanes," Journal of Geophysical Research, vol. 114, pp. E03001 1 to E03001 19, (2009).
Coen, Stephane, et al., "Supercontinuum generation by stimulated Raman scattering and parametric four-wave mixing in photonic crystal fibers", J. Opt. Soc. Am. B, vol. 19, No. 4, Apr. 2002, pp. 753-764.
Compendium of Chemical Terminology Gold Book, International Union of Pure and Applied Chemistry, Version 2.3.3 (Feb. 24, 2014).
Computer Motion, Inc. "HERMES™ O.R. Control Center—510(k) Summary of Safety and Effectiveness," Oct. 11, 2002, 5 pages.
Computer Motion, Inc., "501(k) Summary—ZEUS® MicroWrist™ Surgical System andAccessories," Sep. 24, 2002, 6 pages.
Curriculum Vitae of Brian W. Anthony, PhD (Nov. 18, 2018).
D'Amico, Anthony V., et al., "Optical Coherence Tomography as a Method for Identifying Benign and Malignant Microscopic Structures in the Prostate Gland", Basic Science, Urology 55 (5), 2000, pp. 783-787.
De Boer, Johannes F., et al., "Determination of the depth-resolved Stokes parameters of light backscattered from turbid media by use of polarization-sensitive optical coherence omography", Optics Letters, vol. 24, No. 5; Mar. 1, 1999, pp. 300-302.
De Boer, Johannes F., et al., "Imaging thermally damaged tissue by polarization sensitive optical coherence tomography", Optics Express 212, vol. 3, No. 6, Sep. 14, 1998, pp. 212-218.
Demircan, Ayhan, et al., "Supercontinuum generation by the modulation instability", Optics Communications 244, 2005, pp. 181-185.
Desthieux, B., et al., "111 ?W (0. 5 mJ) pulse amplification at 1.5 um using a gated cascade of three erbium-doped fiber amplifiers," Appl. Phys. Lett. vol. 63, Aug. 2, 1993, pp. 586-588.
District Court Preliminary Claim Constructions in Case No. 2:18-cv-134-RWS from Court at Markman hearing.
Dr. Mohammed Islam, Faculty Profile, University of Michigan, College of Engineering (available at https://islam.engin.umich.edu) (2019 The Regents of the University of Michigan).
Drexler, C., Hirmer, M., Danilov, S., Giglberger, S., Putzger, J., Niklas, A., Jager, A., Hiller, K., Loffler, S., Schmalz, G., Redlich, B., Schulz, I., Monkman, G., Ganichev, S. "Infrared spectroscopy for clinical diagnosis of dental pulp vitality." Infrared, Millimeter, and Terahertz Waves (IRMIMW-THz), 2012 37th International Conference on. IEEE (2012).
Drexler, Wolfgang, "Ultrahigh-resolution optical coherence tomography", Journal of Biomedical Optics, vol. 9, No. 1, Jan./Feb. 2004, pp. 47-74.
Dubois, A., et al., "Three-dimensional cellular-level imaging using full-field optical coherence tomography", Physics in Medicine and Biology, Phys. Med. Biol. 49, 2004, pp. 1227-1234.
Dudley, John M., et al., "Supercontinuum generation in air-silica microstructured fibers with nanosecond and femtosecond pulse pumping", J. Opt. Soc. Am. B, vol. 19, No. 4, Apr. 2002, pp. 765-771.
Edwards, Glenn S., et al., "Advantage of the Mark-III FEL for biophysical research and biomedical applications", J. Synchrotron Rad. vol. 10, 2003, pp. 354-357.
Edwards, Glenn, et al., Tissue ablation by a free-electron laser tuned to the amide II band, Nature, vol. 371, Sep. 29, 1994, pp. 416-419.
Embedded-Lab, Introducing Easy Pulse: A DIY Photoplethysmographic Sensor for Measuring Hearth Rate, posted on www.Embedded-Lab.com Sep. 12, 2012, by R-B, 10 pages.
Enejder, A.M.K., T.G. Scecina, J. Oh, M. Hunter, W.C. Shih, S. Sasic, G.L. Horowitz, M.S. Feld, "Raman spectroscopy for noninvasive glucose measurements," Journal of Biomedical Optics, vol. 10, No. 3, 031114 (2005).

(56) **References Cited**

OTHER PUBLICATIONS

Evers, D.J., B.H.W. Hendriks, G.W. Lucassen, T.J.M. Ruers, "Optical spectroscopy: current advances and future applications in cancer diagnosis and therapy," Future Oncology, vol. 8, No. 3, pp. 307-320 (2012).
Evers, D.J., R. Nachabe, H.M. Klomp, J.W. van Sandick, M.W. Wouters, G.W. Lucassen, B.H.W. Hendriks, J. Wesseling, T.J.M. Ruers, "Diffuse reflectance spectroscopy: a new guidance tool for improvement of biopsy procedures in lung malignancies," Clinical Lung Cancer, article identifier 10.1016/j.clc.2012.02.001, 8 pages, (2012).
Excerpt from Claim Construction Markman Hearing Transcript filed in Case No. 2:18-cv-134-RWS (Feb. 6, 2019) vol. 1, pp. 1, 2, 21, 22.
Excerpts from Merriam-Webster's Collegiate Dictionary Eleventh Edition (2011).
Excerpts from the American Heritage Dictionary, 5th Edition (Jul. 2012).
Extended European Search Report for European Application No. 13867874.3 dated Jul. 15, 2016.
Extended European Search Report for European Application No. 13867892.5 dated Jul. 22, 2016.
Extended European Search Report for European Application No. 17155541.0 dated May 24, 2017.
Extended European Search Report for European Application No. 17156625.0 dated Mar. 20, 2017.
F. Kuhn, K. Oppermann, B. Hong, "Hydrocarbon Index-and algorithm for hyperspectral detection of hydrocarbons," International Journal of Remote Sensing, vol. 25, No. 12, pp. 2467-2473 (Jun. 20, 2004).
Falk, Peter, et al., "Supercontinuum generation in a photonic crystal fiber with two zero-dispersion wavelengths tapered to normal dispersion at all wavelengths", Optics Express, vol. 13, No. 19, Sep. 19, 2005, pp. 7535-7540.
Fantini, S. A. Sassaroli, "Near-infrared optical mammography for breast cancer detection with intrinsic contrast," Annals of Biomedical Engineering, vol. 40, No. 2, pp. 398-407 (Feb. 2012).
Faralli, S., et al., "Impact of Double Rayleigh Scattering Noise in Distributed Higher Order Raman Pumping Schemes", IEEE Photonics Technology Letters, vol. 15, No. 6, Jun. 2003, pp. 804-806.
Fedotova, O., et al., "Supercontinuum generation in planar rib waveguides enabled by anomalous dispersion", Optics Express, vol. 14, No. 4, Feb. 20, 2006, pp. 1512-1517.
File History for U.S. Pat. No. 9,651,533 issued May 16, 2017.
File History for U.S. Pat. No. 9,757,040 issued Sep. 12, 2017.
File History for U.S. Pat. No. 9,861,286 issued Jan. 9, 2018.
File History for U.S. Pat. No. 9,885,698 issued Feb. 6, 2018.
Final Office Action dated Oct. 21, 2016 for U.S. Appl. No. 14/875,709.
Fried, D. M. Staninec, C.L. Darling, "Near-infrared imaging of dental decay at 1310nm," Journal of Laser Dentistry, vol. 18, No. 1, pp. 8-16 (2010).
G. Edwards, et al., "Comparison of OPA and Mark-III FEL for Tissue Ablation at 6.45 Microns," Department of Physics and Free Electron Laser Laboratory, Duke University, 2002, 7 pages.
G.S. Edwards et al., "Free-electron-laser-based biophysical and biomedical instrumentation," American Institute of Physics, vol. 74, No. 7, Jul. 2003, pp. 3207-3245.
Galvis-Sánchez, Andrea C., et al. "Fourier transform near-infrared spectroscopy application for sea salt quality evaluation." Journal of agricultural and food chemistry 59.20 (2011): 11109-11116.
GE Healthcare, GE Ohmeda TufSat Oximeter for Clinicians on the go, (2012), A General Electric Co., www.gehealthcare.com, GE, Finland, 4 pages.
GE Healthcare, TuffSat User's Guide and Service Manual Electromagnetic Compatibility (EMC), (Mar. 2005) Helsinki, Finland, 43 pages.
Genty, G., et al., "Enhanced bandwidth of supercontinuum generated m microstructured fibers", Optics Express, vol. 12, No. 15, Jul. 26, 2004, pp. 3471-3480.
Genty, G., et al., "Supercontinuum generation in large mode-area microstructured fibers", Optics Express, vol. 13, No. 21, Oct. 17, 2005, pp. 8625-8633.
Glenn Edwards, "Biomedical and potential clinical applications for pulsed lasers operating near 6.45 um," Society of Photo-Optical Instrumentation Engineers, 1995, 2 pages.
H. Harry Asada et al.; Mobile Monitoring With Wearable Photoplethysmographic Biosensors; IEEE Engineering in Medicine and Biology Magazine, Jun. 2003; 13 pps.
Haase, Norbert U. "Prediction of potato processing quality by near infrared reflectance spectroscopy of ground raw tubers" Journal of Near Infrared Spectroscopy 19.1 (2011): 37-45.
Hafez, M. I., et al., "The Effect of Irrigation on Peak Temperatures in Nerve Root, Dura, and Intervertebral Disc During Laser-Assisted Foraminoplasty", Lasers in Surgery and Medicine, vol. 29, 2001, pp. 33-37.
Hagen, C. L., et al., "Generation of a Continuum Extending to the Midinfrared by Pumping ZBLAN Fiber With an Ultrafast 1550-nm Source", IEEE Photonics Technology Letters, vol. 18, No. 1, Jan. 1, 2006, pp. 91-93.
Hamilton, James D., et al., "High Frequency Optoacoustic Arrays Using Etalon Detection", IEEE Transactions on Ultrasonics, Ferroelectrics, and Frequency Control, vol. 47, No. 1, Jan. 2000, pp. 160-169.
Hamilton, James D., et al., "High Frequency Ultrasound Imaging Using an Active Optical Detector", IEEE Transactions on Ultrasonics, Ferroelectrics, and Frequency Control, vol. 45, No. 3, May 1998, pp. 719-727.
Hamilton, James D., et al., "High Frequency Ultrasound Imaging with Optical Arrays", IEEE Transactions on Ultrasonics, Ferroelectrics, and Frequency Control, vol. 45, No. 1, Jan. 1998, pp. 216-235.
Harbold, J. M., et al., "Highly nonlinear As—S—Se glasses for all-optical switching", Optics Letters, vol. 27, No. 2, Jan. 15, 2002, pp. 119-121.
Harbold, Jeffrey M., et al., "Highly Nonlinear Ge—As—Se and Ge—As—S—Se Glasses for All-Optical Switching", IEEE Photonics Technology Letters, vol. 14, No. 6, Jun. 2002, pp. 822-824.
Harman-Boehm, I. A. Gal, A.M. Raykhman, J.D. Zahn, E. Naidis, Y. Mayzel, "Noninvasive glucose monitoring: a novel approach," Journal of Diabetes Science and Technology, vol. 3, No. 2 pp. 253-260 (2009).
Harrington, James A., "Infrared Fiber Optics", OSA Handbook, vol. III, white paper, to be published by McGraw Hill, Undated, 13 pages.
Hartmann, R., and H. Büning-Pfaue. "NIR determination of potato constituents." Potato research 41.4 (1998): 327-334.
Hazen, K.H., M.A. Arnold, G.W. Small, "Measurement of glucose and other analytes in undiluted human serum with near-infrared transmission spectroscopy," Analytica Chimica Acta, vol. 371, pp. 255-267 (1998).
Herranz, M., A. Ruibal, "Optical imaging in breast cancer diagnosis: the next evolution," Journal of Oncology, vol. 2012, article ID 863747, 10 pages, (2012).
Hilligsoe, Karen Marie, et al., "Supercontinuum generation in a photonic crystal fiber with two zero dispersion wavelengths", Optics Express, vol. 12, No. 6, Mar. 22, 2004, pp. 1045-1054.
Hirmer, Marion, Danilov, Sergey, Giglberger, Stephan, Putzger, Jurgen, Niklas, Andreas, Jager, Andreas, Hiller, Karl-Anton, Loffler, Susanne, Schmalz, Gottfried, Redlich, Britta, Schulz, Irene, Monkman, Gareth, Ganichev, Sergey. "Spectroscopic Study of Human Teeth and Blood from Visible to Terahertz Frequencies for Clinical Diagnosis of Dental Pulp Vitality." Journal of Infrared, Millimeter, and Terahertz Waves 33.3 (2012): 366-375.
Hirosawa, N. Y. Sakamoto, H. Katayama, S. Tonooka, K. Yano, "In vivo investigation of progressive alternations in rat mammary gland tumors by near-infrared spectroscopy," Analytical Biochemistry, vol. 305, pp. 156-165 (2002).
Hori, Takashi, et al., "Experimental and numerical analysis of widely broadened supercontinuum generation in highly nonlinear dispersion-shifted fiber with a femtosecond pulse", J. Opt. Soc. Am. B, vol. 21, No. 11, Nov. 2004, pp. 1969-1980.

(56) **References Cited**

OTHER PUBLICATIONS

Hori, Takashi, et al., "Flatly broadened, wideband and low noise supercontinuum generation in highly nonlinear hybrid fiber", Optics Express, vol. 12, No. 2, Jan. 26, 2004, pp. 317-324.
Humphreys et al., Noncontact Simultaneous Dual Wavelength Photoplethysmography: A Further Step Toward Noncontact Pulse Oximetry, (2007) Review of Scientific Instruments 78, 044304, American Institute of Physics, 6 pages.
Husakou, Anton V., et al, "Supercontinuum generation, four-wave mixing, and fission of higher-order solitons in photonic-crystal fibers", J. Opt. Soc. Am. B, vol. 19, No. 9, Sep. 2002, pp. 2171-2182.
I.B. Ads, A.A.E. Wagie, N.B. Mariun, A.B.E. Jammal, "An Internet-based blood pressure monitoring system for patients," Journal of Telemedicine and Telecare, 2001, pp. 51-53.
Iatridis, James C., et al., "Is the Nucleus Pulposus a Solid or a Fluid? Mechanical Behaviors of the Nucleus Pulposus of the Human Intervertebral Disc", Spine, vol. 21(10), May 15, 1996, pp. 1174-1184.
Inoue, H., et al., "Computer simulation of the vibrational spectra and properties of fluoride glasses based on ZrF4", Journal of Non-Crystalline Solids, vol. 161, 1993, pp. 118-122.
Inter Partes Review No. IPR2019-00910; Petition for Inter Partes Review of U.S. Pat. No. 9,757,040; *Apple Inc.* v. *Omni Medsci, Inc.*; pp. 1-96; dated Apr. 10, 2019.
Inter Partes Review No. IPR2019-00911; Petition for Inter Partes Review of U.S. Pat. No. 9,861,286; *Apple Inc.* v. *Omni Medsci, Inc.*; pp. 1-83; dated Apr. 10, 2019.
Inter Partes Review No. IPR2019-00912; Petition for Inter Partes Review of U.S. Pat. No. 9,885,698; *Apple Inc.* v. *Omni Medsci, Inc.*; pp. 1-94; dated Apr. 10, 2019.
Inter Partes Review No. IPR2019-00913; Petition for Inter Partes Review of U.S. Pat. No. 9,651,533; *Apple Inc.* v. *Omni Medsci, Inc.*; pp. 1-96; dated Apr. 10, 2019.
Inter Partes Review No. IPR2019-00914; Petition for Inter Partes Review of U.S. Pat. No. 9,861,286; *Apple Inc.* v. *Omni Medsci, Inc.*; pp. 1-90; dated Apr. 10, 2019.
Inter Partes Review No. IPR2019-00915; Petition for Inter Partes Review of U.S. Pat. No. 9,885,698; *Apple Inc.* v. *Omni Medsci, Inc.*; pp. 1-91; dated Apr. 10, 2019.
Inter Partes Review No. IPR2019-00916; Petition for Inter Partes Review of U.S. Pat. No. 9,651,533; *Apple Inc.* v. *Omni Medsci, Inc.*; pp. 1-90; dated Apr. 10, 2019.
Inter Partes Review No. IPR2019-00917; Petition for Inter Partes Review of U.S. Pat. No. 9,757,040; *Apple Inc.* v. *Omni Medsci, Inc.*; pp. 1-93; dated Apr. 10, 2019.
International Preliminary Report on Patentability for International Application No. PCT/US2013/07567 dated Jul. 9, 2015.
International Preliminary Report on Patentability for International Application No. PCT/US2013/075700 dated Jul. 9, 2015.
International Preliminary Report on Patentability for International Application No. PCT/US2013/075736 dated Jul. 9, 2015.
International Search Report and Written Opinion for International Application No. PCT/US2013/075700 dated Apr. 24, 2014.
International Search Report and Written Opinion for International Application No. PCT/US2013/075736 dated Apr. 7, 2014.
International Search Report and Written Opinion for International Application No. PCT/US2013/075767 dated Oct. 14, 2014.
Islam, M. N., et al., "Broad bandwidths from frequency-shifting solitons in fibers", Optics Letters, vol. 14, No. 7, Apr. 1, 1989, pp. 370-372.
Islam, M. N., et al., "Femtosecond distributed soliton spectrum in fibers", J. Opt. Soc. Am. B, vol. 6, No. 6, Jun. 1989, pp. 1149-1158.
Istepanian, Robert H., "The Comparative Performance of Mobile Telemedical Systems based on the IS-54 and GSM Cellular Telephone Standards"; Journal of Telemedicine and Telecare 1999; pp. 97-104.
J. Sanghera, I. Aggarwal, "IR Fiber Optics at NRL," undated, 10 pages.
J. Sanghera, L.B. Shaw, I.D. Aggarwal, "Applications of chalcogenide glass optical fibers," Academic of Science, 2003, pp. 1-11.
J.G. Webster; Design of Pulse Oximeters; Medical Science Series; Taylor & Francis Group; CRC Press; Oct. 23, 1997; 260 pps.
Jackson, Stuart D., et al., "Theory and numerical simulation of nth-order cascaded Raman fiber lasers", J. Opt. Soc. Am. B, vol. 18, No. 9, Sep. 2001, pp. 1297-1306.
Jarman, Richard H., "Novel optical fiber lasers", Current Opinion in Solid State and Materials Science, 1996, pp. 199-203.
Jasco Application Note No. 200DR0188-E, "Rapid Identification of illegal drug using NIR (identification of MDMA tablet)", Sep. 4, 2008.
Jung et al., Design of a Low-Power Consumption Wearable Reflectance Pulse Oximetry for Ubiquitous Healthcare System, International Conference on Control, Automation and Systems (Oct. 2008), in COEX, Seoul, Korea, 4 pages.
K.M. Joos, et al. "Optic Nerve Sheath Fenestration with a Novel Wavelength Produced by the Free Electron Laser (FEL)," Lasers in Surgery and Medicine, 27: 2000,191-205.
Karlsson, L. "Caries detection methods based on changes in optical properties between healthy and carious tissue," International Journal of Dentistry, vol. 2010, Article ID 270729, 9 pages (2010).
Kays, Sandra E., William R. Windham, and Franklin E. Barton. "Prediction of total dietary fiber in cereal products using near-infrared reflectance spectroscopy." Journal of Agricultural and food chemistry 44.8 (1996): 2266-2271.
Kim-K.D., G.S. Son, S.S. Lim, S.S. Lee, "Measurement of glucose level exploiting a relative optical absorption at discrete probe wavelengths," Japanese Journal of Applied Physics, vol. 48, 077001 (2009).
Kobtsev, Serguei M., et al., "Modelling of high-power supercontinuum generation in highly nonlinear, dispersion shifted fibers at CW pump", Optics Express, vol. 13, No. 18, Sep. 5, 2005, pp. 6912-6918.
Konderpati, V.R., H.M. Heise, J. Backhaus, "Recent applications of near-infrared spectroscopy in cancer diagnosis and therapy," Annals of Bioanalytic Chemistry, vol. 390, pp. 125-139 (2008).
Kowalevicz, Andrew M., et al., "Ultrahigh resolution optical coherence tomography using a superluminescent light source" Optics Express 349, vol. 10, No. 7, Apr. 8, 2002, pp. 349-353.
Krantz, M., et al., The mobile fitness coach: Towards individualized skill assessment using personalized mobile devices, Pervasive and Mobile Computing (Jun. 2012).
Kumar, V.V. Ravi Kanth, et al, "Extruded soft glass photonic crystal fiber for ultrabroad supercontinuum generation", Optics Express, vol. 10, No. 25, Dec. 16, 2002, pp. 1520-1525.
Kurylyak et al., Smartphone-Based Photoplethysmogram Measurement, Department of Electronics, Computer and System Sciences, (2012) River Publishers, University of Calabria, Italy, 30 pages.
Kutz, J. Nathan, et al., Enhanced Supercontinuum Generation through Dispersion-Management, Optics Express, vol. 13, No. 11, May 30, 2005, pp. 3989-3998.
Lee, Ju Han, et al., "Continuous-wave supercontinuum laser based on an erbium-doped fiber ring cavity incorporating a highly nonlinear optical fiber", Optics Letters, vol. 30, No. 19, Oct. 1, 2005, pp. 2599-2601.
Lee, Ju Han, et al., "Experimental performance comparison for various continuous-wave supercontinuum schemes: ring cavity and single pass structures", Optics Express, vol. 13, No. 13, Jun. 27, 2005, pp. 4848-4853.
Leff, D.R., O.J. Warren, L.C. Enfield, A. Gibson, T. Athanasion, D.K. Patten, J. Hebden, G.Z. Yang, A. Darzi, "Diffuse optical imaging of the healthy and diseased breast: a systematic review," Breast Cancer Research Treatment, vol. 108, pp. 9-22 (2008).
Leon-Saval, S. G., et al., "Supercontinuum generation in submicron fibre waveguides", Optics Express, vol. 12, No. 13, Jun. 28, 2004, pp. 2864-2869.
Li et al, A Wireless Reflective Pulse Oximeter with Digital Baseline Control for Unfiltered Photoplethysmograms, (Jun. 2012) IEEE Transactions on Biomedical Circuits and Systems, vol. 6, No. 3, 10 pages.
Li Xingde, et al., "Imaging needle for optical coherence tomography", Optics Letters, vol. 25, No. 20, Oct. 15, 2000, pp. 1520-1522.

(56) **References Cited**

OTHER PUBLICATIONS

Lisogurski; Charts 1-3: Lisogurski-533; U.S. Pat. No. 9,651,533 vs. Lisogurski; *Omni MedSci, Inc.* v. *Apple Inc.*, pp. 1-84; May 22, 2019.
Lucas, Jacques, "Infrared glasses", Current Opinion in Solid State & Materials Science 4, 1999. pp. 181-187.
Luo et al., A Non-Invasive Dual-Channel Oximeter Based on Near-Infrared Spectroscopy (NIRS), Biophotonics Lab, Center of Advanced Research in Photonics (2007), The Chinese University of Hong Kong, China, 2 pages.
Lussi, A., R. Hibst, R. Paulus, "Diagnodent: An optical method for caries detection," Journal of Dental Research, vol. 83, special issue C, pp. C80-C83 (2004).
M. Kumar, M.N. Islam, F.L. Terry, M.J. Freeman, A. Chan, M. Neelakandan, T Manzur, "Stand-off detection of solid targets with diffuse reflection spectroscopy using a high-power mid-infrared supercontinuum source," Applied Optics, vol. 51, No. 15, pp. 2794-2807 (May 20, 2012).
Maia, A., L. Karlsson, W. Margulis, A. Gomes, "Evaluation of two imaging techniques: near-infrared transillumination and dental radiographs for the detection of early approximal enamel canes," Dentomaxillofacial Radiology, vol. 40, pp. 429-433 (2011).
Malin, S.F., T.L. Ruchti, T.B. Blank, S.N. Thennadil, S.L. Monfre, "Noninvasive prediction of glucose by near-infrared diffuse reflectance spectroscopy," Clinical Chemistry, vol. 45, No. 9, pp. 1651-1658 (1999).
Marbach, R., T. Koschinsky, F.A. Gries, H.M. Heise, "Noninvasive blood glucose assay by near-infrared diffuse reflectance spectroscopy of the human inner lip," Applied Spectroscopy, vol. 47, No. 7, pp. 875-881 (1993).
McCoy, R.M., J.G. Blake, K.L. Andrews, "Detecting hydrocarbon microseepage," Oil and Gas Journal, pp. 40-45 (May 28, 2001).
Mehrotra, R. A. Gupta, A. Kaushik, N. Prakash, H. Kandpal, "Infrared spectroscopic analysis of tumor pathology," Indian Journal of Experimental Biology, vol. 45, pp. 71-76 (Jan. 2007).
Mendelson et al., A Wearable Reflectance Pulse Oximeter for Remote Physiological Monitoring, (Aug./Sep. 2006) Proceedings of the 28th IEEE EMBS Annual International Conference New York City, Ny, 4 pages.
Michaels, C.A., T. Masiello, P.M. Chu, "Fourier transform spectrometry with a near-infrared supercontinuum source," Applied Spectroscopy, vol. 63, No. 5, pp. 538-543 (2009).
Mizunami, Toru, et al., "Gain saturation characteristics of Raman amplification in silica and fluoride glass optical fibers", Optics Communications 97, 1993, pp. 74-78.
Moon, Sucbei, et al., "Generation of octave-spanning supercontinuum with 1550-nm amplified diode-laser pulses and a dispersion-shifted fiber", Optics Express, vol. 14, No. 1, Jan. 9, 2006, pp. 270-278.
Morón et al, A Wireless Monitoring System for Pulse-Oximetry Sensors, (2005) Electronic Technology Department, University of Malaga, Spain, 6 pages.
Moros, J. N. Gallpienso, R. Vilches, S. Garrigues, M. DeLa Guardia, "Nondestructive direct determination of heroin in seized illicit street drugs by diffuse reflectance near-infrared spectroscopy," Analytical Chemistry, vol. 80, No. 19, pp. 7257-7265 (Oct. 1, 2008).
Moros,J., J. Kuligowski, G. Quintas, S. Garrigues, M. DeLa Guardia, "New cut-off criterion for uninformative variable elimination in multivariate calibration of near-infrared spectra for the determination of heroin in illicit street drugs," Analytica Chimica Acta, vol. 636, pp. 150-160 (2008).
Mussot, Arnaud, et al., "Generation of a broadband single-mode supercontinuum in a conventional dispersion-shifted fiber by use of a subnanosecond microchip laser", Optics Letters, vol. 28, No. 19, Oct. 1, 2003, pp. 1820-1822.
Na, J, J.H. Baek, S.Y. Ryu, C. Lee, B.H. Lee, "Tomographic imaging of incipient dental-caries using optical coherence tomography and comparison with various modalities," Optical Review, vol. 16, No. 4, pp. 426-431 (2009).
Nachabe, R., D.J. Evers, B.H.W. Hendriks, G.W. Lucassen, M.van der Voort, E.J. Rutgers, M.J.V. Peeters, J.A. Van der Hage, H.S. Oldenburg, J. Wesseling, T.J.M. Ruers, "Diagnosis of breast cancer using diffuse optical spectroscopy from 500 to 1600nm: comparison of classification methods," Journal of Biomedical Optics, vol. 16, No. 8, article 087010, 12 pages (Aug. 2011).
Nang, Yimin, et al., "Ultrahigh-resolution optical coherence tomography by broadband continuum generation from a photonic crystal fiber", Optics Letters, vol. 28, No. 3, Feb. 1, 2003, pp. 182-184.
Nassif, N. A., et al., "In vivo high-resolution video-rate spectral-domain optical coherence tomography of the human retina and optic nerve", Optics Express, vol. 12, No. 3, Feb. 9, 2004, pp. 367-375.
Nellcor; Charts 1-3: Nellcor-533; U.S. Pat. No. 9,651,533 vs. Nellcor; *Omni MedSci, Inc.* v. *Apple Inc.*, pp. 1-155; May 22, 2019.
New and Emerging Techniques—Surgical, Rapid Review, Laser Discectomy, Australian Safety and Efficacy Register of New Interventional Procedures—Surgical, Jun. 2003, 12 pages.
Ng, Choo Lum, Randy L. Wehling, and Susan L Cuppett. "Method for determining frying oil degradation by near-infrared spectroscopy." Journal of agricultural and food chemistry 55.3 (2007): 593-597.
Ni, Yongnian, Minghua Mei, and Serge Kokot. "Analysis of complex, processed substances with the use of NIR spectroscopy and chemometrics: Classification and prediction of properties—The potato crisps example." Chemometrics and Intelligent Laboratory Systems 105.2 (2011): 147-156.
Nicholson, J. W., "Supercontinuum generation in ultraviolet-irradiated fibers", Optics Letters, vol. 29, No. 20, Oct. 15, 2004, pp. 2363-2365.
Nicholson, J. W., et al., "All-fiber, octave-spanning supercontinuum", Optics Letters, vol. 28, No. 8, Apr. 15, 2003, pp. 643-645.
Nicholson, J. W., et al., "High power, single mode, all-fiber source of femtosecond pulses at 1550 nm and its use in supercontinuum generation", Optics Express, vol. 12, No. 13, Jun. 28, 2004, pp. 3025-3034.
Nicholson, J. W., et al., "Pulsed and continuous-wave supercontinuum generation in highly nonlinear, dispersion-shifted fibers", Applied Physics B 77, 2003, pp. 211-218.
Nishida, Yoshiki, et al., "Reliability of Fluoride Fiber Module for Optical Amplifier Use", IEEE Photonics Technology Letters, vol. 11, No. 12, Dec. 1999, pp. 1596-1598.
Nishizawa, N., "Generation and application of high-quality supercontinuum sources," Optical Fiber Technology, vol. 18, pp. 394-402 (2012).
Non-Final Office Action for U.S. Appl. No. 14/875,709 dated May 26, 2016.
Noreen, R., C.C. Chien, M. Delugin, S. Yao, R. Pineau, Y. Hwu, M. Moenner, C. Petibois, "Detection of collagens in brain tumors based on FTIR imaging and chemometrics," Annals of Bioanalytic Chemistry, vol. 401, pp. 845-852 (2011).
Notice of Allowance for U.S. Appl. No. 14/875,709 dated Jan. 10, 2017.
Nowak, G. A., et al., "Low-power high-efficiency wavelength conversion based on modulational instability in high-nonlinearity fiber," Optics Letters, vol. 23, No. 12, Jun. 15, 1998, pp. 936-938.
Nowak, George A., et al., "Stable supercontinuum generation in short lengths of conventional dispersion-shifted fiber", Applied Optics, vol. 38, No. 36, Dec. 20, 1999, pp. 7364-7369.
Nunnally, W.C., S.K. Holland, G. Laufer, "Wide field of view solar occultation gas filter correlation radiometer for stratospheric methane measurements from a sounding rocket," Thermosense XXV, K.E. Elliot, X.P. Maldague, Editors, Proceedings of SPIE, vol. 5073, pp. 122-130 (2003).
Olesberg, J.T., L. Liu, V.V. Zee, M.A. Arnold, "In vivo near-infrared spectroscopy of rat skin tissue with varying blood glucose levels," Analytic Chemistry, vol. 78, No. 1, pp. 215-223 (2006).
Olesberg, J.T., M.A. Arnold, C. Mermelstein, J. Schmitz, J. Wagner, "Tunable laser diode system for noninvasive blood glucose measurements," Applied Spectroscopy, vol. 59, No. 12, pp. 1480-1484 (2005).
Olsen, B.A., M.W. Borer, F.M. Perry, R.A. Forbes, "Screening for counterfeit drugs using near-infrared spectroscopy," Pharmaceutical Technology, pp. 62-71 (Jun. 2002).
Omni MedSci Inc.'s Opening Claim Construction Brief filed in Case No. 2:18-cv-134-RWS (Dec. 20, 2018).

(56) **References Cited**

OTHER PUBLICATIONS

Omni Medsci, Inc. V. *Apple Inc.*; Case No. 2:18-cv-134-RWS (E.D. Tex.); Defendant's Invalidity Contentions, Aug. 28, 2018 (Exhibit A), 66 pps.
Omni Medsci, Inc. V. *Apple Inc.*; Case No. 2:18-cv-134-RWS (E.D. Tex.); Defendants Invalidity Contentions, Aug. 28, 2018 (Exhibit AA), 75 pps.
Omni Medsci, Inc. V. *Apple Inc.*; Case No. 2:18-cv-134-RWS (E.D. Tex.); Defendant's Invalidity Contentions, Aug. 28, 2018 (Exhibit B), 73 pps.
Omni Medsci, Inc. V. *Apple Inc.*; Case No. 2:18-cv-134-RWS (E.D. Tex.); Defendants Invalidity Contentions, Aug. 28, 2018 (Exhibit BB), 65 pps.
Omni Medsci, Inc. V. *Apple Inc.*; Case No. 2:18-cv-134-RWS (E.D. Tex.); Defendant's Invalidity Contentions, Aug. 28, 2018 (Exhibit C), 85 pps.
Omni Medsci, Inc. V. *Apple Inc.*; Case No. 2:18-cv-134-RWS (E.D. Tex.); Defendants Invalidity Contentions, Aug. 28, 2018 (Exhibit CC), 320 pps.
Omni Medsci, Inc. V. *Apple Inc.*; Case No. 2:18-cv-134-RWS (E.D. Tex.); Defendant's Invalidity Contentions, Aug. 28, 2018 (Exhibit D), 38 pps.
Omni Medsci, Inc. V. *Apple Inc.*; Case No. 2:18-cv-134-RWS (E.D. Tex.); Defendants Invalidity Contentions, Aug. 28, 2018 (Exhibit DD), 240 pps.
Omni Medsci, Inc. V. *Apple Inc.*; Case No. 2:18-cv-134-RWS (E.D. Tex.); Defendants Invalidity Contentions, Aug. 28, 2018 (Exhibit E), 120 pps.
Omni Medsci, Inc. V. *Apple Inc.*; Case No. 2:18-cv-134-RWS (E.D. Tex.); Defendants Invalidity Contentions, Aug. 28, 2018 (Exhibit F), 40 pps.
Omni Medsci, Inc. V. *Apple Inc.*; Case No. 2:18-cv-134-RWS (E.D. Tex.); Defendants Invalidity Contentions, Aug. 28, 2018 (Exhibit G), 66 pps.
Omni Medsci, Inc. V. *Apple Inc.*; Case No. 2:18-cv-134-RWS (E.D. Tex.); Defendants Invalidity Contentions, Aug. 28, 2018 (Exhibit H), 74 pps.
Omni Medsci, Inc. V. *Apple Inc.*; Case No. 2:18-cv-134-RWS (E.D. Tex.); Defendants Invalidity Contentions, Aug. 28, 2018 (Exhibit I), 102 pps.
Omni Medsci, Inc. V. *Apple Inc.*; Case No. 2:18-cv-134-RWS (E.D. Tex.); Defendants Invalidity Contentions, Aug. 28, 2018 (Exhibit J), 64 pps.
Omni Medsci, Inc. V. *Apple Inc.*; Case No. 2:18-cv-134-RWS (E.D. Tex.); Defendants Invalidity Contentions, Aug. 28, 2018 (Exhibit K), 77 pps.
Omni Medsci, Inc. V. *Apple Inc.*; Case No. 2:18-cv-134-RWS (E.D. Tex.); Defendants Invalidity Contentions, Aug. 28, 2018 (Exhibit L), 64 pps.
Omni Medsci, Inc. V. *Apple Inc.*; Case No. 2:18-cv-134-RWS (E.D. Tex.); Defendants Invalidity Contentions, Aug. 28, 2018 (Exhibit M), 119 pps.
Omni Medsci, Inc. V. *Apple Inc.*; Case No. 2:18-cv-134-RWS (E.D. Tex.); Defendants Invalidity Contentions, Aug. 28, 2018 (Exhibit N), 50 pps.
Omni Medsci, Inc. V. *Apple Inc.*; Case No. 2:18-cv-134-RWS (E.D. Tex.); Defendants Invalidity Contentions, Aug. 28, 2018 (Exhibit O), 63 pps.
Omni Medsci, Inc. V. *Apple Inc.*; Case No. 2:18-cv-134-RWS (E.D. Tex.); Defendants Invalidity Contentions, Aug. 28, 2018 (Exhibit P), 78 pps.
Omni Medsci, Inc. V. *Apple Inc.*; Case No. 2:18-cv-134-RWS (E.D. Tex.); Defendants Invalidity Contentions, Aug. 28, 2018 (Exhibit Q), 69 pps.
Omni Medsci, Inc. V. *Apple Inc.*; Case No. 2:18-cv-134-RWS (E.D. Tex.); Defendants Invalidity Contentions, Aug. 28, 2018 (Exhibit R), 61 pps.
Omni Medsci, Inc. V. *Apple Inc.*; Case No. 2:18-cv-134-RWS (E.D. Tex.); Defendants Invalidity Contentions, Aug. 28, 2018 (Exhibit S), 50 pps.
Omni Medsci, Inc. V. *Apple Inc.*; Case No. 2:18-cv-134-RWS (E.D. Tex.); Defendants Invalidity.Contentions, Aug. 28, 2018 (Exhibit T), 174 pps.
Omni Medsci, Inc. V. *Apple Inc.*; Case No. 2:18-cv-134-RWS (E.D. Tex.); Defendants Invalidity Contentions, Aug. 28, 2018 (Exhibit U), 334 pps.
Omni Medsci, Inc. V. *Apple Inc.*; Case No. 2:18-cv-134-RWS (E.D. Tex.); Defendants Invalidity Contentions, Aug. 28, 2018 (Exhibit V), 137 pps.
Omni Medsci, Inc. V. *Apple Inc.*; Case No. 2:18-cv-134-RWS (E.D. Tex.); Defendants Invalidity Contentions, Aug. 28, 2018 (Exhibit W), 384 pps.
Omni Medsci, Inc. V. *Apple Inc.*; Case No. 2:18-cv-134-RWS (E.D. Tex.); Defendants Invalidity Contentions, Aug. 28, 2018 (Exhibit X), 291 pps.
Omni Medsci, Inc. V. *Apple Inc.*; Case No. 2:18-cv-134-RWS (E.D. Tex.); Defendants Invalidity Contentions, Aug. 28, 2018 (Exhibit Y), 120 pps.
Omni Medsci, Inc. V. *Apple Inc.*; Case No. 2:18-cv-134-RWS (E.D. Tex.); Defendants Invalidity Contentions, Aug. 28, 2018 (Exhibit Z), 53 pps.
Omre, A., Bluetooth Low Energy: Wireless Connectivity for Medical Monitoring, Journal of Diabetes Science & Technology , vol. 4, Issue 2 (Mar. 2010).
Ooen, Stephane, et al., "Supercontinuum generation by stimulated Raman scattering and Darametric four-wave mixing in photonic crystal fibers", J. Opt. Soc. Am. B, vol. 19, No. 4, Apr. 2002, pp. 753-764.
Ooi ET, Zhang XQ, Chen JH, Soh PH, Ng K, Yeo JH, "Non-invasive glucose measurement using multiple laser diodes," Optical Diagnostic and Sensing VII, edited by Gerard L. Cote, Alexander V. Priezzhev, Proc. of SPIE vol. 6445, 64450K , (2007).
Oughstun, Kurt E., "Influence of precursor fields on ultrashort pulse autocorrelation measurements and pulse width evolution", Optics Express, vol. 8, No. 8, Apr. 9, 2001, pp. 481-491.
P.A. Thielen and L.B. Shaw, et al., "Small-core As—Se fiber for Raman amplification," Optics Leti-ers, vol. 28, No. 16, Aug. 15, 2003, 3 pages.
Palou, A. J. Cruz, M. Blanco, J. Tomas, J. De Los Rios, M. Alcala, "Determination of drug, excipients and coating distribution in pharmaceutical tablets using NIR-CI," Journal of Pharmaceutical Analysis, vol. 2, No. 2, pp. 90-97 (2012).
Pan, Yingtian, et al., "Hand-held arthroscopic optical coherence tomography for in vivo high-resolution imaging of articular cartilage", Journal of Biomedical Optics 8(4), Oct. 2003, pp. 648-654.
Papemyi, S. B., et al., "Sixth-Order Cascaded Raman Amplification", OFC/NFOEC, 2005, 3 pages.
Parawira, S. "Classification of hyperspectral breast images for cancer detection," Dec. 4, 2009, downloaded from WWW, 5 pages.
Park, Jesung, et al., "Analysis of birefringent image in the retinal nerve fiber layer by polarization sensitive optical coherence tomography", Ophthalmic Technologies XIV, Proceedings of SPIE, vol. 5314, 2004, pp. 188-194.
Park; Charts 1-3: Park-533; U.S. Pat. No. 9,651,533 vs. Park; *Omni MedSci, Inc.* v. *Apple Inc.*, pp. 1-171; May 22, 2019.
Passat, "Solid-State Lasers and Optical Components," Jul. 14, 2003, 5 pages.
Patel, S., et al., A review of wearable sensors and systems with application rehabilitation, Journal of Neuroengineering & Rehabilitation 2012 9:21.
Patterson et al., Ratiometric Artifact Reduction in Low Power Reflective Photoplethysmography, (Aug. 2011) IEEE Transactions on Biomedical Circuits and Systems, vol. 5, No. 4, 9 pages.
PCT/US06/44451, Notification of Transmittal of the International Search Report and the Written Opinion of the International Searching Authority, or the Declaration, dated Nov. 29, 2007, 12 pages.
Pedreschi, F., V. H. Segtnan, and S. H. Knutsen. "On-line monitoring of fat, dry matter and acrylamide contents in potato chips using near infrared interactance and visual reflectance imaging." Food Chemistry 121.2 (2010): 616-620.
Peláez, LED Power Reduction Trade-Offs for Ambulatory Pulse Oximetry, Conference Proceedings of the 29th Annual International Conference of the IEEE EMBS (Aug. 2007) Lyon, France, 4 pages.

(56) **References Cited**

OTHER PUBLICATIONS

U.S. Appl. No. 12/206,432, "System and Method for Voice Control of Medical Devices," by Mohammed N. Islam, filed Sep. 8, 2008.
Pezzaniti, J.L., T.W. Jeng, L. McDowell, G.M. Oosta, "Preliminary investigation of near-infrared spectroscopic measurements of urea, creatinine, glucose, protein and ketone in urine," Clinical Biochemistry, vol. 34, pp. 239-246 (2001).
Pierce, Mark C., et al., "Advances in Optical Coherence Tomography imaging for Dermatology", Optical Coherence Tomography Advances, The Journal of Investigative Dermatology, Sep. 3, 2004, pp. 458-463.
Pojic, M. J. Mastilovic, N. Majcen, "The application of near infrared spectroscopy in wheat quality control," Infrared Spectroscopy—Life and Biomedical Sciences, pp. 167-184 (2012).
Povazay, B., et al., "Submicrometer axial resolution optical coherence tomography", Optical Letters, vol. 27, No. 20, Oct. 15, 2002, pp. 1800-1802.
Proof of Service of Summons in *Omni MedSci, Inc.* v. *Apple Inc.*, No. 2:18-cv-134 (E.D. Tex.) (Apr. 13, 2018).
R.H. Istepanian, B. Woodward, P.A. Bales, S. Chen, B. Luk, "The comparative performance of mobile telemediCal systems based on the IS-54 and GSM cellular telephone standards," Journal of Telemedicine and Telecare, 1999, pp. 97-104.
R.Rox Anderson, et al., "Selective Photothermolysis: Precise Microsurgery by Selective Absorption of Pulsed Radiation," Department of Dermatology, Harvard Medical School, Science, vol. 220, Apr. 29, 1983, 4 pages.
Rambla, F.J., S. Garrigues, M. DeLa Guardia, "PLS-NIR determination of total sugar, glucose, fructose and sucrose in aqueous solutions of fruit juices," Analytica Chimica Acta, vol. 344, pp. 41-53 (1997).
Ranka, Jinendra K., et al., "Visible continuum generation in air-silica microstructure optical fibers with anomalous dispersion at 800 nm", Optics Letters, vol. 25, No. 1, Jan. 1, 2000, pp. 25-27.
Rauf Adil, "The Usage of Tablets in the HealthCare Industry," available at https://www.healthcareitnews.com/blog/usage-tablets-healthcare-industry (Aug. 2, 2012).
Reese, E.L, E.E. Fisher, D.A. Horowitz, "Photoelectric densitometry of the circulation of the human dental pulp," The Journal of the Baltimore College of Dental Surgery, vol. 26, No. 1, pp. 6-18 (1971).
Reich, G. "Near-infrared spectroscopy and imaging: basic principles and pharmaceutical applications," Advanced Drug Delivery Reviews, vol. 57, pp. 1109-1143 (2005).
Rein, Alan, and Luis Rodriguez-Saona. "Measurement of Acrylamide in Potato Chips by Portable FTIR Analyzers." (2013).
Rhee et al., Artifact-Resistant Power-Efficient Design of Finger-Ring Plethysmographic Sensors, IEEE Transactions on Biomedical Engineering (Jul. 2001), vol. 48, No. 7, Cambridge, MA, 11 pages.
Robert S. Jones et al.; Near-Infrared Transillumination at 1310-nm for the Imaging of Early Dental Decay; vol. 11; No. 18; Optics Express 2259; Sep. 8, 2003.
Rodionova, O.Y., L.P. Houmoller, A.L. Pomerantsev, P. Geladi, J. Burger, V.L. Dorofeyev, A.P. Arzamastsev, "NIR spectrometry for counterfeit drug detection: A feasibility study," Analytica Chimica Acta, vol. 549, pp. 151-158 (2005).
Roggan, Andre, et al., "Optical Properties of Circulating Human Blood in the Wavelength Range 400-2500 NM", Journal of Biomedical Optics, vol. 4, No. 1, Jan. 1999, pp. 36-46.
Roggo, Y. P. Chalus, L. Maurer, C. Lema-Martinez, A. Edmond, N. Jent, "A review of near infrared spectroscopy and chemometrics in pharmaceutical technologies," Journal of Pharmaceutical and Biomedical Analysis, vol. 44, pp. 683-700 (2007).
Rollins, Andrew M., et al., "Real-time in vivo imaging of human gastrointestinal ultrastructure by use of endoscopic optical coherence tomography with a novel efficient interferometer design", Optics Letters, vol. 24, No. 19, Oct. 1, 1999, pp. 1358-1360.
S.D. Khan, S. Jacobson, "Remote sensing and geochemistry for detecting hydrocarbon microseepages," GSA Bulletin, vol. 120, No. 1/2, pp. 96-105 (Jan./Feb. 2008).
Saliminia, A., et al., "Ultra-broad and coherent white light generation in silica glass by focused femtosecond pulses at 1.5pm", Optics Express, vol. 13, No. 15, Jul. 25, 2005, pp. 5731-5738.
Sanghera, J. S., et al., Active and passive chalcogenide glass optical fibers for IR applications: A review, Journal of Non-Crystalline Solids 256 & 257, 1999, pp. 6-16.
Scafi, S.H.F., C. Pasquini, "Identification of counterfeit drugs using near-infrared spectroscopy," Analyst, vol. 126, pp. 2218-2224 (2001).
Schmitt, Joseph, et al., "Intravascular Optical Coherence Tomography Opens a Window Onto Coronary Artery Disease", Optics & Photonics News, Feb. 2004, pp. 20-25.
Schneider, R.C., K.A. Kovar, "Analysis of ecstasy tablets: comparison of reflectance and transmittance near infrared spectroscopy," Forensic Science International, vol. 134, pp. 187-195 (2003).
Schreiber, T., et al., "Supercontinuum generation by femtosecond single and dual wavelength pumping in photonic crystal fibers with two zero dispersion wavelengths", Optics Express, vol. 13, No. 23, Nov. 14, 2005, pp. 9556-9569.
Schreiner et al., Blood Oxygen Level Measurement with a Chest-Based Pulse Oximetry Prototype System, Computing in Cardiology (2010) NIBEC, University of Ulster, Newtownabbey, Northern Ireland, 4 pages.
Schubert, E.F., Light-Emitting Diodes (Cambridge Univ. Press, 2nd ed. Reprinted 2014).
Schulz, I., J. Putzger, A. Niklas, M. Brandt, A. Jager, A. Hardt, S. Knorzer, K.A. Hiller, S. Loffler, G. Schmalz, S.N. Danilov, S. Giglberger, M. Hirmer, S.D. Ganichev, G. Monkman, "PPG signal acquisition and analysis on in vitro tooth model for dental pulp vitality assessment," ARC Submission 16, (2012).
Seefeldt, Michael, et al., "Compact white-light source with an average output power of 2.4 Wand 900 nm spectral bandwidth", Optics Communications 216, pp. 199-202.
Segtnan, Vegard H., et al. "Screening of acrylamide contents in potato crisps using process variable settings and near-infrared spectroscopy." Molecular nutrition & food research 50.9 (2006): 811-817.
September, Danwille Jacqwin Franco. Detection and quantification of spice adulteration by near infrared hyperspectral imaging. Diss. Stellenbosch: University of Stellenbosch, 2011.
Shaw, et al, IR Supercontinuum Generation in As—Se Photonic Crystal Fiber, Optical Society of America, Copyright 2005, 3 pages.
Shiroma, Cecilia, and Luis Rodriguez-Saona. "Application of NIR and MIR spectroscopy in quality control of potato chips." Journal of Food Composition and Analysis 22.6 (2009): 596-605.
Shiroma, Cecilia. "Rapid quality control of potato chips using near and mid-infrared spectroscopy." (2007).
Shu-Fang, T. C. Jian-Ping, Z. Mi, "The information of oil and gas micro-seepage in Dongsheng Region of Inner Mongolia extraction based on the airborne hyperspectral remote sensing image," Remote Sensing of the Environment, 16th National Symposium on Remote Sensing of China, edited by Q. Tong, Proceedings of SPIE, vol. 7123, 71230K-1 to 8, (2008).
Slusher, Richard, et al., "Highly nonlinear composite chalcogenide/polymer fibers", OSA 2004, 1 page.
Slusher, Richart E., et al., "Large Raman gain and nonlinear phase shills in high-purity As2So3 chalcogenide fibers", J. Opt. Soc. Am. B, vol. 21, No. 6, Jun. 2004, pp. 1146-1155.
Smektala, F., et al., "Chalcogenide glasses with large non-linear refractive indices", Journal of Non-Crystalline Solids 239, 1998, pp. 139-142.
Smith, J.L., "The Pursuit of Noninvasive Glucose: Hunting the Deceitful Turkey," 2nd Edition, pp. 1-141 (2011).
Sobol, Emil, et al., "Time-resolved, light scattering measurements of cartilage and cornea denaturation due to free electron laser radiation", Journal of Biomedical Optics, vol. 8, No. 2, Apr. 2003, pp. 216-222.
Sondermann, N., K.A. Kovar, "Identification of ecstasy in complex matrices using near-infrared spectroscopy," Forensic Science International, vol. 102, pp. 133-147 (1999).
Staninec, M., S.M. Douglas, C.L. Darling, K. Chan, H. Kang, R. C. Lee, D. Fried, "Nondestructive clinical assessment of occlusal caries lesions using near-IR imaging methods," Lasers in Surgery and Medicine, vol. 43, No. 10, pp. 951-959 (2011).

(56) **References Cited**

OTHER PUBLICATIONS

State-Specific Trends in Chronic Kidney Failure-United States, 1990-2001, Morbidity and Mortality Weekly Report, Department of Health and Human Services Centers for Disease Control and Prevention, vol. 53, No. 39, copied from internet: file:// C:\Documents and Settings\eturlo\Desktop\State-Speciflc Trends in Chronic Kidney . . . Feb. 12, 2010, Oct. 8, 2004, pp. 918-920.
Sun, Y., C.F. Booker, S. Kumari, R.N. Day, M. Davidson, A. Periasamy, "Characterization of an orange acceptor fluorescent protein for sensitized spectral fluorescence resonant energy transfer microscopy using a white-light laser," Journal of Biomedical Optics, vol. 14, No. 5, paper 054009 (2009).
Swan, M., Sensor Mania! the Internet of Things, Wearable Computing, Objective Metrics, and the Quantified Self 2.0, Journal of Sensor and Actuator Networks (2012).
Takushima, Yuichi, High average power, depolarized supercontinuum generation using a 1.55-um ASE noise source, Optics Express, vol. 13, No. 15, Jul. 25, 2005, pp. 5871-5877.
Tanaka, Keiji, "Optical nonlinearity in photonic glasses", Journal of Materials Science: Materials in Electronics 16, 2005, pp. 633-643.
Taos, Inc., Infrared Light-to-Voltage Optical Sensors, (2006) Texas Advanced Optoelectronic Solutions Inc., The Lumenology Company, TX, 14 pages.
Taroni, P. D. Cornelli, A. Giusto, A. Pifferi, N. Shah, L. Spinelli, A. Torricelli, R. Cubeddu, "Assessment of collagen absorption and related potential diagnostic applications," Diffuse Optical Imaging of Tissue, edited by B.W. Pogue, R. Cubeddu, Proceedings of SPIE-OSA Biomedical Optics, SPIE vol. 6629, paper 66290D, 5 pages, (2007).
Taroni, P., "Diffuse optical imaging and spectroscopy of the breast: a brief outline of history and perspectives," Photochemical Photobiological Science, vol. 11, pp. 241-250 (2012).
Tearney, Guillermo J., et al., "In vivo Endoscopic Optical Biopsy with Optical Coherence Tomography", Science, New Series, vol. 276, Jun. 27, 1997, pp. 2037-2039.
Technology Transfer Policy, Office of Technology Transfer—University of Michigan (available at https://techtransfer.umich.edu/for-inventors/policies/technology-transfer- -policy/) (revision effective Jun. 1, 2009).
The Bylaws of the University of Michigan Board of Regents, (available at http://www.regents.umich.edu/bylaws/bylawsrevised_09-18.pdf) (last updated Sep. 20, 2018).
Thennadil, S.N., J.L. Rennert, B.J. Wenzel, K.H. Hazen, T.L. Ruchti, M.B. Block, "Comparison of glucose concentration in interstitial fluid, and capillary and venous blood during rapid changes in blood glucose levels," Diabetes Technology & Therapeutics, vol. 3, No. 3, pp. 357-365 (2001).
Thongtrangan, Issada, et al., "Minimally invasive spinal surgery: a historical perspective", Neurosurg. Focus, vol. 16, Article 13, Jan. 2004, pp. 1-10.
Thybo, Anette Kistrup, et al. "Prediction of sensory texture of cooked potatoes using uniaxial compression, near infrared spectroscopy and low field1H NMR spectroscopy." LWT—Food Science and Technology 33.2 (2000): 103-111.
Tolton, B.T., "A concept for a gas-filter correlation radiometer to remotely sense the atmospheric carbon dioxide column from space," Notes and Correspondence, Journal of Atmospheric and Oceanic Technology, vol. 21, pp. 837-852, (May 2004).
Tombelaine, Vincent, et al., "Ultra wide band supercontinuum generation in air-silica holey fibers by SHG-induced modulation instabilities", Optics Express, vol. 13, No. 19, Sep. 19, 2005, pp. 7399-7404.
Travers, J. C., et al., "Extended blue supercontinuum generation in cascaded holey fibers", Optics Letters, vol. 30, No. 23, Dec. 1, 2005, pp. 3132-3134.
Travers, J. C., et al., "Extended continuous-wave supercontinuum generation in a low-water-loss holey fiber", Optics Letters, vol. 30, No. 15, Aug. 1, 2005, pp. 1938-1940.
Troy, T.L., S.N. Thennadil, "Optical properties of human skin in the near infrared wavelength range of 1000 to 2200nm," Journal of Biomedical Optics, vol. 6, No. 2, pp. 167-176, (2001).
U.S. Appl. No. 10/652,276, "System and Method for Voice Control of Medical devices," by Mohammed N. Islam, abandoned, filed Aug. 29, 2003.
U.S. Appl. No. 10/757,341, "System and Method for Voice Control of Medical devices," by Mohammed N. Islam, filed Jan. 13, 2004.
U.S. Appl. No. 12/206,432, "System and Method for Voice Control of Medical Devices," by Mohammed N. Islam, pending filed Sep. 8, 2008.
U.S. Appl. No. 61/350,673; titled: Opticoustic Sensor; Inventor: Massi Joe E. Kiani, filed Jun. 2, 2010.
U.S. Appl. No. 61/747,472, filed Dec. 31, 2012.
U.S. Appl. No. 61/747,477, filed Dec. 31, 2012.
U.S. Appl. No. 61/747,487, filed Dec. 31, 2012.
U.S. Appl. No. 61/754,698, filed Jan. 21, 2013.
U.S. Patent and Trademark Office, Notice of Allowance and Fee(s) Due for U.S. Appl. No. 12/206,432, filed Sep. 8, 2008, Mohammed N. Islam, Date filed: Aug. 28, 2009.
U.S. Patent and Trademark Office, Office Action for U.S. Appl. No. 12/206,432, filed Sep. 8, 2008, Mohammed N, Islam, Date Filed: Mar. 12, 2009.
United States District Court Eastern District of Texas Marshall Division; Defendant and Counter Claimant Apple Inc.'s Amended Answer, Affirmative Defenses, and Counterclaims to Complaint of Plaintiff and Counter Defendant Omni Medsci, Inc.; Document 38; Jul. 19, 2018; 32 pps.
United States District Court Eastern District of Texas Marshall Division; *Omni Medsci, Inc.* vs. *Apple Inc.*; Civil Action No. 2:18-cv-00134 Jury Trial Demanded; Defendant's Invalidity Contentions; Aug. 28, 2018; 33 pps.
Unterhuber, A., et al., "Advances in broad bandwidth light sources for ultrahigh resolution optical coherence tomography", Physics in Medicine and Biology, Phys. Med. Biol. 49, 2004, pp. 1235-1246.
Urban, J. P. G., et al., "The Nucleus of the Intervertebral Disc from Development to Degeneration" Amer. Zool., vol. 40, 2000, pp. 53-61.
Urbas, A., M.W. Manning, A. Daugherty, L.A. Cassis, R.A. Lodder, "Near-infrared spectrometry of abdominal aortic aneurysm in the ApoE Mouse," Analytical Chemistry, vol. 75, No. 15, pp. 3650-3655 (Jul. 15, 2003).
Valencell; Charts 1-3: Valencell-533; U.S. Pat. No. 9,651,533 vs. Valencell; *Omni MedSci, Inc.* v. *Apple Inc.*, pp. 1-122; May 22, 2019.
Van Der Meer, F. P. Van Dijk, H. Van Der Werff, H. Yang, "Remote sensing and petroleum seepage: a review and case study," Terra Nova, vol. 14, No. 1, pp. 1-17 (2002).
Van Der Meer, F., P. Van Dijk, S. Kroonenberg, Y. Hong, H. Lang, "Hyperspectral hydrocarbon microseepage detection and monitoring: potentials and limitations," Second EARSEI workshop on imaging spectroscopy, pp. 1-9 (2000).
Venugopalan, V., "Optical Society of America BIOMED Topical Meeting Tutorial on Tissue Optics", Apr. 27, 2004, pp. 1-32.
Vinay V. Alexander et al; Modulation Instability High Power All-Fiber Supercontinuum Lasers and Their Applications; Optical Fiber Technology 18; 2012; pp. 349-374.
Wadsworth, W. J., et al., "Supercontinuum and four-wave mixing with Q-switched pulses in endlessly single-mode photonic crystal fibres", Optics Express, vol. 12, No. 2, Jan. 26, 2004, pp. 299-309.
Wadsworth, William J., et al., "Supercontinuum generation in photonic crystal fibers and Optical fiber tapers: a novel light source", J. Opt. Soc. Am. B, vol. 19, No. 9, Sep. 2002, pp. 2148-2155.
Walsh, M.J., R.K. Reddy, R. Bhargava, "Label-free biomedical imaging with mid-IR spectroscopy," IEEE Journal of Selected Topics in Quantum Electronics, article identifier 10.1109/JSTQE.2011.2182635, 12 pages, (2011).
Wang et al., Multichannel Reflective PPG Earpiece Sensor with Passive Motion Cancellation, (Dec. 2007) IEEE Transactions on Biomedical Circuits and Systems, vol. 1, No. 4, 7 pages.

(56) **References Cited**

OTHER PUBLICATIONS

Wang, Lihong V., Multiscale photoacoustic microscopy and computed tomography, Sep. 2009, Nature Photonics, vol. 3, pp. 503-509.
Wang, Yimin, et al., "Ultrahigh-resolution optical coherence tomography by broadband continuum generation from a photonic crystal fiber", Optics Letters, vol. 28, No. 3, Feb. 1, 2003, pp. 182-184.
Watari, M., H. Migashiyama, N. Mitsui, M. Tomo, Y. Ozaki, "On-line monitoring of the density of linear low-density polyethylene in a real plant by near-infrared spectroscopy and chemometrics," Applied Spectroscopy, vol. 58, No. 2, pp. 248-255 (2004).
Webster, Design of Pulse Oximeters, Medical Science Series (1997), Department of Electrical and Computer Engineering, University of Wisconsin-Madison, Institute of Physics Publishing, Bristol and Philadelphia, 267 pages.
Wedding, B.B., C. Wright, S. Grauf, R.D. White, "The application of near infrared spectroscopy for the assessment of avocado quality attributes," Infrared Spectroscopy—Life and Biomedical Sciences, pp. 211-230 (2011).
Werle, Peter, et al., "Near- and mid-infrared laser-optical sensors for gas analysis", Optics and Lasers in Engineering 37, 2002, pp. 101-114.
Westbrook, Paul S., "Improved Supercontinuum Generation Through UV Processing of Highly Nonlinear Fibers", Journal of Lightwave Technology, vol. 23, No. 1, Jan. 2005, pp. 13-18.
Williams, Phil. "Near-Infrared Spectroscopy of Cereals." Handbook of vibrational spectroscopy (2006).
Wuthrich, Stefan, et al., "Optical damage thresholds at 2.94 um in fluoride glass fibers", Applied Optics, vol. 31, No. 27, Sep. 20, 1992, pp. 5833-5837.
Xiao, J. Q. Tian, Y. Lu, L. Wang, X. Qi, B. Wen, "Extraction of hydrocarbon content information by using hyperspectral image at Liaodong Bay, China," downloaded from world wide web on Apr. 6, 2012.
Xie, T.-Q., et al., "Detection of tumorigenesis in urinary bladder with optical coherence tomography: optical characterization of morphological changes", Optics Express, vol. 10, No. 24, Dec. 2, 2002, 2003, pp. 1431-1443.
Xie, Tuqiang, et al., "Endoscopic optical coherence tomography with a modified microelectromechanical systems mirror for detection of bladder cancers", Applied Optics, vol. 42, No. 31, Nov. 1, 2003, pp. 6422-6426.
Xu, D., G. Ni, T. Jiang, L. Jiang, M. Chi, "Integration of field work and hyperspectral data for oil and gas exploration," IEEE Jan. 4244-1212-9/07, pp. 3194-3197 (2007).
Xu, D-Q, G-Q Ni, L-L Jiang, Y-T Shen, T. Li, S-L Ge, X-B Shu, "Exploring for natural gas using reflectance spectra of surface soils," Advances in Space Research, vol. 41, pp. 1800-1817 (2008).
Yamaha, BODiBEAT, Body, Music, in Sync., BF-1 Quick Guide, Player/Heart Rate Monitor: Quick Manual, 120 pages.
Yeh, S-J, C.F. Hanna, O.S. Khalil, "Monitoring blood glucose changes in cutaneous tissue by temperature-modulated localized reflectance measurements," Clinical Chemistry, vol. 49, No. 6, pp. 924-934 (2003).
Zakian, C.I. Pretty, R. Ellwood, "Near-infrared hyperspectral imaging of teeth for dental canes detection," Journal of Biomedical Optics, vol. 16, No. 6, 064047 (2009).
Ziegler, U., A.G. Bittermann, M. Hoechli, "Introduction to Confocal Laser Scanning Microscopy (LEICA)," www.zmb.unizh.ch, May 29, 2013.
Claim Construction Memorandum Opinion and Order. Case No. 2:18-CV-000134-RWS (Jun. 24, 2019).
Claim Construction Memorandum Opinion and Order. Case No. 2:18-CV-000429-RWS (Aug. 14, 2019).
Declaration of Brian W. Anthony, PhD regarding U.S. Pat. No. 10,098,546 filed in IPR2020-00029 (Oct. 17, 2019).
Declaration of Brian W. Anthony, PhD regarding U.S. Pat. No. 9,651,533 filed in IPR2019-00913 (Apr. 10, 2019).
Declaration of Brian W. Anthony, PhD regarding U.S. Pat. No. 9,651,533 filed in IPR2019-00916 (Apr. 10, 2019).
Declaration of Brian W. Anthony, PhD regarding U.S. Pat. No. 9,757,040 filed in IPR2019-00910 (Apr. 10, 2019).
Declaration of Brian W. Anthony, PhD regarding U.S. Pat. No. 9,757,040 filed in IPR2019-00917 (Apr. 10, 2019).
Declaration of Brian W. Anthony, PhD regarding U.S. Pat. No. 9,861,286 filed in IPR2019-00911 (Apr. 10, 2019).
Declaration of Brian W. Anthony, PhD regarding U.S. Pat. No. 9,861,286 filed in IPR2019-00914 (Apr. 10, 2019).
Declaration of Brian W. Anthony, PhD regarding U.S. Pat. No. 9,885,698 filed in IPR2019-00912 (Apr. 10, 2019).
Declaration of Brian W. Anthony, PhD regarding U.S. Pat. No. 9,885,698 filed in IPR2019-00915 (Apr. 10, 2019).
File History for U.S. Pat. No. 10,098,546, issued Oct. 16, 2018.
Inter Partes Review No. IPR2020-00029; Petition for Inter Partes Review of U.S. Pat. No. 10,098,546; *Apple Inc.* v. *Omni Medsci, Inc.*; dated Oct. 17, 2019.
Lister et al., Optical properties of human skin (Journal of Biomedical Optics 2012).
Mark Nelson & Jean-Loup Gailly, The Data Compression Book (Cary Sullivan et al. eds.) (2nd ed. 1996).
Newton, H., Newton's Telecom Dictionary (18th ed. 2002).
Order, *Omni MedSci, Inc.* v. *Apple Inc.*, No. 2:18-cv-134-RWS in the United States District Court for the Eastern District of Texas Marshall Division (Aug. 16, 2019), ECF No. 283.
Proof of Service of Summons in *Omni MedSci*, Inc. v. *Apple Inc.*, No. 2:18-cv-429 (E.D. Tex.).

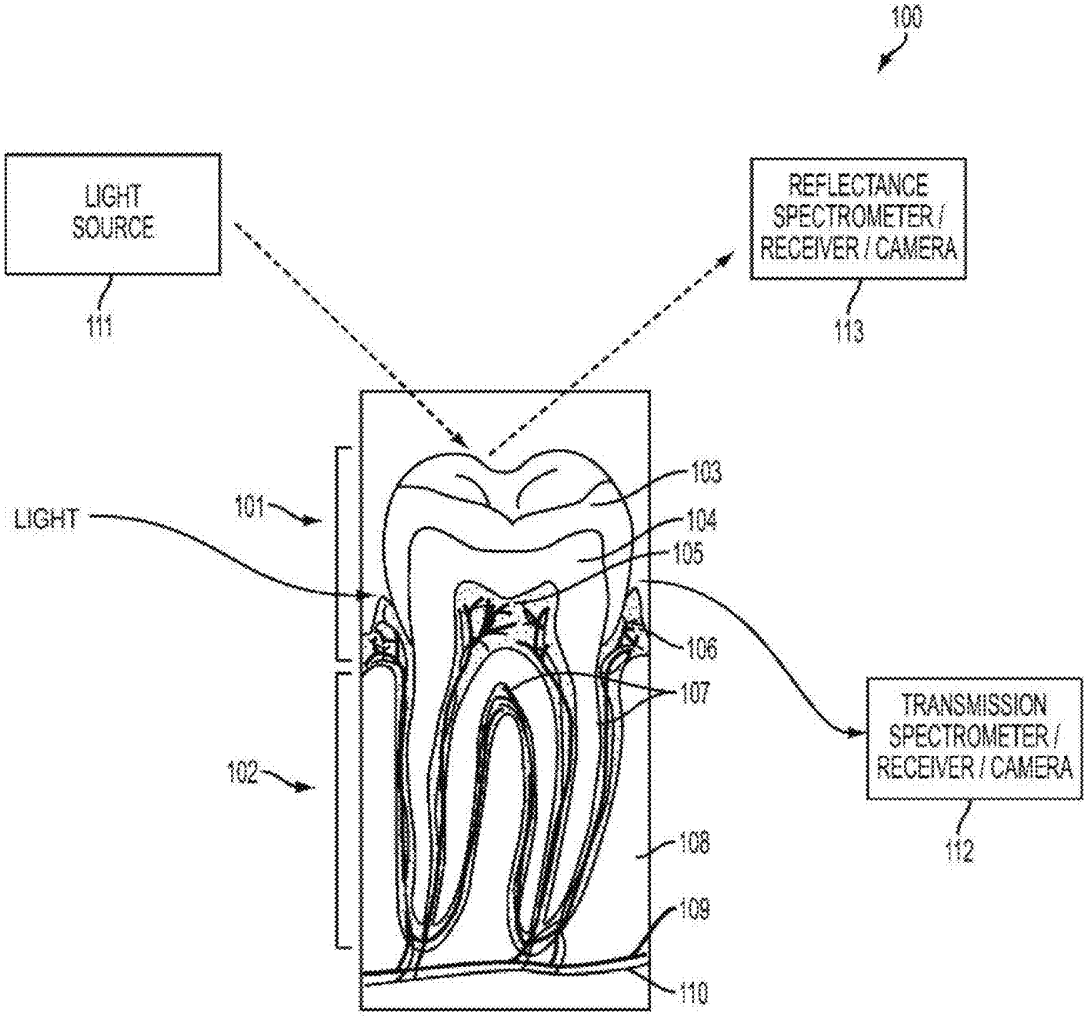
100
LIGHT SOURCE
111
REFLECTANCE SPECTROMETER / RECEIVER / CAMERA
113
LIGHT
101
102
103
104
105
106
107
108
109
110
TRANSMISSION SPECTROMETER / RECEIVER / CAMERA
112

FIG. 1

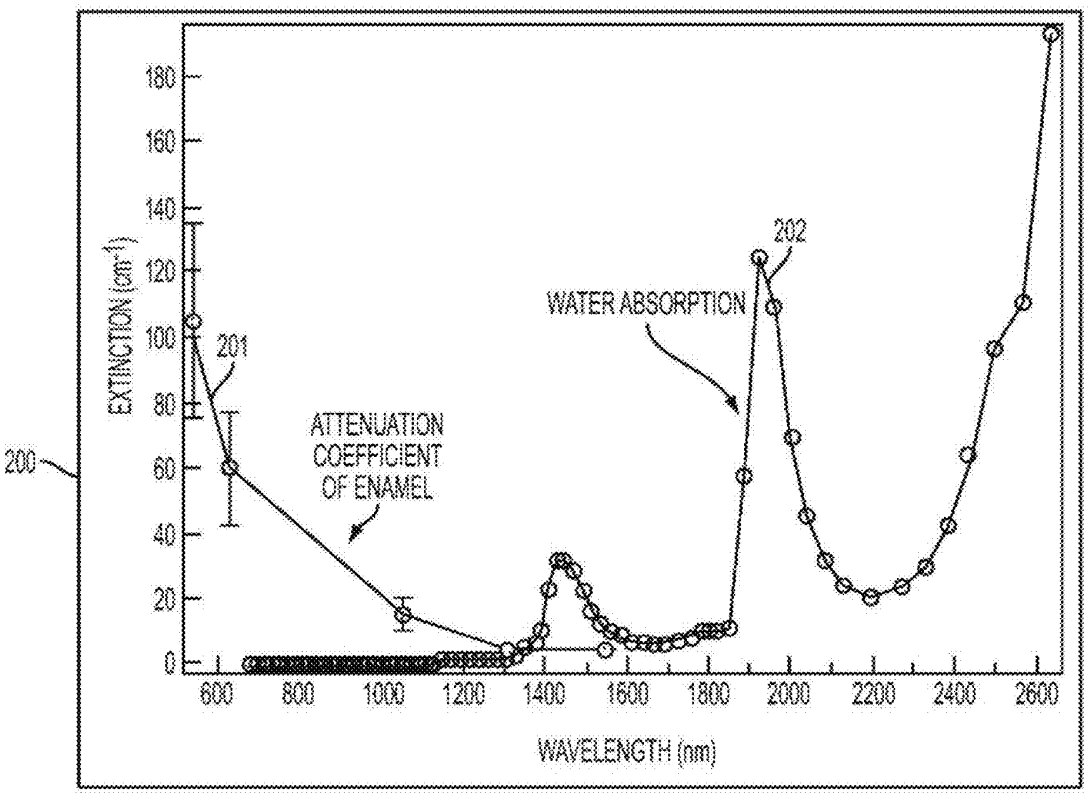
200
EXTINCTION (cm-1)
180
160
140
120
100
80
60
40
20
0
201
202
WATER ABSORPTION
ATTENUATION
COEFFICIENT
OF ENAMEL
600
800
1000
1200
1400
1600
1800
2000
2200
2400
2600
WAVELENGTH (nm)

FIG. 2A

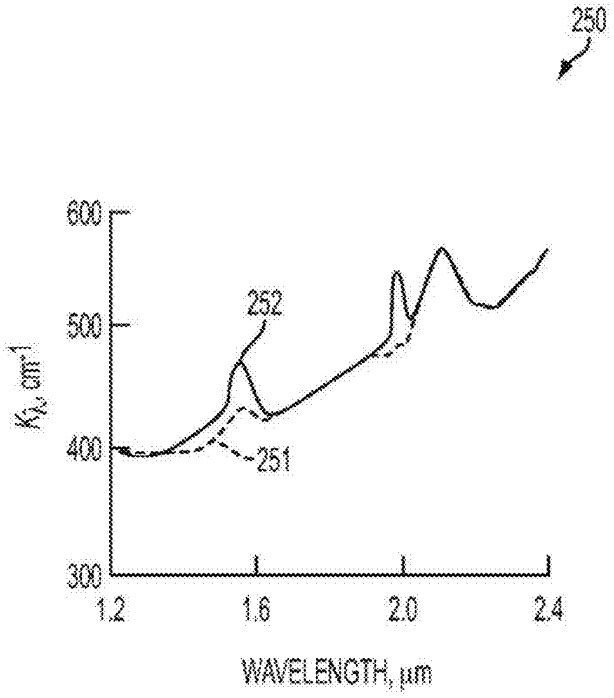
250
600
500
400
300
K_λ, cm^{-1}
252
251
1.2
1.6
2.0
2.4
WAVELENGTH, μm

FIG. 2B

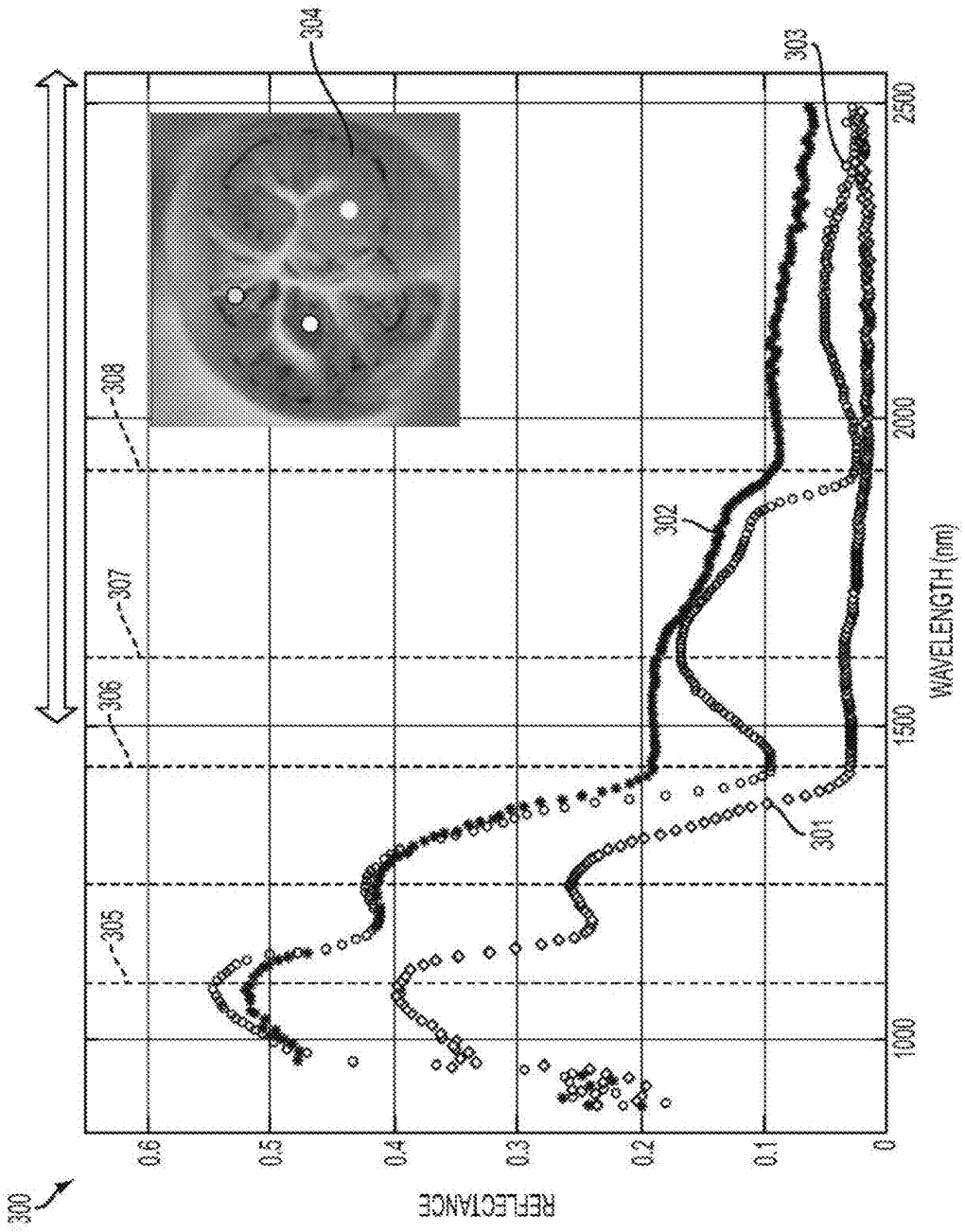
300
REFLECTANCE
0.6
0.5
0.4
0.3
0.2
0.1
0
1000
1500
2000
2500
WAVELENGTH (nm)
301
302
303
304
305
306
307
308

FIG. 3

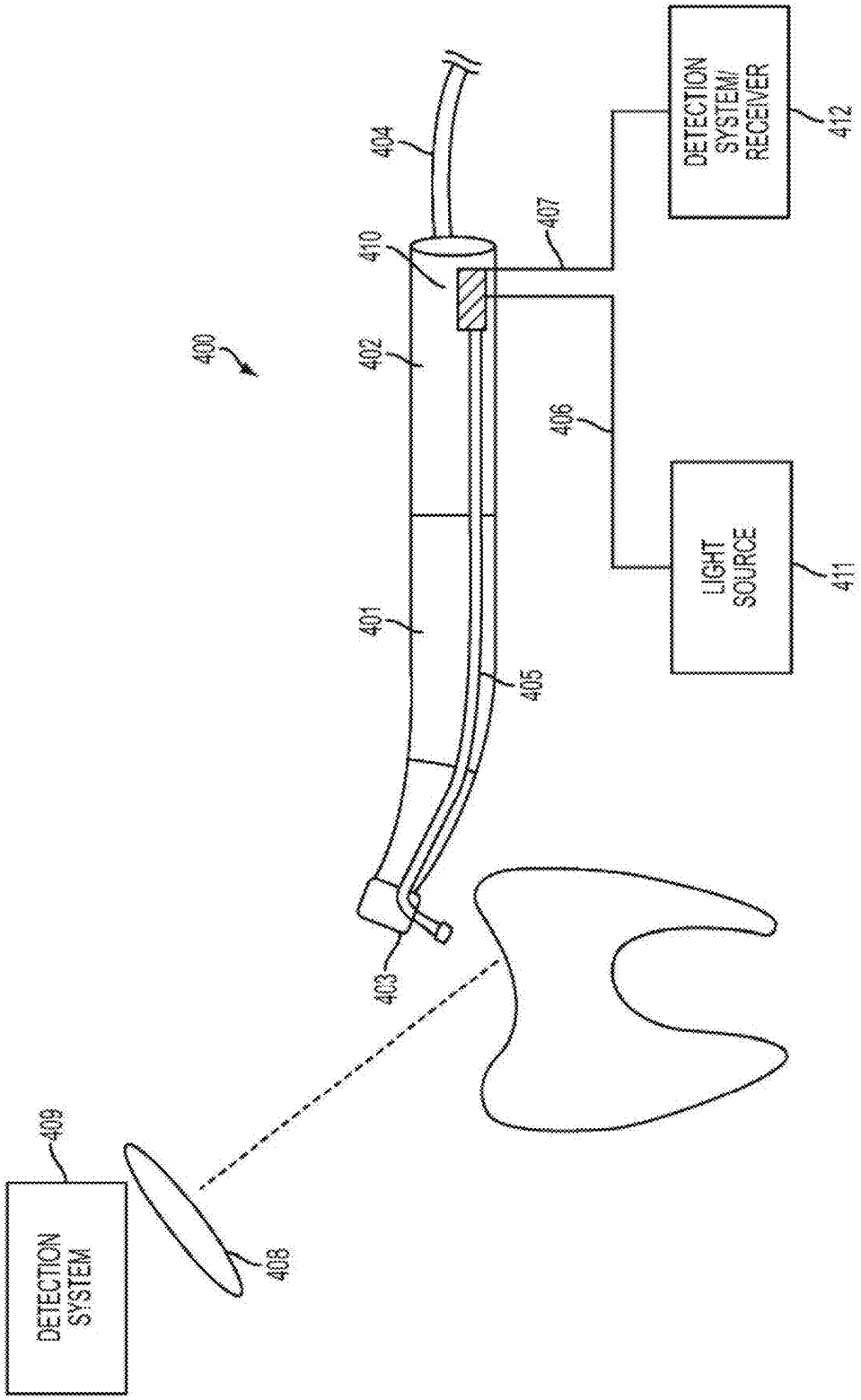
400
401
402
403
404
405
406
407
408
409
410
411
412
DETECTION SYSTEM
LIGHT SOURCE
DETECTION SYSTEM/ RECEIVER

FIG. 4

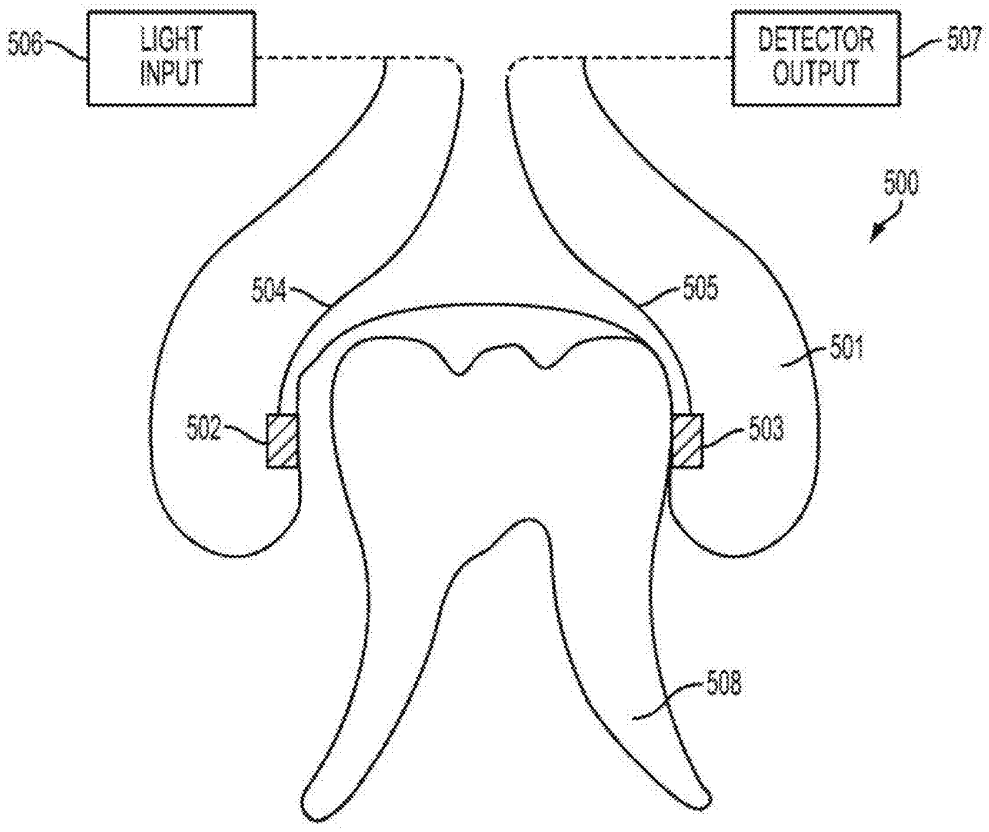
506
LIGHT INPUT
DETECTOR OUTPUT
507
500
504
505
501
502
503
508

FIG. 5A

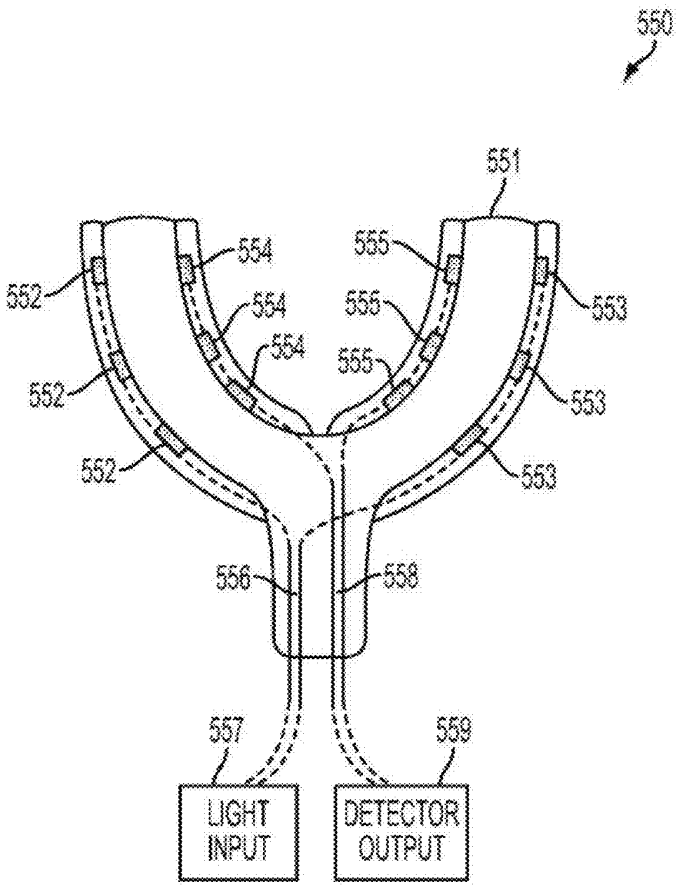
550
551
552
552
552
553
553
553
554
554
554
555
555
555
556
558
557
559
LIGHT INPUT
DETECTOR OUTPUT

FIG. 5B

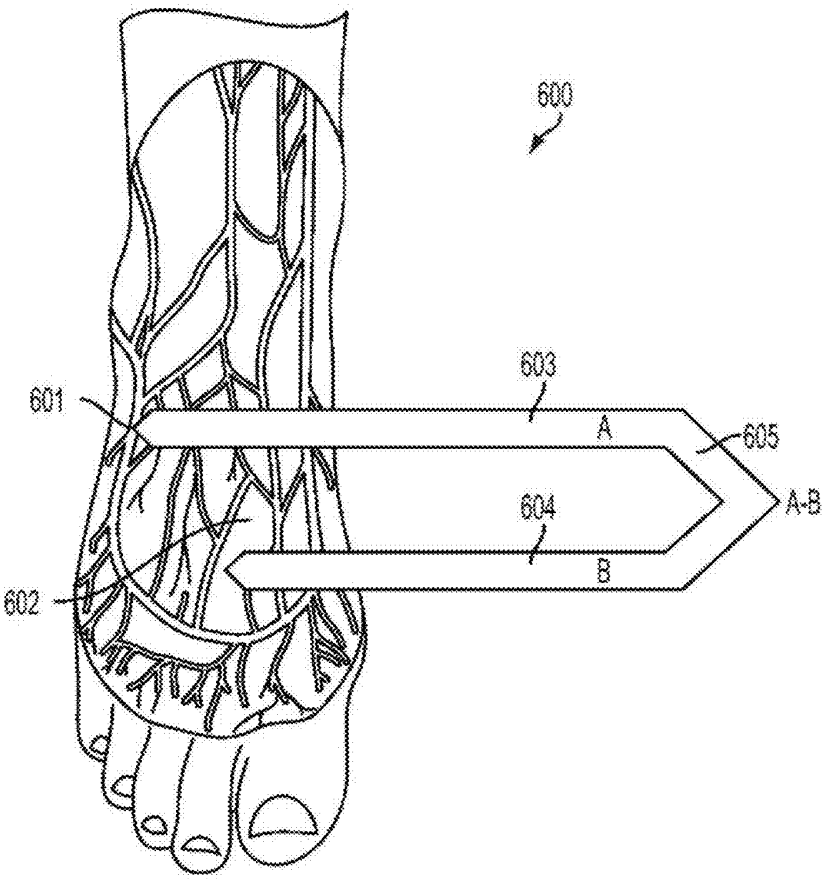

FIG. 6A

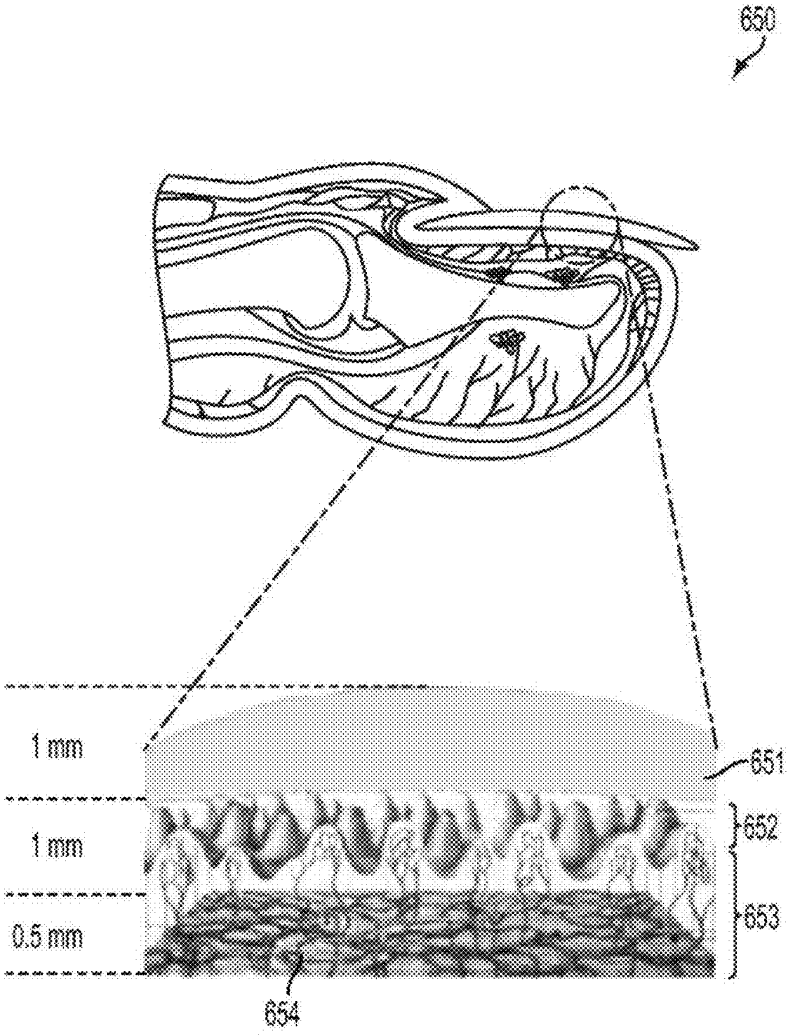

FIG. 6B

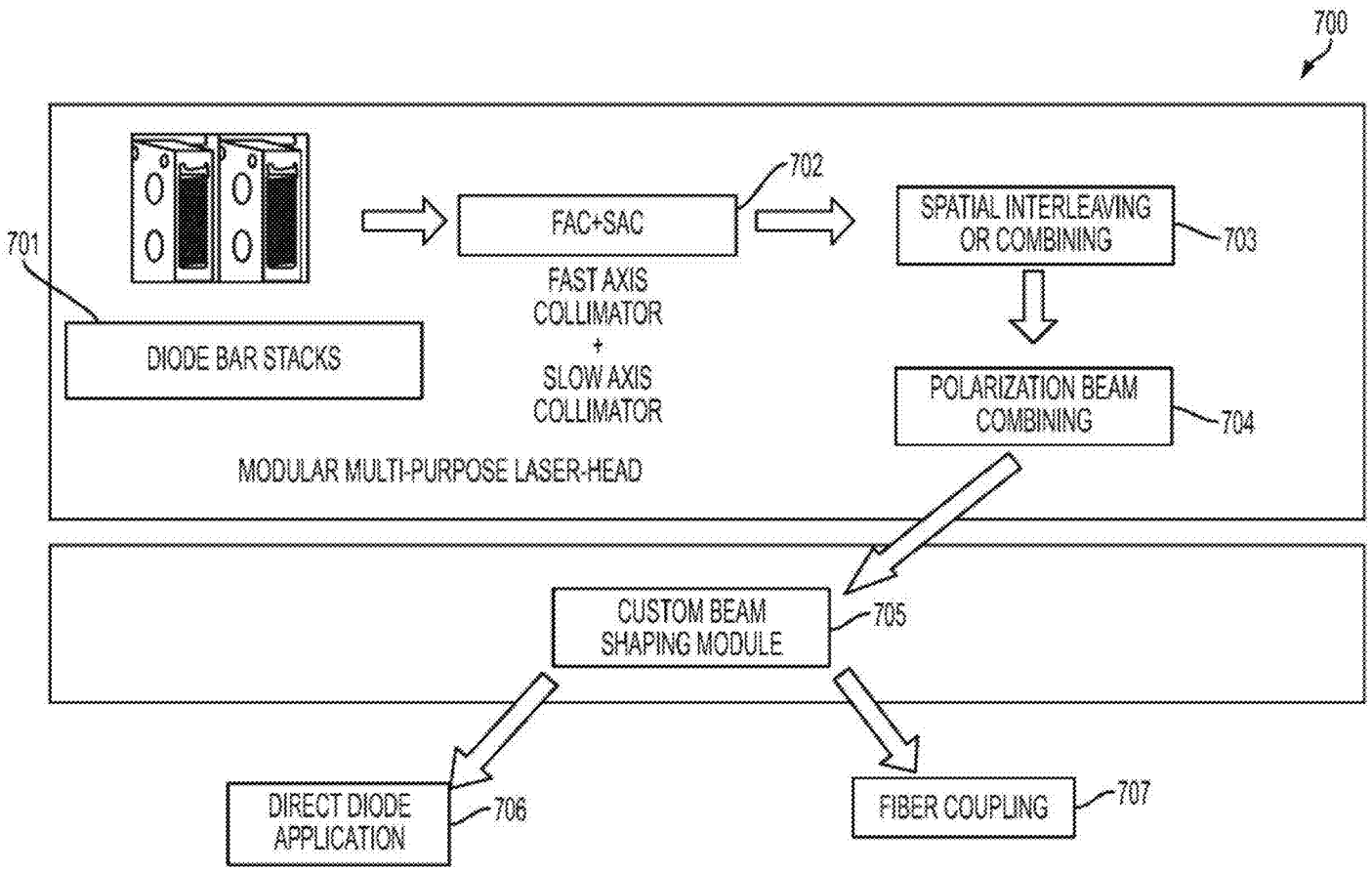
700
701
DIODE BAR STACKS
FAC+SAC
702
FAST AXIS
COLLIMATOR
+
SLOW AXIS
COLLIMATOR
SPATIAL INTERLEAVING
OR COMBINING
703
POLARIZATION BEAM
COMBINING
704
MODULAR MULTI-PURPOSE LASER-HEAD
CUSTOM BEAM
SHAPING MODULE
705
DIRECT DIODE
APPLICATION
706
FIBER COUPLING
707

FIG. 7

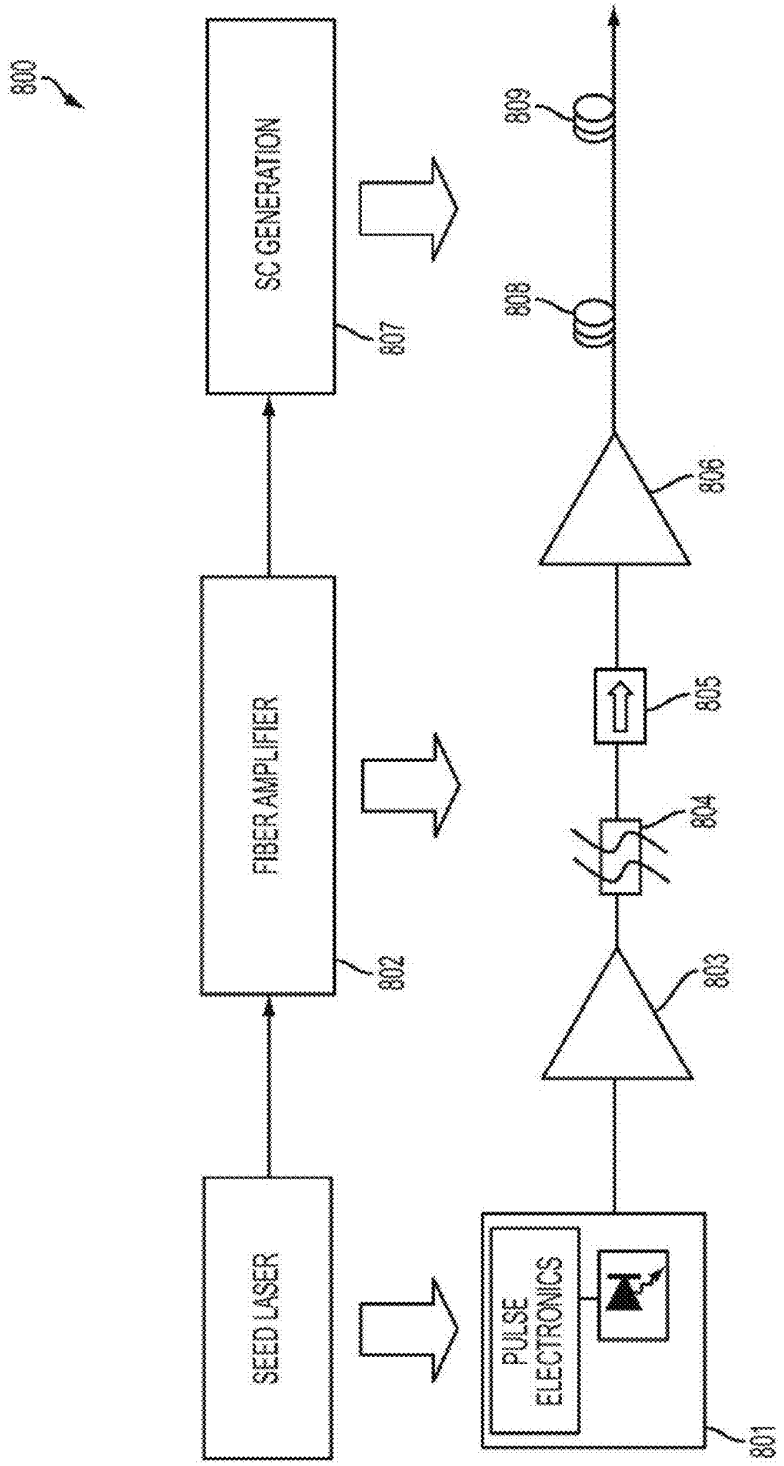
800
SEED LASER
FIBER AMPLIFIER
SC GENERATION
PULSE ELECTRONICS
801
802
803
804
805
806
807
808
809

FIG. 8

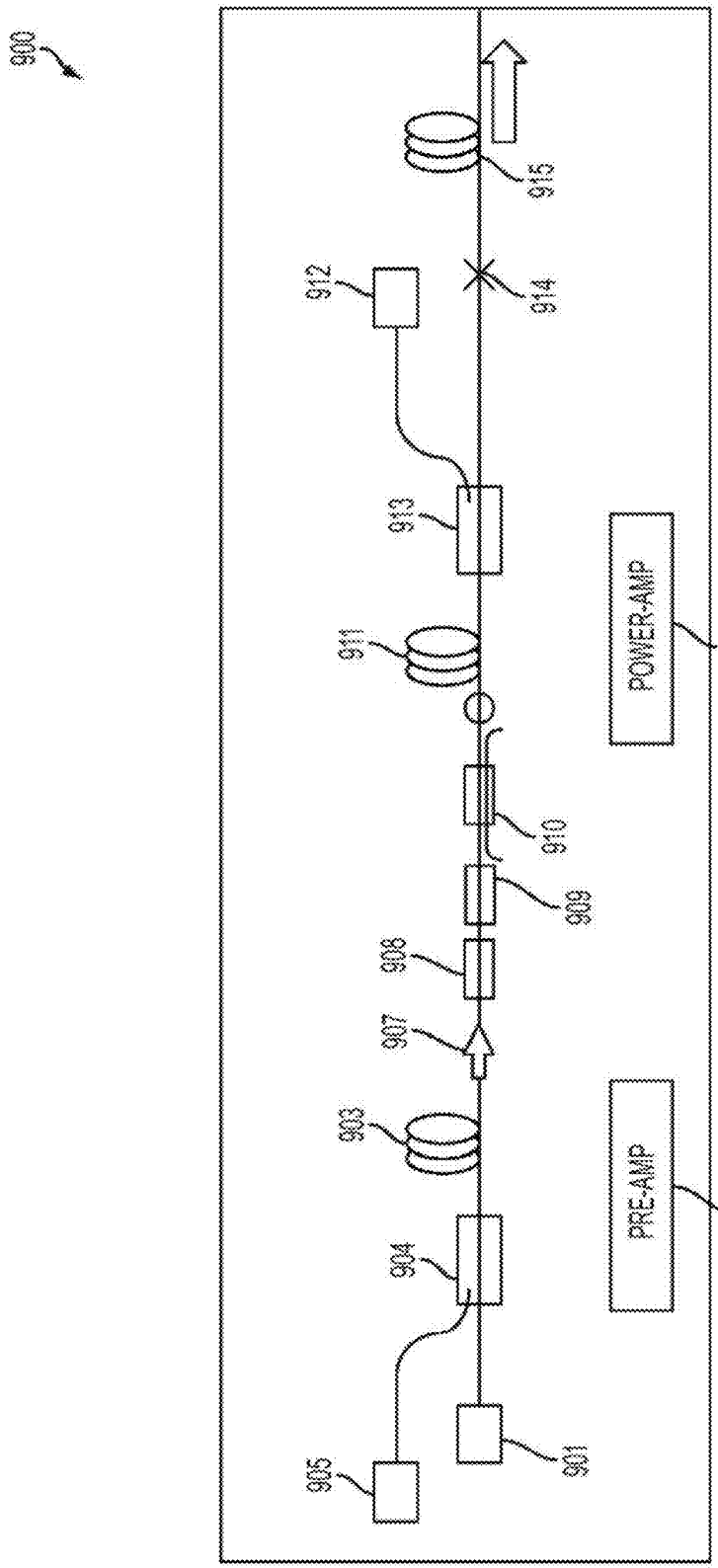
900
905
904
903
907
908
909
910
911
912
913
914
915
901
PRE-AMP
902
POWER-AMP
906

FIG. 9

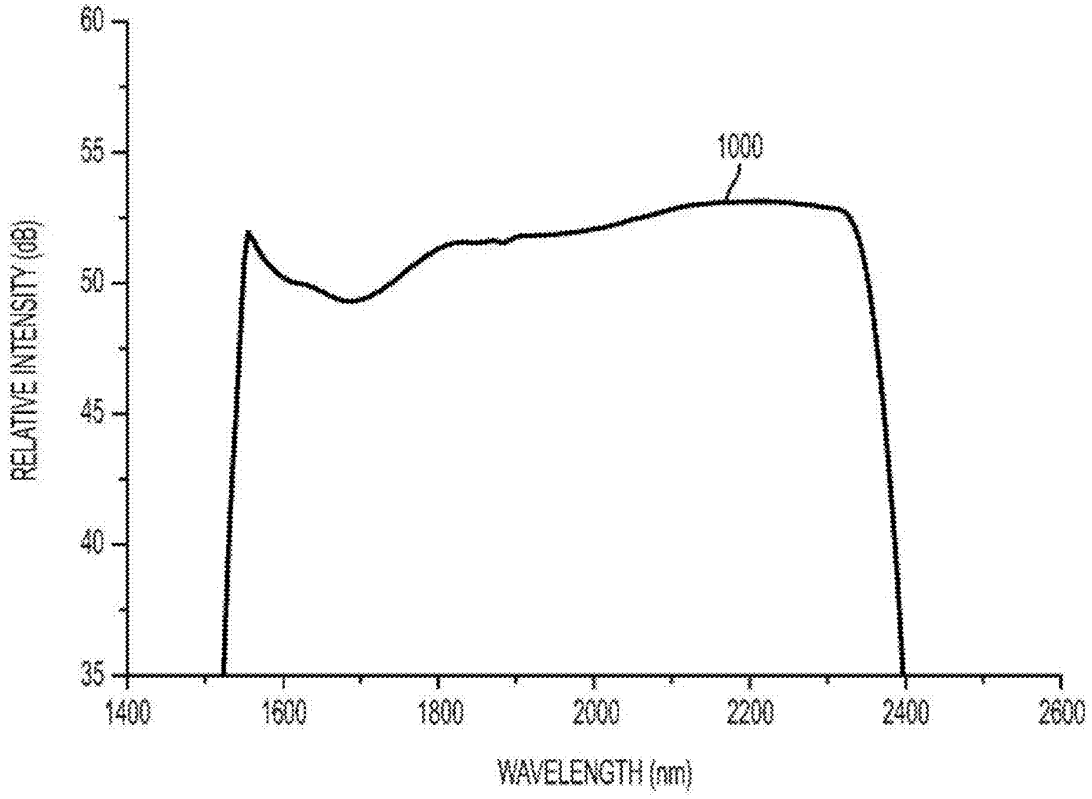
60
55
50
45
40
35
RELATIVE INTENSITY (dB)
1000
1400
1600
1800
2000
2200
2400
2600
WAVELENGTH (nm)

FIG. 10

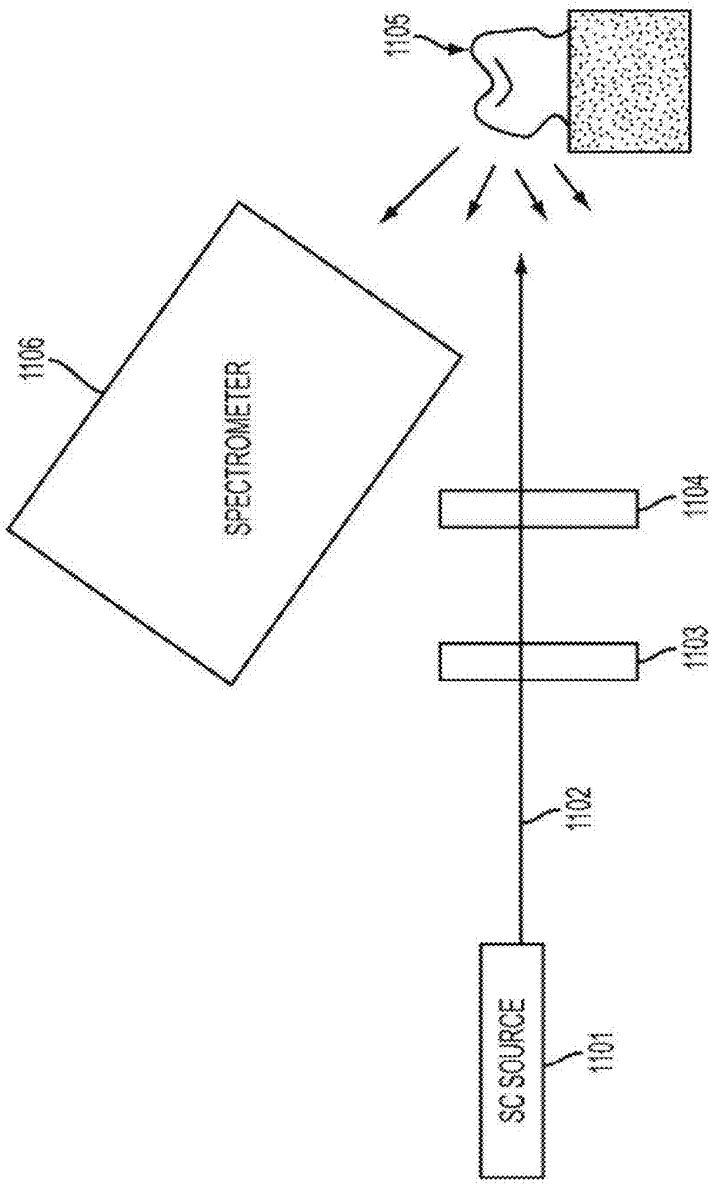

FIG. 11A

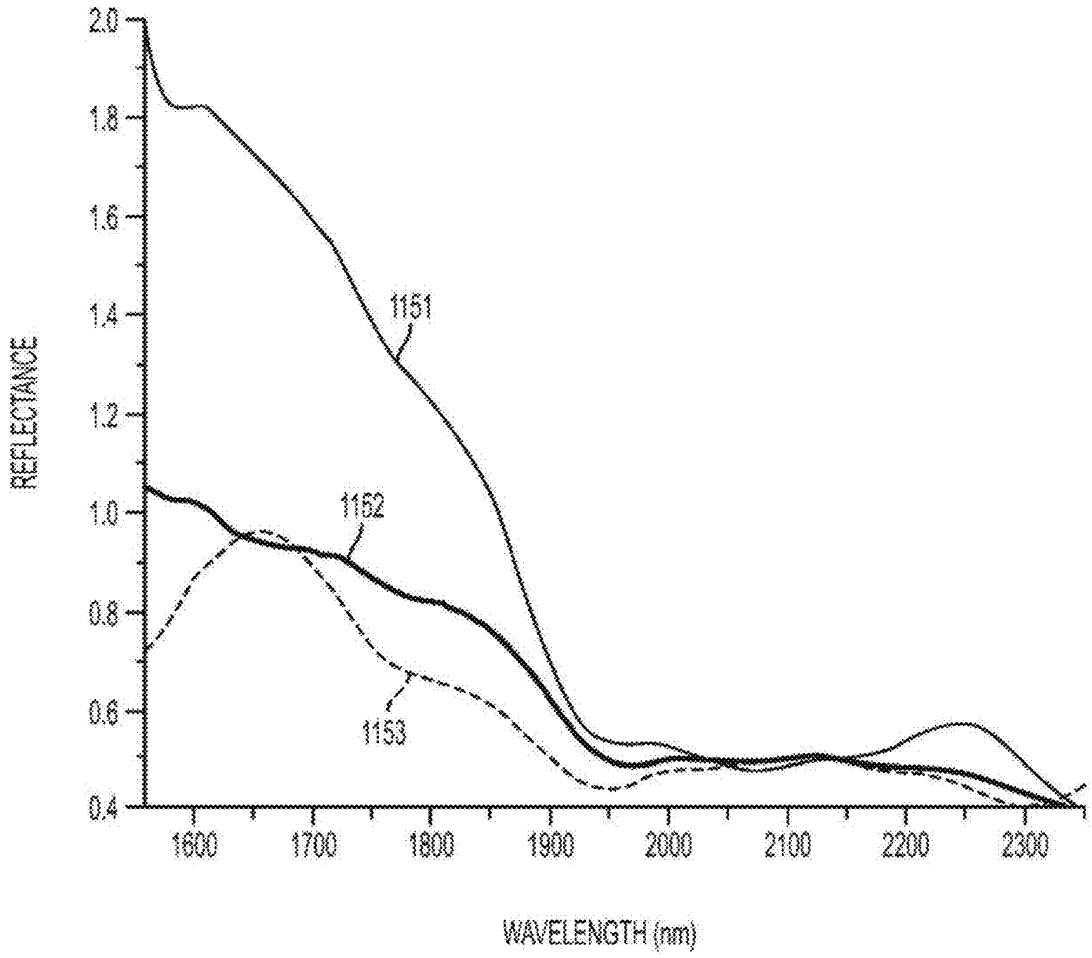
2.0
1.8
1.6
1.4
1.2
1.0
0.8
0.6
0.4
REFLECTANCE
1151
1152
1153
1600
1700
1800
1900
2000
2100
2200
2300
WAVELENGTH (nm)

FIG. 11B

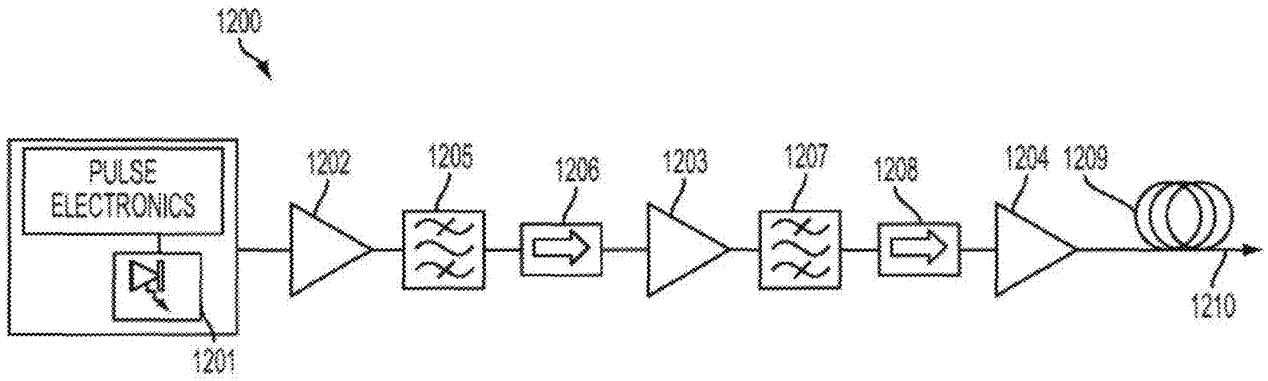

FIG. 12A

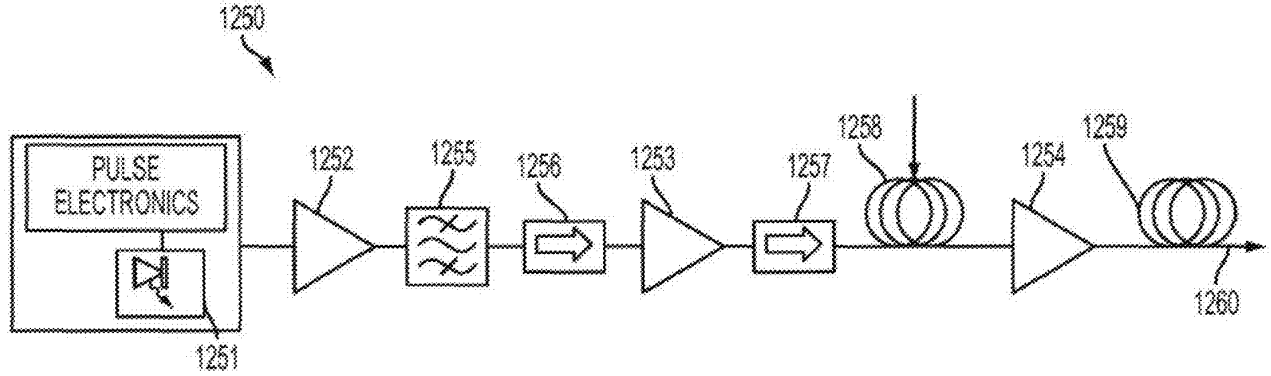

FIG. 12B

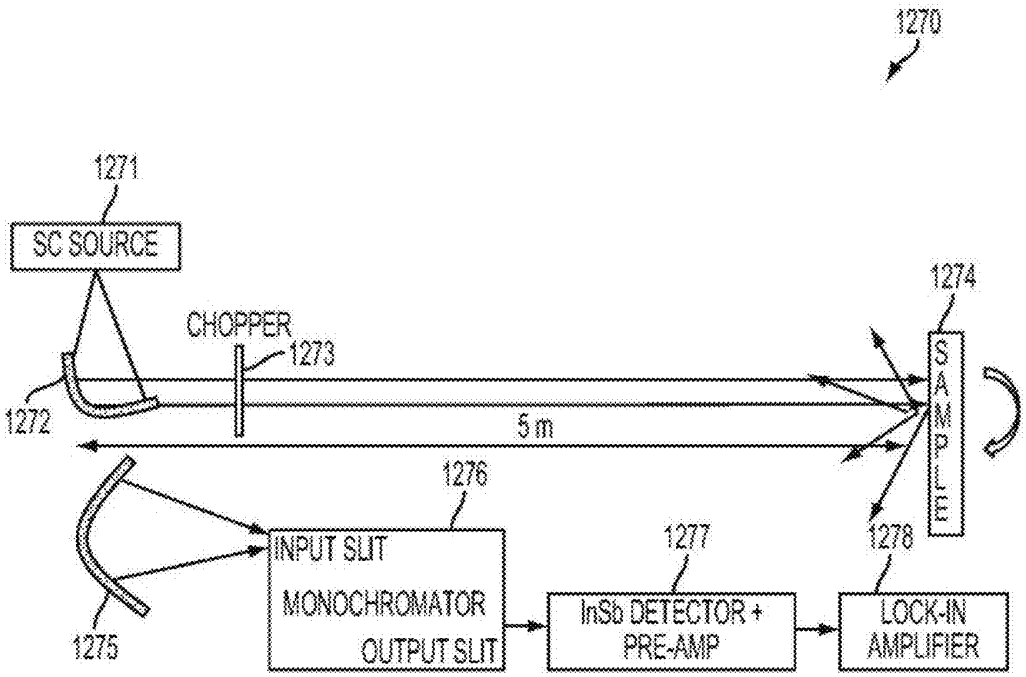
1270
1271
SC SOURCE
CHOPPER
1273
1272
5 m
1274
SAMPLE
1276
INPUT SLIT
MONOCHROMATOR
OUTPUT SLIT
1277
InSb DETECTOR +
PRE-AMP
1278
LOCK-IN
AMPLIFIER
1275

FIG. 12C

IPR2025-01254 Page 31

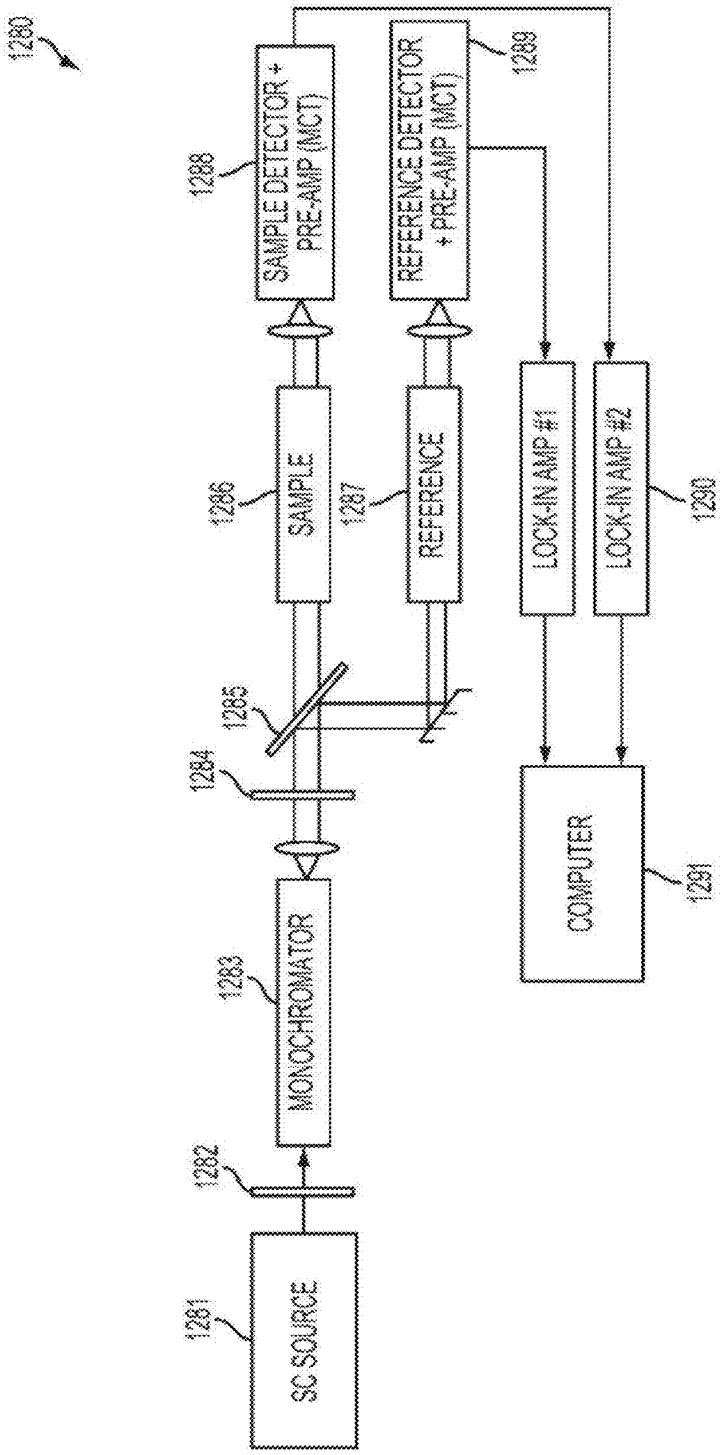

FIG. 12D

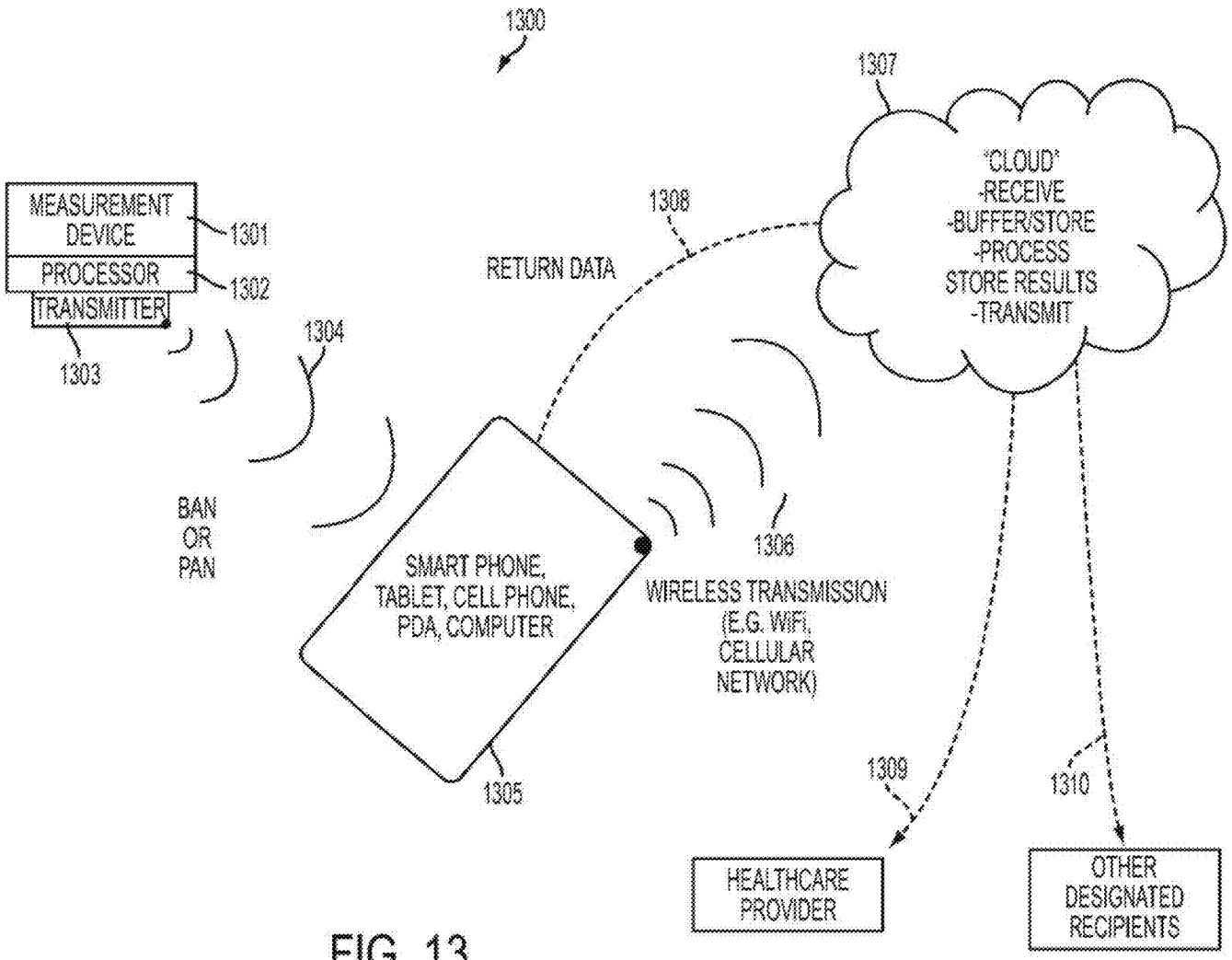
1300
MEASUREMENT DEVICE
1301
PROCESSOR
1302
TRANSMITTER
1303
1304
BAN OR PAN
RETURN DATA
1308
1307
"CLOUD"
-RECEIVE
-BUFFER/STORE
-PROCESS
STORE RESULTS
-TRANSMIT
SMART PHONE, TABLET, CELL PHONE, PDA, COMPUTER
1305
1306
WIRELESS TRANSMISSION (E.G. WIFI, CELLULAR NETWORK)
1309
1310
HEALTHCARE PROVIDER
OTHER DESIGNATED RECIPIENTS

FIG. 13

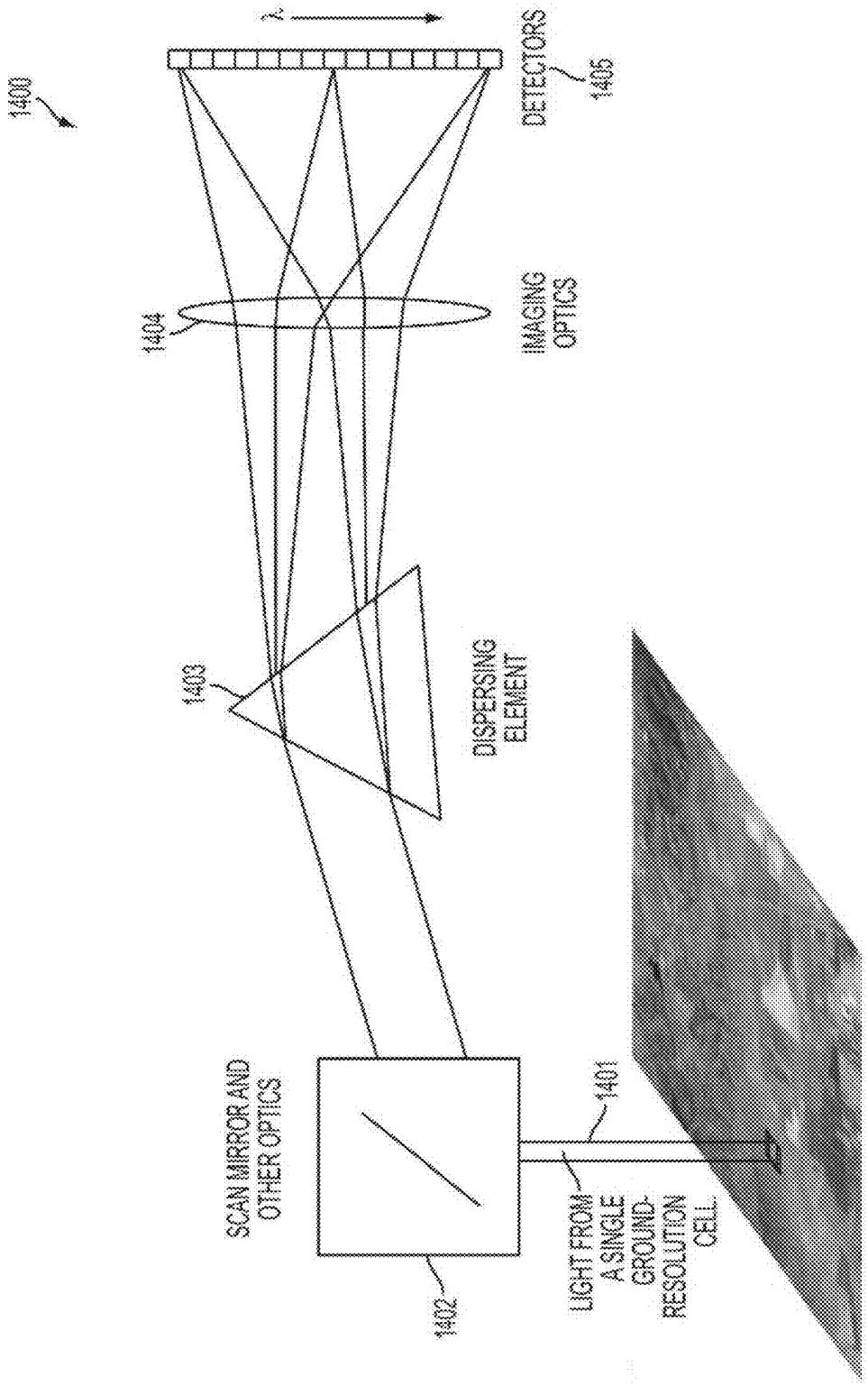
1400
λ
DETECTORS
1405
1404
IMAGING OPTICS
1403
DISPERSING ELEMENT
SCAN MIRROR AND OTHER OPTICS
1402
1401
LIGHT FROM A SINGLE GROUND-RESOLUTION CELL

FIG. 14A

IPR2025-01254 Page 34

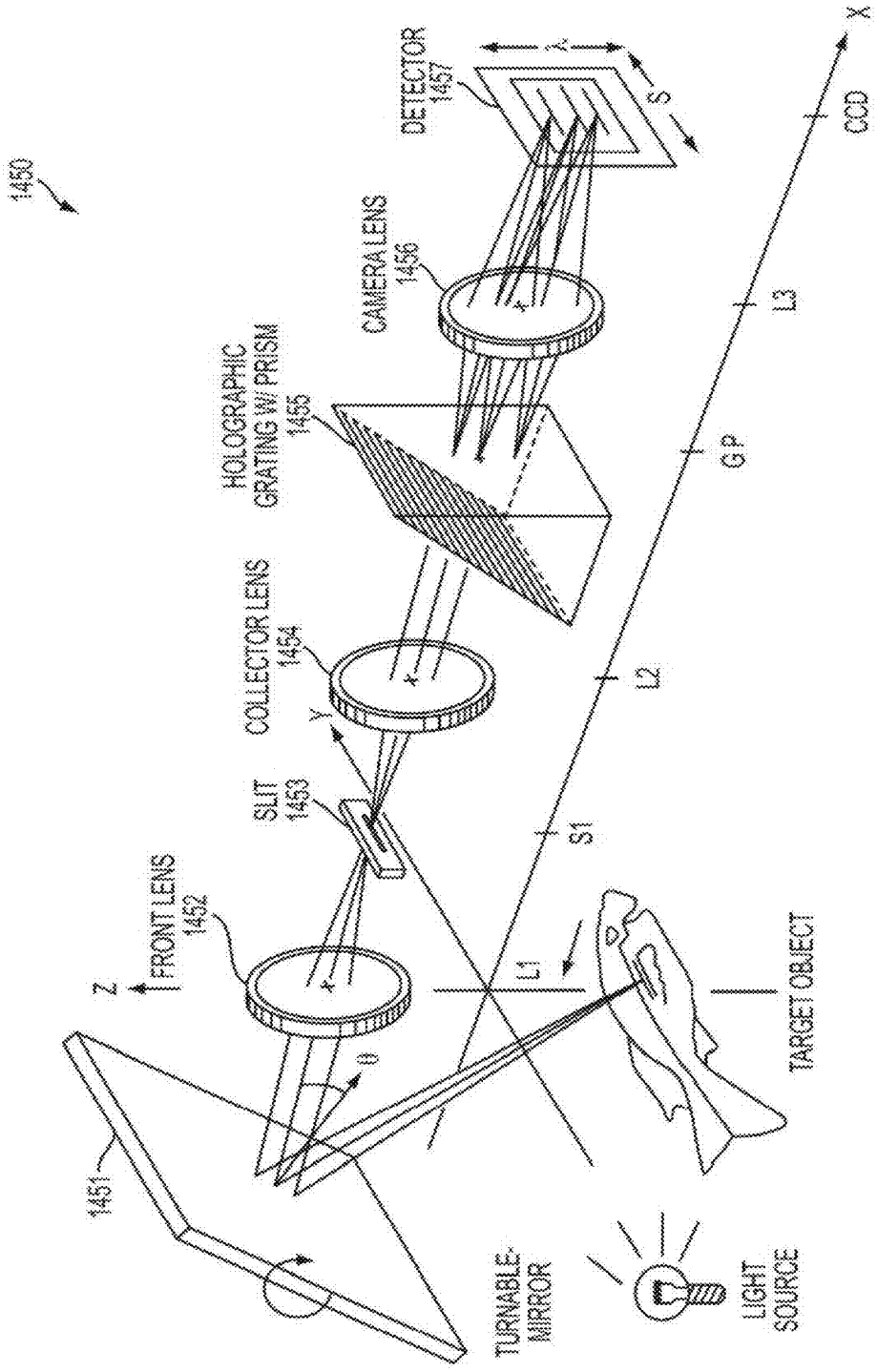

FIG. 14B

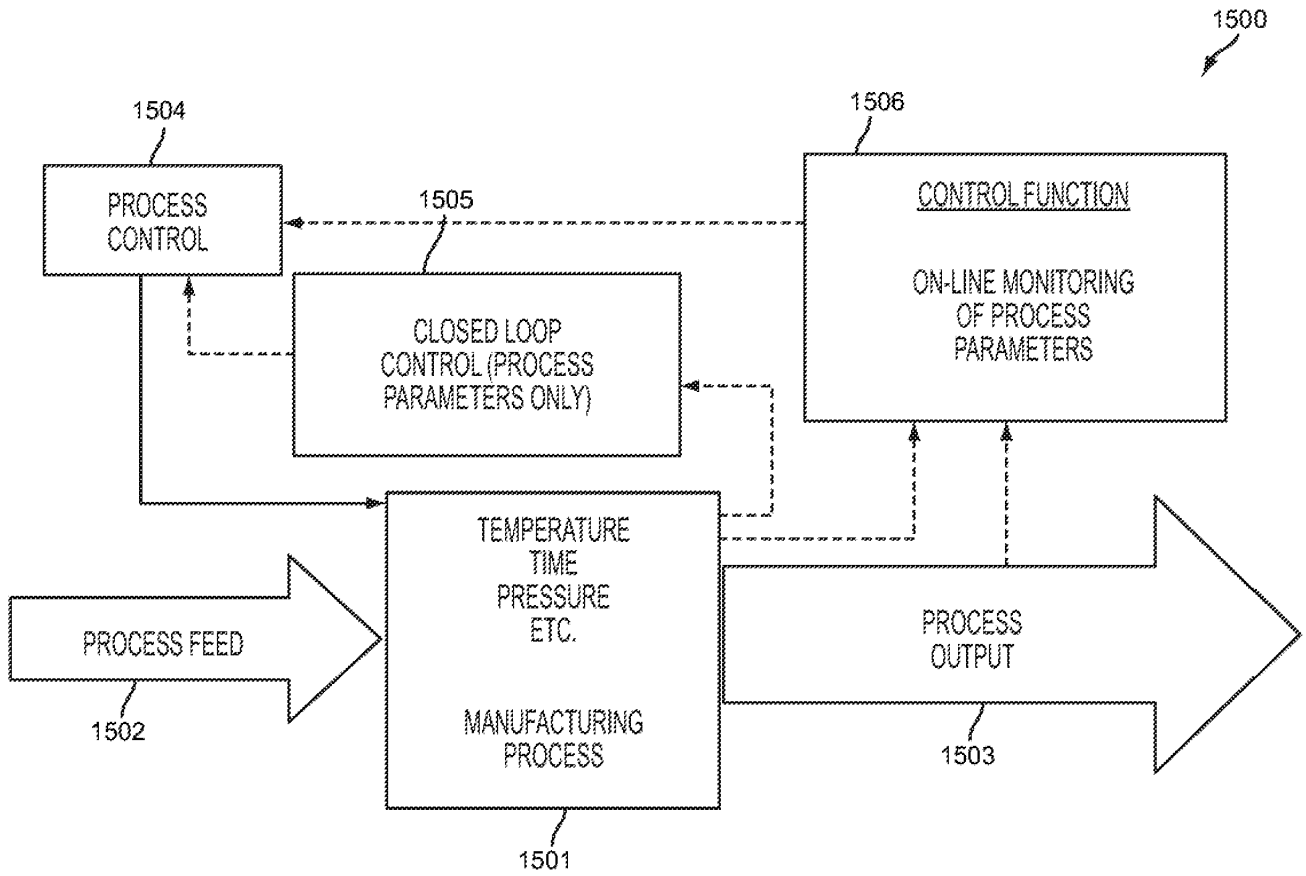
1500
1504
PROCESS CONTROL
1505
CLOSED LOOP CONTROL (PROCESS PARAMETERS ONLY)
1506
CONTROL FUNCTION
ON-LINE MONITORING OF PROCESS PARAMETERS
TEMPERATURE
TIME
PRESSURE
ETC.
MANUFACTURING PROCESS
1501
PROCESS FEED
1502
PROCESS OUTPUT
1503

FIG. 15

SEMICONDUCTOR SOURCE BASED NEAR INFRARED MEASUREMENT DEVICE WITH IMPROVED SIGNAL-TO-NOISE RATIO

CROSS-REFERENCE TO RELATED APPLICATIONS

This application is a Continuation of U.S. application Ser. No. 16/284,514 filed Feb. 25, 2019, which is a Continuation of U.S. application Ser. No. 16/016,649 filed Jun. 24, 2018 (now U.S. Pat. No. 10,213,113), which is a Continuation of U.S. application Ser. No. 15/860,065 filed Jan. 2, 2018 (now U.S. Pat. No. 10,098,546), which is a Continuation of U.S. application Ser. No. 15/686,198 filed Aug. 25, 2017 (now U.S. Pat. No. 9,861,286), which is a Continuation of U.S. application Ser. No. 15/357,136 filed Nov. 21, 2016 (now U.S. Pat. No. 9,757,040), which is a Continuation of U.S. application Ser. No. 14/651,367 filed Jun. 11, 2015 (now U.S. Pat. No. 9,500,635), which is the U.S. national phase of PCT Application No. PCT/US2013/075736 filed Dec. 17, 2013, which claims the benefit of U.S. provisional application Ser. No. 61/747,477 filed Dec. 31, 2012 and U.S. provisional application Ser. No. 61/754,698 filed Jan. 21, 2013, the disclosures of which are hereby incorporated by reference in their entirety.

This application is also a continuation of U.S. application Ser. No. 16/506,885 filed Jul. 9, 2019, which is a continuation of U.S. application Ser. No. 16/272,069 filed Feb. 11, 2019, which is a continuation of U.S. application Ser. No. 16/029,611 filed Jul. 8, 2018 (now U.S. Pat. No. 10,201, 283), which is a continuation of U.S. application Ser. No. 15/888,052 filed Feb. 4, 2018 (now U.S. Pat. No. 10,136, 819), which is a continuation of U.S. application Ser. No. 15/212,549 filed Jul. 18, 2016 (now U.S. Pat. No. 9,885, 698), which is a continuation of U.S. application Ser. No. 14/650,897 filed Jun. 10, 2015 (now U.S. Pat. No. 9,494, 567), which is a U.S. National Phase of PCT/US2013/075700 filed Dec. 17, 2013, which claims the benefit of U.S. provisional application Ser. No. 61/747,472 filed Dec. 31, 2012, the disclosures of all of which are hereby incorporated in their entirety by reference herein.

U.S. application Ser. No. 16/506,885 is also a continuation of U.S. application Ser. No. 16/004,359 filed Jun. 9, 2018, which is a continuation of U.S. application Ser. No. 14/109,007 filed Dec. 17, 2013 (now U.S. Pat. No. 9,993, 159), which claims the benefit of U.S. provisional application Ser. No. 61/747,553 filed Dec. 31, 2012, the disclosures of all of which are hereby incorporated in their entirety by reference herein.

U.S. application Ser. No. 16/506,885 is also a continuation of U.S. application Ser. No. 16/188,194 filed Nov. 12, 2018 (now U.S. Pat. No. 10,386,230), which is a continuation of U.S. application Ser. No. 16/004,154 filed Jun. 8, 2018 (now U.S. Pat. No. 10,126,283), which is a continuation of U.S. application Ser. No. 15/855,201 filed Dec. 27, 2017 (now U.S. Pat. No. 9,995,722), which is a continuation of U.S. application Ser. No. 15/711,907 filed Sep. 21, 2017 (now U.S. Pat. No. 9,897,584), which is a divisional of U.S. application Ser. No. 15/357,225 filed Nov. 21, 2016 (now U.S. Pat. No. 9,797,876), which is a continuation of U.S. application Ser. No. 14/650,981 filed Jun. 10, 2015 (now U.S. Pat. No. 9,500,634), which is the U.S. national phase of PCT Application No. PCT/US2013/075767 filed Dec. 17, 2013, which claims the benefit of U.S. provisional application Ser. No. 61/747,485 filed Dec. 31, 2012, the disclosures of all of which are hereby incorporated by reference in their entirety.

U.S. application Ser. No. 16/506,885 is also a continuation of U.S. application Ser. No. 16/241,628 filed Jan. 7, 2019 (now U.S. Pat. No. 10,441,176), which is a continuation of U.S. Ser. No. 16/015,737 filed Jun. 22, 2018 (now U.S. Pat. No. 10,172,523), which is a continuation of U.S. Ser. No. 15/594,053 filed May 12, 2017 (now U.S. Pat. No. 10,188,299), which is a continuation of U.S. application Ser. No. 14/875,709 filed Oct. 6, 2015 (now U.S. Pat. No. 9,651,533), which is a continuation of U.S. application Ser. No. 14/108,986 filed Dec. 17, 2013 (now U.S. Pat. No. 9,164,032), which claims the benefit of U.S. provisional application Ser. No. 61/747,487 filed Dec. 31, 2012, the disclosures of all of which are hereby incorporated in their entirety by reference herein.

U.S. application Ser. No. 16/506,885 is also a continuation of U.S. application Ser. No. 16/284,514 filed Feb. 25, 2019, which is a continuation of U.S. application Ser. No. 16/016,649 filed Jun. 24, 2018 (now U.S. Pat. No. 10,213, 113), which is a continuation of U.S. application Ser. No. 15/860,065 filed Jan. 2, 2018 (now U.S. Pat. No. 10,098, 546), which is a Continuation of U.S. application Ser. No. 15/686,198 filed Aug. 25, 2017 (now U.S. Pat. No. 9,861, 286), which is a continuation of U.S. application Ser. No. 15/357,136 filed Nov. 21, 2016 (now U.S. Pat. No. 9,757, 040), which is a continuation of U.S. application Ser. No. 14/651,367 filed Jun. 11, 2015 (now U.S. Pat. No. 9,500, 635), which is the U.S. national phase of PCT Application No. PCT/US2013/075736 filed Dec. 17, 2013, which claims the benefit of U.S. provisional application Ser. No. 61/747, 477 filed Dec. 31, 2012 and U.S. provisional application Ser. No. 61/754,698 filed Jan. 21, 2013, the disclosures of all of which are hereby incorporated by reference in their entirety.

This application is related to U.S. provisional application Ser. No. 61/747,472 filed Dec. 31, 2012; Ser. No. 61/747, 481 filed Dec. 31, 2012; Ser. No. 61/747,485 filed Dec. 31, 2012; Ser. No. 61/747,487 filed Dec. 31, 2012; Ser. No. 61/747,492 filed Dec. 31, 2012; and Ser. No. 61/747,553 filed Dec. 31, 2012, the disclosures of which are hereby incorporated by reference in their entirety herein.

This application has a common priority date with commonly owned U.S. application Ser. No. 14/650,897 filed Jun. 10, 2015 (now U.S. Pat. No. 9,494,567), which is the U.S. national phase of International Application PCT/US2013/075700 entitled Near-Infrared Lasers For Non-Invasive Monitoring Of Glucose, Ketones, HBAlC, And Other Blood Constituents; U.S. application Ser. No. 14/108,995 filed Dec. 17, 2013 (published as US 2014/0188092) entitled Focused Near-Infrared Lasers For Non-Invasive Vasectomy And Other Thermal Coagulation Or Occlusion Procedures; U.S. application Ser. No. 14/650,981 filed Jun. 10, 2015 (now U.S. Pat. No. 9,500,634), which is the U.S. national phase of International Application PCT/US2013/075767 entitled Short-Wave Infrared Super-Continuum Lasers For Natural Gas Leak Detection, Exploration, And Other Active Remote Sensing Applications; U.S. application Ser. No. 14/108,986 filed Dec. 17, 2013 (now U.S. Pat. No. 9,164, 032) entitled Short-Wave Infrared Super-Continuum Lasers For Detecting Counterfeit Or Illicit Drugs And Pharmaceutical Process Control; U.S. application Ser. No. 14/108,974 filed Dec. 17, 2013 (Published as US2014/0188094) entitled Non-Invasive Treatment Of Varicose Veins; and U.S. application Ser. No. 14/109,007 filed Dec. 17, 2013 (Published as US2014/0236021) entitled Near-Infrared Super-Continuum Lasers For Early Detection Of Breast And Other Cancers,

the disclosures of all of which are hereby incorporated in their entirety by reference herein.

TECHNICAL FIELD

This disclosure relates to lasers and light sources for healthcare, medical, dental, or bio-technology applications, including systems and methods for using near-infrared or short-wave infrared light sources for early detection of dental caries, often called cavities.

BACKGROUND AND SUMMARY

Dental care and the prevention of dental decay or dental caries has changed in the United States over the past several decades, due to the introduction of fluoride to drinking water, the use of fluoride dentifrices and rinses, application of topical fluoride in the dental office, and improved dental hygiene. Despite these advances, dental decay continues to be the leading cause of tooth loss. With the improvements over the past several decades, the majority of newly discovered carious lesions tend to be localized to the occlusal pits and fissures of the posterior dentition and the proximal contact sites. These early carious lesions may be often obscured in the complex and convoluted topography of the pits and fissures or may be concealed by debris that frequently accumulates in those regions of the posterior teeth. Moreover, such lesions are difficult to detect in the early stages of development.

Dental caries may be a dynamic disease that is characterized by tooth demineralization leading to an increase in the porosity of the enamel surface. Leaving these lesions untreated may potentially lead to cavities reaching the dentine and pulp and perhaps eventually causing tooth loss. Occlusal surfaces (bite surfaces) and approximal surfaces (between the teeth) are among the most susceptible sites of demineralization due to acid attack from bacterial by-products in the biofilm. Therefore, there is a need for detection of lesions at an early stage, so that preventive agents may be used to inhibit or reverse the demineralization.

Traditional methods for caries detection include visual examination and tactile probing with a sharp dental exploration tool, often assisted by radiographic (x-ray) imaging. However, detection using these methods may be somewhat subjective; and, by the time that caries are evident under visual and tactile examination, the disease may have already progressed to an advanced stage. Also, because of the ionizing nature of x-rays, they are dangerous to use (limited use with adults, and even less used with children). Although x-ray methods are suitable for approximal surface lesion detection, they offer reduced utility for screening early caries in occlusal surfaces due to their lack of sensitivity at very early stages of the disease.

Some of the current imaging methods are based on the observation of the changes of the light transport within the tooth, namely absorption, scattering, transmission, reflection and/or fluorescence of light. Porous media may scatter light more than uniform media. Taking advantage of this effect, the Fiber-optic trans-illumination is a qualitative method used to highlight the lesions within teeth by observing the patterns formed when white light, pumped from one side of the tooth, is scattered away and/or absorbed by the lesion. This technique may be difficult to quantify due to an uneven light distribution inside the tooth.

Another method called quantitative light-induced fluorescence—QLF—relies on different fluorescence from solid teeth and caries regions when excited with bright light in the visible. For example, when excited by relatively high intensity blue light, healthy tooth enamel yields a higher intensity of fluorescence than does demineralized enamel that has been damaged by caries infection or any other cause. On the other hand, for excitation by relatively high intensity of red light, the opposite magnitude change occurs, since this is the region of the spectrum for which bacteria and bacterial by-products in carious regions absorb and fluoresce more pronouncedly than do healthy areas. However, the image provided by QLF may be difficult to assess due to relatively poor contrast between healthy and infected areas. Moreover, QLF may have difficulty discriminating between white spots and stains because both produce similar effects. Stains on teeth are commonly observed in the occlusal sites of teeth, and this obscures the detection of caries using visible light.

As described in this disclosure, the near-infrared region of the spectrum offers a novel approach to imaging carious regions because scattering is reduced and absorption by stains is low. For example, it has been demonstrated that the scattering by enamel tissues reduces in the form of $1/(\text{wavelength})^3$, e.g., inversely as the cube of wavelength. By using a broadband light source in the short-wave infrared (SWIR) part of the spectrum, which corresponds approximately to 1400 nm to 2500 nm, lesions in the enamel and dentine may be observed. In one embodiment, intact teeth have low reflection over the SWIR wavelength range. In the presence of caries, the scattering increases, and the scattering is a function of wavelength; hence, the reflected signal decreases with increasing wavelength. Moreover, particularly when caries exist in the dentine region, water build up may occur, and dips in the SWIR spectrum corresponding to the water absorption lines may be observed. The scattering and water absorption as a function of wavelength may thus be used for early detection of caries and for quantifying the degree of demineralization.

SWIR light may be generated by light sources such as lamps, light emitting diodes, one or more laser diodes, super-luminescent laser diodes, and fiber-based super-continuum sources. The SWIR super-continuum light sources advantageously may produce high intensity and power, as well as being a nearly transform-limited beam that may also be modulated. Also, apparatuses for caries detection may include C-clamps over teeth, a handheld device with light input and light detection, which may also be attached to other dental equipment such as drills. Alternatively, a mouth-guard type apparatus may be used to simultaneously illuminate one or more teeth. Fiber optics may be conveniently used to guide the light to the patient as well as to transport the signal back to one or more detectors and receivers.

One approach to non-invasive monitoring of blood constituents or blood analytes is to use near-infrared spectroscopy, such as absorption spectroscopy or near-infrared diffuse reflection or transmission spectroscopy. Some attempts have been made to use broadband light sources, such as tungsten lamps, to perform the spectroscopy. However, several challenges have arisen in these efforts. First, many other constituents in the blood also have signatures in the near-infrared, so spectroscopy and pattern matching, often called spectral fingerprinting, is required to distinguish the glucose with sufficient confidence. Second, the non-invasive procedures have often transmitted or reflected light through the skin, but skin has many spectral artifacts in the near-infrared that may mask the glucose signatures. Moreover, the skin may have significant water and blood content. These difficulties become particularly complicated when a weak

light source is used, such as a lamp. More light intensity can help to increase the signal levels, and, hence, the signal-to-noise ratio.

In one embodiment, a wearable device includes a measurement device including a light source comprising a plurality of light emitting diodes (LEDs) for measuring one or more physiological parameters, the measurement device configured to generate, by modulating at least one of the LEDs having an initial light intensity, an optical beam having a plurality of optical wavelengths, wherein at least a portion of the plurality of optical wavelengths is a near-infrared wavelength between 700 nanometers and 2500 nanometers. The measurement device comprises one or more lenses configured to receive and to deliver a portion of the optical beam to tissue, wherein the tissue reflects at least a portion of the optical beam delivered to the tissue, and wherein the measurement device is adapted to be placed on a wrist or an ear of a user. The measurement device further comprises a receiver, the receiver having a plurality of spatially separated detectors and one or more analog to digital converters coupled to the spatially separated detectors, the one or more analog to digital converters configured to generate at least two receiver outputs. The measurement device is configured to improve a signal-to-noise ratio of the optical beam reflected from the tissue by comparing the at least two receiver outputs. The measurement device is also configured to further improve the signal-to-noise ratio of the optical beam reflected from the tissue by increasing the light intensity relative to the initial light intensity from at least one of the LEDs. The measurement device is further configured to generate an output signal representing at least in part a non-invasive measurement on blood contained within the tissue. The receiver further comprises one or more spectral filters positioned in front of at least some of the plurality of spatially separated detectors, wherein the receiver is configured to be synchronized to the modulation of the at least one of the LED, and wherein the modulating at least one of the LEDs has a modulation frequency, and wherein the receiver is configured to use a lock-in technique that detects the modulation frequency.

In one or more embodiments, a wearable device comprises a measurement device including a light source comprising a plurality of light emitting diodes (LEDs) for measuring one or more physiological parameters, the measurement device configured to generate, by modulating at least one of the LEDs having an initial light intensity, an optical beam having a plurality of optical wavelengths, wherein at least a portion of the plurality of optical wavelengths is a near-infrared wavelength between 700 nanometers and 2500 nanometers. The measurement device comprises one or more lenses configured to receive and to deliver a portion of the optical beam to tissue, wherein the tissue reflects at least a portion of the optical beam delivered to the tissue, and wherein the measurement device is adapted to be placed on a wrist or an ear of a user. The measurement device is configured to generate an output signal representing at least in part a non-invasive measurement on blood contained within the tissue. The measurement device is configured to improve a signal-to-noise ratio of the optical beam reflected from the tissue by increasing the light intensity relative to the initial light intensity from at least one of the LEDs. The measurement device further comprises a receiver having one or more detectors, wherein one of the one or more detectors is located a first distance from a first one of the LEDs and a different distance from a second one of the LEDs such that the receiver can compare light received from the first LED and light received from the second LED, and wherein the output signal is generated in part by comparing signals associated with the light received from the first and second LEDs. The receiver is configured to be synchronized to the modulation of the at least one of the LEDs, wherein the modulating at least one of the LEDs has a modulation frequency, and wherein the receiver is configured to use a lock-in technique that detects the modulation frequency.

In at least one embodiment, a wearable device comprises a measurement device including a light source comprising a plurality of light emitting diodes (LEDs) for measuring one or more physiological parameters, the measurement device configured to generate, by modulating at least one of the LEDs having an initial light intensity, an optical beam having a plurality of optical wavelengths, wherein at least a portion of the plurality of optical wavelengths is a near-infrared wavelength between 700 nanometers and 2500 nanometers. The measurement device comprises one or more lenses configured to receive and to deliver a portion of the optical beam to tissue, wherein the tissue reflects at least a portion of the optical beam delivered to the tissue, and wherein the measurement device is adapted to be placed on a wrist or an ear of a user. The measurement device is further configured to generate an output signal representing at least in part a non-invasive measurement on blood contained within the tissue. The measurement device is configured to improve a signal-to-noise ratio of the optical beam reflected from the tissue by increasing the light intensity relative to the initial light intensity from at least one of the LEDs. The measurement device further comprises a receiver, the receiver having a plurality of spatially separated detectors configured to generate at least two receiver outputs, and the measurement device configured to further improve the signal-to-noise ratio of the optical beam reflected from the tissue by comparing the at least two receiver outputs. One of the plurality of detectors is located a first distance from a first one of the LEDs and a different distance from a second one of the LEDs such that the receiver can generate a third signal responsive to light received from the first LED and a fourth signal responsive to light received from the second LED, and wherein the output signal is generated in part by comparing the third and fourth signals, wherein the receiver is configured to be synchronized to the modulation of the at least one of the LEDs, and wherein the modulating at least one of the LEDs has a modulation frequency, and wherein the receiver is configured to use a lock-in technique that detects the modulation frequency.

In one or more embodiments, a wearable device includes a measurement device having a light source comprising a plurality of light emitting diodes (LEDs) for measuring one or more physiological parameters. The measurement device is configured to generate, by modulating at least one of the LEDs having an initial light intensity, an optical beam having a plurality of optical wavelengths, wherein at least a portion of the optical beam includes a near-infrared wavelength between 700 nanometers and 2500 nanometers. The measurement device comprises one or more lenses configured to receive and to deliver at least a portion of the optical beam to tissue, wherein the tissue reflects at least a portion of the optical beam delivered to the tissue. The measurement device further comprises a receiver having a plurality of spatially separated detectors and one or more analog to digital converters coupled to the spatially separated detectors, the one or more analog to digital converters being configured to generate at least two receiver outputs. The receiver is configured to capture light while the LEDs are off and convert the captured light into a first signal, and to

capture light while at least one of the LEDs is on and to convert the captured light into a second signal, the captured light including at least a portion of the optical beam reflected from the tissue. The measurement device is configured to improve a signal-to-noise ratio of the optical beam reflected from the tissue by differencing the first signal and the second signal and by differencing the two receiver outputs. The measurement device is configured to further improve the signal-to-noise ratio of the optical beam reflected from the tissue by increasing the light intensity relative to the initial light intensity from at least one of the LEDs. The measurement device is further configured to generate an output signal representing at least in part a non-invasive measurement on blood contained within the tissue.

Embodiments may include a wearable device comprising a measurement device including a light source comprising a plurality of light emitting diodes (LEDs) for measuring one or more physiological parameters. The measurement device is configured to generate, by modulating at least one of the LEDs having an initial light intensity, an optical beam having a plurality of optical wavelengths, wherein at least a portion of the plurality of optical wavelengths is a near-infrared wavelength between 700 nanometers and 2500 nanometers. The measurement device comprises one or more lenses configured to receive and to deliver a portion of the optical beam to tissue, wherein the tissue reflects at least a portion of the optical beam delivered to the tissue, and wherein the measurement device is adapted to be placed on a wrist or an ear of a user. The measurement device further comprises a receiver having a plurality of spatially separated detectors and one or more analog to digital converters coupled to the spatially separated detectors. The one or more analog to digital converters is configured to generate at least two receiver outputs. The receiver is configured to capture light while the LEDs are off and convert the captured light into a first signal, and to capture light while at least one of the LEDs is on and convert the captured light into a second signal, the captured light including at least a portion of the optical beam reflected from the tissue. The measurement device is configured to improve a signal-to-noise ratio of the optical beam reflected from the tissue by differencing the first signal and the second signal and by differencing the two receiver outputs. The measurement device is also configured to further improve the signal-to-noise ratio of the optical beam reflected from the tissue by increasing the light intensity relative to the initial light intensity from at least one of the LEDs. The measurement device is further configured to generate an output signal representing at least in part a non-invasive measurement on blood contained within the tissue.

In one or more embodiments, a wearable device comprises a measurement device including a light source comprising a plurality of light emitting diodes (LEDs) for measuring one or more physiological parameters. The measurement device is configured to generate, by modulating at least one of the LEDs having an initial light intensity, an optical beam having a plurality of optical wavelengths, wherein at least a portion of the plurality of optical wavelengths is a near-infrared wavelength between 700 nanometers and 2500 nanometers. The measurement device comprises one or more lenses configured to receive and to deliver a portion of the optical beam to tissue, wherein the tissue reflects at least a portion of the optical beam delivered to the tissue, and wherein the measurement device is adapted to be placed on a wrist or an ear of a user. The measurement device further comprises a receiver having a plurality of spatially separated detectors and one or more analog to digital converters coupled to the spatially separated detectors, the one or more analog to digital converters configured to generate at least two receiver outputs. The receiver is configured to capture light while the LEDs are off and convert the captured light into a first signal, and to capture light while at least one of the LEDs is on and convert the captured light into a second signal, the captured light including at least a portion of the optical beam reflected from the tissue. The measurement device is configured to improve a signal-to-noise ratio of the optical beam reflected from the tissue by differencing the first signal and the second signal and by differencing the two receiver outputs. The measurement device is configured to further improve the signal-to-noise ratio of the optical beam reflected from the tissue by increasing the light intensity relative to the initial light intensity from at least one of the LEDs. The measurement device is further configured to generate an output signal representing at least in part a non-invasive measurement on blood contained within the tissue, wherein the output signal is generated at least in part by using a Fourier transform and mathematical manipulation of a signal resulting from the captured light. The receiver further comprises one or more spectral filters positioned in front of at least some of the plurality of spatially separated detectors.

In one embodiment a measurement system is provided with a light source, an apparatus, a receiver, a smart phone or tablet, and a remote device. The light source comprises a plurality of semiconductor sources that are configured to generate an output optical beam with one or more optical wavelengths, the light source is configured to increase signal-to-noise ratio by increasing a light intensity from at least one of the plurality of semiconductor sources. The apparatus is configured to: receive a portion of the output optical beam, and deliver an analysis output beam to a sample. The receiver is configured to: receive and process at least a portion of the analysis output beam reflected or transmitted from the sample, generate an output signal, and synchronize to the light source. The smart phone or tablet comprises a wireless receiver, a wireless transmitter, a display, a microphone, a speaker, one or more buttons or knobs, a microprocessor and a touch screen. The smart phone or tablet is configured to: receive and process at least a portion of the output signal, store and display the processed output signal, and transmit at least a portion of the processed output signal over a wireless transmission link. The remote device is configured to: receive, over the wireless transmission link, an output status comprising the at least a portion of the processed output signal, process the received output status to generate processed data, and store the processed data.

In another embodiment a measurement system is provided with a wearable measurement device for measuring one or more physiological parameters, including a light source comprising a plurality of semiconductor sources that are configured to generate an output optical beam with one or more optical wavelengths. The light source is configured to increase signal-to-noise ratio by increasing a light intensity from at least one of the plurality of semiconductor sources. The wearable measurement device is configured to receive a portion of the output optical beam and to deliver an analysis output beam to a sample. The wearable measurement device further comprises a receiver configured to receive and process at least a portion of the analysis output beam reflected or transmitted from the sample and to generate an output signal, wherein the wearable measurement device receiver is configured to be synchronized to pulses of the light source. The measurement system is also provided

with a smart phone or tablet and a remote device. The smart phone or tablet comprises a wireless receiver, a wireless transmitter, a display, a microphone, a speaker, one or more buttons or knobs, a microprocessor and a touch screen. The smart phone or tablet is configured to receive and process at least a portion of the output signal, to store and display the processed output signal, and to transmit a portion of the processed output signal over a wireless transmission link. The remote device is configured to receive over the wireless transmission link an output status comprising the at least a portion of the processed output signal, to process the received output status to generate processed data and to store the processed data. The remote device is capable of storing a history of at least a portion of the received output status over a specified period of time.

In yet another embodiment a wearable device for use with a smart phone or tablet is provided with a measurement device including a light source comprising a plurality of semiconductor sources for measuring one or more physiological parameters. The measurement device is configured to: generate, by modulating at least one of the semiconductor sources having an initial light intensity, an input optical beam having one or more optical wavelengths, and receive and to deliver a portion of the input optical beam to tissue, wherein the tissue reflects at least a portion of the input optical beam delivered to the tissue. The measurement device further comprises a receiver that is configured to: capture light while the semiconductor sources are off and convert the captured light into a first signal, and capture light while at least one of the semiconductor sources is on and convert the captured light into a second signal, the captured light including at least a portion of the input optical beam reflected from the tissue; synchronize to the modulation of the at least one of the semiconductor sources. The measurement device is further configured to improve a signal-to-noise ratio of the input optical beam reflected from the tissue by: differencing the first signal and the second signal, and increasing the light intensity relative to the initial light intensity from at least one of the semiconductor sources. The measurement device is further configured to generate an output signal representing at least in part a non-invasive measurement on blood contained within the tissue. The wearable device is configured to communicate with the smart phone or tablet. The smart phone or tablet comprises a wireless receiver, a wireless transmitter, a display, a voice input module, a speaker, and a touch screen. The smart phone or tablet is configured to: receive and to process at least a portion of the output signal, store and display the processed output signal, and transmit at least a portion of the processed output signal over a wireless transmission link.

BRIEF DESCRIPTION OF THE DRAWINGS

For a more complete understanding of the present disclosure, and for further features and advantages thereof, reference is now made to the following description taken in conjunction with the accompanying drawings, in which:

FIG. **1** illustrates the structure of a tooth.

FIG. **2**A shows the attenuation coefficient for dental enamel and water versus wavelength from approximately 600 nm to 2600 nm.

FIG. **2**B illustrates the absorption spectrum of intact enamel and dentine in the wavelength range of approximately 1.2 to 2.4 microns.

FIG. **3** shows the near infrared spectral reflectance over the wavelength range of approximately 800 nm to 2500 nm from an occlusal tooth surface. The black diamonds correspond to the reflectance from a sound, intact tooth section. The asterisks correspond to a tooth section with an enamel lesion. The circles correspond to a tooth section with a dentine lesion.

FIG. **4** illustrates a hand-held dental tool design of a human interface that may also be coupled with other dental tools.

FIG. **5**A illustrates a clamp design of a human interface to cap over one or more teeth and perform a non-invasive measurement for dental caries.

FIG. **5**B shows a mouth guard design of a human interface to perform a non-invasive measurement for dental caries.

FIG. **6**A illustrates the dorsal of a hand for performing a differential measurement for measuring blood constituents or analytes.

FIG. **6**B illustrates the dorsal of a foot for performing a differential measurement for measuring blood constituents or analytes.

FIG. **7** illustrates a block diagram or building blocks for constructing high power laser diode assemblies.

FIG. **8** shows a platform architecture for different wavelength ranges for an all-fiber-integrated, high powered, super-continuum light source.

FIG. **9** illustrates one embodiment for a short-wave infrared super-continuum light source.

FIG. **10** shows the output spectrum from the SWIR SC laser of FIG. **9** when about 10 m length of fiber for SC generation is used. This fiber is a single-mode, non-dispersion shifted fiber that is optimized for operation near 1550 nm.

FIG. **11**A illustrates a schematic of the experimental set-up for measuring the diffuse reflectance spectroscopy using the SWIR-SC light source of FIGS. **9** and **10**.

FIG. **11**B shows exemplary reflectance from a sound enamel region, an enamel lesion region, and a dentine lesion region. The spectra are normalized to have equal value near 2050 nm.

FIGS. **12**A-B illustrate high power SWIR-SC lasers that may generate light between approximately 1.4-1.8 microns (FIG. **12**A) or approximately 2-2.5 microns (FIG. **12**B).

FIG. **12**C shows a reflection-spectroscopy based stand-off detection system having an SC laser source.

FIG. **12**D shows one example of a dual-beam experimental set-up that may be used to subtract out (or at least minimize the adverse effects of) light source fluctuations.

FIG. **13** schematically shows that the medical measurement device can be part of a personal or body area network that communicates with another device (e.g., smart phone or tablet) that communicates with the cloud. The cloud may in turn communicate information with the user, dental or healthcare providers, or other designated recipients.

FIG. **14**A is a schematic diagram of the basic elements of an imaging spectrometer.

FIG. **14**B illustrates one example of a typical imaging spectrometer used in hyper-spectral imaging systems.

FIG. **15** illustrates a flowchart of a smart manufacturing process.

DETAILED DESCRIPTION OF EXAMPLE EMBODIMENTS

As required, detailed embodiments of the present disclosure are disclosed herein; however, it is to be understood that the disclosed embodiments are merely exemplary of the disclosure that may be embodied in various and alternative forms. The figures are not necessarily to scale; some features may be exaggerated or minimized to show details of par-

ticular components. Therefore, specific structural and functional details disclosed herein are not to be interpreted as limiting, but merely as a representative basis for teaching one skilled in the art to variously employ the present disclosure.

Near-infrared (NIR) and SWIR light may be preferred for caries detection compared to visible light imaging because the NIR/SWIR wavelengths generally have lower absorption by stains and deeper penetration into teeth. Hence, NIR/SWIR light may provide a caries detection method that can be non-invasive, non-contact and relatively stain insensitive. Broadband light may provide further advantages because carious regions may demonstrate spectral signatures from water absorption and the wavelength dependence of porosity in the scattering of light.

The wavelength of light should be selected appropriately to achieve a non-invasive procedure. For example, the light should be able to penetrate deep enough to reach through the dermis and subcutaneous fat layers to reach varicose veins. For example, the penetration depth may be defined as the inverse of the absorption coefficient, although it may also be necessary to include the scattering for the calculation. To achieve penetration deep enough to reach the varicose veins, wavelengths may correspond to local minima in water **501** and adipose **502** absorption, as well as potentially local minima in collagen **503** and elastin **504** absorption. For example, wavelengths near approximately 1100 nm, 1310 nm, or 1650 nm may be advantageous for non-invasive procedures. More generally, wavelength ranges of approximately 900 nm to 1150 nm, 1280 nm to 1340 nm, or 1550 nm to 1680 nm may be advantageous for non-invasive procedures.

In general, the near-infrared region of the electromagnetic spectrum covers between approximately 0.7 microns (700 nm) to about 2.5 microns (2500 nm). However, it may also be advantageous to use just the short-wave infrared between approximately 1.4 microns (1400 nm) and about 2.5 microns (2500 nm). One reason for preferring the SWIR over the entire NIR may be to operate in the so-called "eye safe" window, which corresponds to wavelengths longer than about 1400 nm. Therefore, for the remainder of the disclosure the SWIR will be used for illustrative purposes. However, it should be clear that the discussion that follows could also apply to using the NIR wavelength range, or other wavelength bands.

In particular, wavelengths in the eye safe window may not transmit down to the retina of the eye, and therefore, these wavelengths may be less likely to create permanent eye damage from inadvertent exposure. The near-infrared wavelengths have the potential to be dangerous, because the eye cannot see the wavelengths (as it can in the visible), yet they can penetrate and cause damage to the eye. Even if a practitioner is not looking directly at the laser beam, the practitioner's eyes may receive stray light from a reflection or scattering from some surface. Hence, it can always be a good practice to use eye protection when working around lasers. Since wavelengths longer than about 1400 nm are substantially not transmitted to the retina or substantially absorbed in the retina, this wavelength range is known as the eye safe window. For wavelengths longer than 1400 nm, in general only the cornea of the eye may receive or absorb the light radiation.

FIG. **1** illustrates the structure of an exemplary cross-section of a tooth **100**. The tooth **100** has a top layer called the crown **101** and below that a root **102** that reaches well into the gum **106** and bone **108** of the mouth. The exterior of the crown **101** is an enamel layer **103**, and below the enamel is a layer of dentine **104** that sits atop a layer of cementum **107**. Below the dentine **104** is a pulp region **105**, which comprises within it blood vessels **109** and nerves **110**. If the light can penetrate the enamel **103** and dentine **104**, then the blood flow and blood constituents may be measured through the blood vessels in the dental pulp **105**. While the amount of blood flow in the capillaries of the dental pulp **105** may be less than an artery or vein, the smaller blood flow could still be advantageous for detecting or measuring blood constituents as compared to detection through the skin if there is less interfering spectral features from the tooth. Although the structure of a molar tooth is illustrated in FIG. **1**, other types of teeth also have similar structure. For example, different types of teeth include molars, pre-molars, canine and incisor teeth.

As used throughout this document, the term "couple" and or "coupled" refers to any direct or indirect communication between two or more elements, whether or not those elements are physically connected to one another. As used throughout this disclosure, the term "spectroscopy" means that a tissue or sample is inspected by comparing different features, such as wavelength (or frequency), spatial location, transmission, absorption, reflectivity, scattering, refractive index, or opacity. In one embodiment, "spectroscopy" may mean that the wavelength of the light source is varied, and the transmission, absorption, or reflectivity of the tissue or sample is measured as a function of wavelength. In another embodiment, "spectroscopy" may mean that the wavelength dependence of the transmission, absorption or reflectivity is compared between different spatial locations on a tissue or sample. As an illustration, the "spectroscopy" may be performed by varying the wavelength of the light source, or by using a broadband light source and analyzing the signal using a spectrometer, wavemeter, or optical spectrum analyzer.

As used throughout this disclosure, the term "fiber laser" refers to a laser or oscillator that has as an output light or an optical beam, wherein at least a part of the laser comprises an optical fiber. For instance, the fiber in the "fiber laser" may comprise one of or a combination of a single mode fiber, a multi-mode fiber, a mid-infrared fiber, a photonic crystal fiber, a doped fiber, a gain fiber, or, more generally, an approximately cylindrically shaped waveguide or light-pipe. In one embodiment, the gain fiber may be doped with rare earth material, such as ytterbium, erbium, and/or thulium, for example. In another embodiment, the mid-infrared fiber may comprise one or a combination of fluoride fiber, ZBLAN fiber, chalcogenide fiber, tellurite fiber, or germanium doped fiber. In yet another embodiment, the single mode fiber may include standard single-mode fiber, dispersion shifted fiber, non-zero dispersion shifted fiber, high-nonlinearity fiber, and small core size fibers.

As used throughout this disclosure, the term "pump laser" refers to a laser or oscillator that has as an output light or an optical beam, wherein the output light or optical beam is coupled to a gain medium to excite the gain medium, which in turn may amplify another input optical signal or beam. In one particular example, the gain medium may be a doped fiber, such as a fiber doped with ytterbium, erbium, and/or thulium. In one embodiment, the "pump laser" may be a fiber laser, a solid state laser, a laser involving a nonlinear crystal, an optical parametric oscillator, a semiconductor laser, or a plurality of semiconductor lasers that may be multiplexed together. In another embodiment, the "pump laser" may be coupled to the gain medium by using a fiber coupler, a dichroic mirror, a multiplexer, a wavelength division multiplexer, a grating, or a fused fiber coupler.

As used throughout this document, the term "super-continuum" and or "supercontinuum" and or "SC" refers to a broadband light beam or output that comprises a plurality of wavelengths. In a particular example, the plurality of wavelengths may be adjacent to one-another, so that the spectrum of the light beam or output appears as a continuous band when measured with a spectrometer. In one embodiment, the broadband light beam may have a bandwidth or at least 10 nm. In another embodiment, the "super-continuum" may be generated through nonlinear optical interactions in a medium, such as an optical fiber or nonlinear crystal. For example, the "super-continuum" may be generated through one or a combination of nonlinear activities such as four-wave mixing, the Raman effect, modulational instability, and self-phase modulation.

As used throughout this disclosure, the terms "optical light" and or "optical beam" and or "light beam" refer to photons or light transmitted to a particular location in space. The "optical light" and or "optical beam" and or "light beam" may be modulated or unmodulated, which also means that they may or may not contain information. In one embodiment, the "optical light" and or "optical beam" and or "light beam" may originate from a fiber, a fiber laser, a laser, a light emitting diode, a lamp, a pump laser, or a light source.

Transmission or Reflection Through Teeth

The transmission, absorption and reflection from teeth has been studied in the near infrared, and, although there are some features, the enamel and dentine appear to be fairly transparent in the near infrared (particularly SWIR wavelengths between about 1400 and 2500 nm). For example, the absorption or extinction ratio for light transmission has been studied. FIG. **2**A illustrates the attenuation coefficient **200** for dental enamel **201** (filled circles) and the absorption coefficient of water **202** (open circles) versus wavelength. Near-infrared light may penetrate much further without scattering through all the tooth enamel, due to the reduced scattering coefficient in normal enamel. Scattering in enamel may be fairly strong in the visible, but decreases as approximately $1/(\text{wavelength})^3$ [i.e., inverse of the cube of the wavelength] with increasing wavelength to a value of only 2-3 cm-1 at 1310 nm and 1550 nm in the near infrared. Therefore, enamel may be virtually transparent in the near infrared with optical attenuation 1-2 orders of magnitude less than in the visible range.

As another example, FIG. **2**B illustrates the absorption spectrum **250** of intact enamel **251** (dashed line) and dentine **252** (solid line) in the wavelength range of approximately 1.2 to 2.4 microns. In the near infrared there are two absorption bands in the areas of about 1.5 and 2 microns. The band with a peak around 1.57 microns may be attributed to the overtone of valent vibration of water present in both enamel and dentine. In this band, the absorption is greater for dentine than for enamel, which may be related to the large water content in this tissue. In the region of 2 microns, dentine may have two absorption bands, and enamel one. The band with a maximum near 2.1 microns may belong to the overtone of vibration of PO hydroxyapatite groups, which is the main substance of both enamel and dentine. Moreover, the band with a peak near 1.96 microns in dentine may correspond to water absorption (dentine may contain substantially higher water than enamel).

In addition to the absorption coefficient, the reflectance from intact teeth and teeth with dental caries (e.g., cavities) has been studied. In one embodiment, FIG. **3** shows the near infrared spectral reflectance **300** over the wavelength range of approximately 800 nm to 2500 nm from an occlusal (e.g., top) tooth surface **304**. The curve with black diamonds **301** corresponds to the reflectance from a sound, intact tooth section. The curve with asterisks (*) **302** corresponds to a tooth section with an enamel lesion. The curve with circles **303** corresponds to a tooth section with a dentine lesion. Thus, when there is a lesion, more scattering occurs and there may be an increase in the reflected light.

For wavelengths shorter than approximately 1400 nm, the shapes of the spectra remain similar, but the amplitude of the reflection changes with lesions. Between approximately 1400 nm and 2500 nm, an intact tooth **301** has low reflectance (e.g., high transmission), and the reflectance appears to be more or less independent of wavelength. On the other hand, in the presence of lesions **302** and **303**, there is increased scattering, and the scattering loss may be wavelength dependent. For example, the scattering loss may decrease as the inverse of some power of wavelength, such as $1/(\text{wavelength})^3$—so, the scattering loss decreases with longer wavelengths. When there is a lesion in the dentine **303**, more water can accumulate in the area, so there is also increased water absorption. For example, the dips near 1450 nm and 1900 nm may correspond to water absorption, and the reflectance dips are particularly pronounced in the dentine lesion **303**.

FIG. **3** may point to several novel techniques for early detection and quantification of carious regions. One method may be to use a relatively narrow wavelength range (for example, from a laser diode or super-luminescent laser diode) in the wavelength window below 1400 nm. In one embodiment, wavelengths in the vicinity of 1310 nm may be used, which is a standard telecommunications wavelength where appropriate light sources are available. Also, it may be advantageous to use a super-luminescent laser diode rather than a laser diode, because the broader bandwidth may avoid the production of laser speckle that can produce interference patterns due to light's scattering after striking irregular surfaces. As FIG. **3** shows, the amplitude of the reflected light (which may also be proportional to the inverse of the transmission) may increase with dental caries. Hence, comparing the reflected light from a known intact region with a suspect region may help identify carious regions. However, one difficulty with using a relatively narrow wavelength range and relying on amplitude changes may be the calibration of the measurement. For example, the amplitude of the reflected light may depend on many factors, such as irregularities in the dental surface, placement of the light source and detector, distance of the measurement instrument from the tooth, etc.

In one embodiment, use of a plurality of wavelengths can help to better calibrate the dental caries measurement. For example, a plurality of laser diodes or super-luminescent laser diodes may be used at different center wavelengths. Alternately, a lamp or alternate broadband light source may be used followed by appropriate filters, which may be placed after the light source or before the detectors. In one example, wavelengths near 1090 nm, 1440 nm and 1610 nm may be employed. The reflection from the tooth **305** appears to reach a local maximum near 1090 nm in the representative embodiment illustrated. Also, the reflectance near 1440 nm **306** is higher for dental caries, with a distinct dip particularly for dentine caries **303**. Near 1610 nm **307**, the reflection is also higher for carious regions. By using a plurality of wavelengths, the values at different wavelengths may help quantify a caries score. In one embodiment, the degree of enamel lesions may be proportional to the ratio of the

reflectance near 1610 nm divided by the reflectance near 1090 nm. Also, the degree of dentine lesion may be proportional to the difference between the reflectance near 1610 nm and 1440 nm, with the difference then divided by the reflectance near 1090 nm. Although one set of wavelengths has been described, other wavelengths may also be used and are intended to be covered by this disclosure.

In yet another embodiment, it may be further advantageous to use all of some fraction of the SWIR between approximately 1400 and 2500 nm. For example, a SWIR super-continuum light source could be used, or a lamp source could be used. On the receiver side, a spectrometer and/or dispersive element could be used to discriminate the various wavelengths. As FIG. **3** shows, an intact tooth **301** has a relatively low and featureless reflectance over the SWIR. On the other hand, with a carious region there is more scattering, so the reflectance **302**,**303** increases in amplitude. Since the scattering is inversely proportional to wavelength or some power of wavelength, the carious region reflectance **302**, **303** also decreases with increasing wavelength. Moreover, the carious region may contain more water, so there are dips in the reflectance near the water absorption lines **306** and **308**. The degree of caries or caries score may be quantified by the shape of the spectrum over the SWIR, taking ratios of different parts of the spectrum, or some combination of this and other spectral processing methods.

Although several methods of early caries detection using spectral reflectance have been described, other techniques could also be used and are intended to be covered by this disclosure. For example, transmittance may be used rather than reflectance, or a combination of the two could be used. Moreover, the transmittance, reflectance and/or absorbance could also be combined with other techniques, such as quantitative light-induced fluorescence or fiber-optic trans-illumination. Also, the SWIR could be advantageous, but other parts of the infrared, near-infrared or visible wavelengths may also be used consistent with this disclosure.

One other benefit of the absorption, transmission or reflectance in the near infrared and SWIR may be that stains and non-calcified plaque are not visible in this wavelength range, enabling better discrimination of defects, cracks, and demineralized areas. For example, dental calculus, accumulated plaque, and organic stains and debris may interfere significantly with visual diagnosis and fluorescence-based caries detection schemes in occlusal surfaces. In the case of using quantitative light-induced fluorescence, such confounding factors typically may need to be removed by prophylaxis (abrasive cleaning) before reliable measurements can be taken. Surface staining at visible wavelengths may further complicate the problem, and it may be difficult to determine whether pits and fissures are simply stained or demineralized. On the other hand, staining and pigmentation generally interfere less with NIR or SWIR imaging. For example, NIR and SWIR light may not be absorbed by melanin and porphyrins produced by bacteria and those found in food dyes that accumulate in dental plaque and are responsible for the pigmentation.

Human Interface for Measurement System

A number of different types of measurements may be used to image for dental caries, particularly early detection of dental caries. A basic feature of the measurements may be that the optical properties are measured as a function of wavelength at a plurality of wavelengths. As further described below, the light source may output a plurality of wavelengths, or a continuous spectrum over a range of wavelengths. In one embodiment, the light source may cover some or all of the wavelength range between approximately 1400 nm and 2500 nm. The signal may be received at a receiver, which may also comprise a spectrometer or filters to discriminate between different wavelengths. The signal may also be received at a camera, which may also comprise filters or a spectrometer. In one embodiment, the spectral discrimination using filters or a spectrometer may be placed after the light source rather than at the receiver. The receiver usually comprises one or more detectors (optical-to-electrical conversion element) and electrical circuitry. The receiver may also be coupled to analog to digital converters, particularly if the signal is to be fed to a digital device.

Referring to FIG. **1**, one or more light sources **111** may be used for illumination. In one embodiment, a transmission measurement may be performed by directing the light source output **111** to the region near the interface between the gum **106** and dentine **104**. In one embodiment, the light may be directed using a light guide or a fiber optic. The light may then propagate through the dental pulp **105** to the other side, where the light may be incident on one or more detectors or another light guide to transport the signal to **112** a spectrometer, receiver, and/or camera, for example. In one embodiment, the light source may be directed to one or more locations near the interface between the gum **106** and dentine **104** (in one example, could be from the two sides of the tooth). The transmitted light may then be detected in the occlusal surface above the tooth using a **112** spectrometer, receiver, or camera, for example. In another embodiment, a reflectance measurement may be conducted by directing the light source output **111** to, for example, the occlusal surface of the tooth, and then detecting the reflectance at a **113** spectrometer, receiver or camera. Although a few embodiments for imaging the tooth are described, other embodiments and techniques may also be used and are intended to be covered by this disclosure. These optical techniques may measure optical properties such as reflectance, transmittance, absorption, or luminescence.

In one embodiment, FIG. **4** shows that the light source and/or detection system may be integrated with a dental hand-piece **400**. The hand-piece **400** may also include other dental equipment, such as a drill, pick, air spray or water cooling stream. The dental hand-piece **400** may include a housing **401** and a motor housing **402** (in some embodiments such as with a drill, a motor may be placed in this section). The end of hand-piece **403** that interfaces with the tooth may be detachable, and it may also have the light input and output end. The dental hand-piece **400** may also have an umbilical cord **404** for connecting to power supplies, diagnostics, or other equipment, for example.

A light guide **405** may be integrated with the hand-piece **400**, either inside the housing **401**, **402** or adjacent to the housing. In one embodiment, a light source **410** may be contained within the housing **401**, **402**. In an alternative embodiment, the hand-piece **400** may have a coupler **410** to couple to an external light source **411** and/or detection system or receiver **412**. The light source **411** may be coupled to the hand-piece **400** using a light guide or fiber optic cable **406**. In addition, the detection system or receiver **412** may be coupled to the hand-piece **400** using one or more light guides, fiber optic cable or a bundle of fibers **407**.

The light incident on the tooth may exit the hand-piece **400** through the end **403**. The end **403** may also have a lens system or curved mirror system to collimate or focus the light. In one embodiment, if the light source is integrated with a tool such as a drill, then the light may reach the tooth

at the same point as the tip of the drill. The reflected or transmitted light from the tooth may then be observed externally and/or guided back through the light guide **405** in the hand-piece **400**. If observed externally, there may be a lens system **408** for collecting the light and a detection system **409** that may have one or more detectors and electronics. If the light is to be guided back through the hand-piece **400**, then the reflected light may transmit through the light guide **405** back to the detection system or receiver **412**. In one embodiment, the incident light may be guided by a fiber optic through the light guide **405**, and the reflected light may be captured by a series of fibers forming a bundle adjacent to or surrounding the incident light fiber.

In another embodiment, a "clamp" design **500** may be used as a cap over one or more teeth, as illustrated in FIG. **5**A. The clamp design may be different for different types of teeth, or it may be flexible enough to fit over different types of teeth. For example, different types of teeth include the molars (toward the back of the mouth), the premolars, the canine, and the incisors (toward the front of the mouth). One embodiment of the clamp-type design is illustrated in FIG. **5**A for a molar tooth **508**. The C-clamp **501** may be made of a plastic or rubber material, and it may comprise a light source input **502** and a detector output **503** on the front or back of the tooth, for example.

The light source input **502** may comprise a light source directly, or it may have light guided to it from an external light source. Also, the light source input **502** may comprise a lens system to collimate or focus the light across the tooth. The detector output **503** may comprise a detector directly, or it may have a light guide to transport the signal to an external detector element. The light source input **502** may be coupled electrically or optically through **504** to a light input **506**. For example, if the light source is external in **506**, then the coupling element **504** may be a light guide, such as a fiber optic. Alternately, if the light source is contained in **502**, then the coupling element **504** may be electrical wires connecting to a power supply in **506**. Similarly, the detector output **503** may be coupled to a detector output unit **507** with a coupling element **505**, which may be one or more electrical wires or a light guide, such as a fiber optic. This is just one example of a clamp over one or more teeth, but other embodiments may also be used and are intended to be covered by this disclosure. For example, if reflectance from the teeth is to be used in the measurement, then the light input **502** and detected light input **503** may be on the same side of the tooth.

In yet another embodiment, one or more light source ports and sensor ports may be used in a mouth-guard type design. For example, one embodiment of a dental mouth guard **550** is illustrated in FIG. **5**B. The structure of the mouth guard **551** may be similar to mouth guards used in sports (e.g., when playing football or boxing) or in dental trays used for applying fluoride treatment, and the mouth guard may be made from plastic, rubber, or any other suitable materials. As an example, the mouth guard may have one or more light source input ports **552**, **553** and one or more detector output ports **554**, **555**. Although six input and output ports are illustrated, any number of ports may be used.

Similar to the clamp design described above, the light source inputs **552**, **553** may comprise one or more light sources directly, or they may have light guided to them from an external light source. Also, the light source inputs **552**, **553** may comprise lens systems to collimate or focus the light across the teeth. The detector outputs **554**, **555** may comprise one or more detectors directly, or they may have one or more light guides to transport the signals to an external detector element. The light source inputs **552**, **553** may be coupled electrically or optically through **556** to a light input **557**. For example, if the light source is external in **557**, then the one or more coupling elements **556** may be one or more light guides, such as a fiber optic. Alternately, if the light sources are contained in **552**, **553**, then the coupling element **556** may be one or more electrical wires connecting to a power supply in **557**. Similarly, the detector outputs **554**, **555** may be coupled to a detector output unit **559** with one or more coupling elements **558**, which may be one or more electrical wires or one or more light guides, such as a fiber optic. This is just one example of a mouth guard design covering a plurality of teeth, but other embodiments may also be used and are intended to be covered by this disclosure. For instance, the position of the light source inputs and detector output ports could be exchanged, or some mixture of locations of light source inputs and detector output ports could be used. Also, if reflectance from the teeth is to be measured, then the light sources and detectors may be on the same side of the tooth. Moreover, it may be advantageous to pulse the light source with a particular pulse width and pulse repetition rate, and then the detection system can measure the pulsed light returned from or transmitted through the tooth. Using a lock-in type technique (e.g., detecting at the same frequency as the pulsed light source and also possibly phase locked to the same signal), the detection system may be able to reject background or spurious signals and increase the signal-to-noise ratio of the measurement.

Other elements may be added to the human interface designs of FIGS. **4**-**6** and are also intended to be covered by this disclosure. For instance, in one embodiment it may be desirable to have replaceable inserts that may be disposable. Particularly in a dentist's or doctor's office or hospital setting, the same instrument may be used with a plurality of patients. Rather than disinfecting the human interface after each use, it may be preferable to have disposable inserts that can be thrown away after each use. In one embodiment, a thin plastic coating material may enclose the clamp design of FIG. **5**A or mouth guard design of FIG. **5**B. The coating material may be inserted before each use, and then after the measurement is exercised the coating material may be peeled off and replaced. The coating or covering material may be selected based on suitable optical properties that do not affect the measurement, or known optical properties that can be calibrated or compensated for during measurement. Such a design may save the dentist or physician or user considerable time, while at the same time provide the business venture with a recurring cost revenue source.

Thus, beyond the problem of other blood constituents or analytes having overlapping spectral features, it may be difficult to observe glucose spectral signatures through the skin and its constituents of water, adipose, collagen and elastin. One approach to overcoming this difficulty may be to try to measure the blood constituents in veins that are located at relatively shallow distances below the skin. Veins may be more beneficial for the measurement than arteries, since arteries tend to be located at deeper levels below the skin. Also, in one embodiment it may be advantageous to use a differential measurement to subtract out some of the interfering absorption lines from the skin. For example, an instrument head may be designed to place one probe above a region of skin over a blood vein, while a second probe may be placed at a region of the skin without a noticeable blood vein below it. Then, by differencing the signals from the two probes, at least part of the skin interference may be cancelled out.

Two representative embodiments for performing such a differential measurement are illustrated in FIG. **6**A and FIG. **6**B. In one embodiment shown in FIG. **6**A, the dorsal of the hand **600** may be used for measuring blood constituents or analytes. The dorsal of the hand **600** may have regions that have distinct veins **601** as well as regions where the veins are not as shallow or pronounced **602**. By stretching the hand and leaning it backwards, the veins **601** may be accentuated in some cases. A near-infrared diffuse reflectance measurement may be performed by placing one probe **603** above the vein-rich region **601**. To turn this into a differential measurement, a second probe **604** may be placed above a region without distinct veins **602**. Then, the outputs from the two probes may be subtracted **605** to at least partially cancel out the features from the skin. The subtraction may be done preferably in the electrical domain, although it can also be performed in the optical domain or digitally/mathematically using sampled data based on the electrical and/or optical signals. Although one example of using the dorsal of the hand **600** is shown, many other parts of the hand can be used within the scope of this disclosure. For example, alternate methods may use transmission through the webbing between the thumb and the fingers **606**, or transmission or diffuse reflection through the tips of the fingers **607**.

In another embodiment, the dorsal of the foot **650** may be used instead of the hand. One advantage of such a configuration may be that for self-testing by a user, the foot may be easier to position the instrument using both hands. One probe **653** may be placed over regions where there are more distinct veins **651**, and a near-infrared diffuse reflectance measurement may be made. For a differential measurement, a second probe **654** may be placed over a region with less prominent veins **652**, and then the two probe signals may be subtracted, either electronically or optically, or may be digitized/sampled and processed mathematically depending on the particular application and implementation. As with the hand, the differential measurements may be intended to compensate for or subtract out (at least in part) the interference from the skin. Since two regions are used in close proximity on the same body part, this may also aid in removing some variability in the skin from environmental effects such as temperature, humidity, or pressure. In addition, it may be advantageous to first treat the skin before the measurement, by perhaps wiping with a cloth or treated cotton ball, applying some sort of cream, or placing an ice cube or chilled bag over the region of interest.

Although two embodiments have been described, many other locations on the body may be used using a single or differential probe within the scope of this disclosure. In yet another embodiment, the wrist may be advantageously used, particularly where a pulse rate is typically monitored. Since the pulse may be easily felt on the wrist, there is underlying the region a distinct blood flow. Other embodiments may use other parts of the body, such as the ear lobes, the tongue, the inner lip, the nails, the eye, or the teeth. Some of these embodiments will be further described below. The ear lobes or the tip of the tongue may be advantageous because they are thinner skin regions, thus permitting transmission rather than diffuse reflection. However, the interference from the skin is still a problem in these embodiments. Other regions such as the inner lip or the bottom of the tongue may be contemplated because distinct veins are observable, but still the interference from the skin may be problematic in these embodiments. The eye may seem as a viable alternative because it is more transparent than skin. However, there are still issues with scattering in the eye. For example, the anterior chamber of the eye (the space between the cornea and the iris) comprises a fluid known as aqueous humor. However, the glucose level in the eye chamber may have a significant temporal lag on changes in the glucose level compared to the blood glucose level.

One of the issues in measuring a particular blood constituent is the interfering and overlapping signal from other blood constituents. The selection of the constituent of interest may be improved using a number of techniques. For example, a higher light level or intensity may improve the signal-to-noise ratio for the measurement. Second, mathematical modeling and signal processing methodologies may help to reduce the interference, such as multivariate techniques, multiple linear regression, and factor-based algorithms, for example. For instance, a number of mathematical approaches include multiple linear regression, partial least squares, and principal component regression (PCR). Various mathematical derivatives, including the first and second derivatives, may help to accentuate differences between spectra. In addition, by using a wider wavelength range and using more sampling wavelengths may improve the ability to discriminate one signal from another. These are just examples of some of the methods of improving the ability to discriminate between different constituents, but other techniques may also be used and are intended to be covered by this disclosure.

Light Sources for Near Infrared

There are a number of light sources that may be used in the near infrared. To be more specific, the discussion below will consider light sources operating in the short wave infrared (SWIR), which may cover the wavelength range of approximately 1400 nm to 2500 nm. Other wavelength ranges may also be used for the applications described in this disclosure, so the discussion below is merely provided as exemplary types of light sources. The SWIR wavelength range may be valuable for a number of reasons. First, the SWIR corresponds to a transmission window through water and the atmosphere. Second, the so-called "eye-safe" wavelengths are wavelengths longer than approximately 1400 nm. Third, the SWIR covers the wavelength range for nonlinear combinations of stretching and bending modes as well as the first overtone of C—H stretching modes. Thus, for example, glucose and ketones among other substances may have unique signatures in the SWIR. Moreover, many solids have distinct spectral signatures in the SWIR, so particular solids may be identified using stand-off detection or remote sensing. For instance, many explosives have unique signatures in the SWIR.

Different light sources may be selected for the SWIR based on the needs of the application. Some of the features for selecting a particular light source include power or intensity, wavelength range or bandwidth, spatial or temporal coherence, spatial beam quality for focusing or transmission over long distance, and pulse width or pulse repetition rate. Depending on the application, lamps, light emitting diodes (LEDs), laser diodes (LD's), tunable LD's, super-luminescent laser diodes (SLDs), fiber lasers or supercontinuum sources (SC) may be advantageously used. Also, different fibers may be used for transporting the light, such as fused silica fibers, plastic fibers, mid-infrared fibers (e.g., tellurite, chalcogenides, fluorides, ZBLAN, etc), or a hybrid of these fibers.

Lamps may be used if low power or intensity of light is required in the SWIR, and if an incoherent beam is suitable. In one embodiment, in the SWIR an incandescent lamp that can be used is based on tungsten and halogen, which have

an emission wavelength between approximately 500 nm to 2500 nm. For low intensity applications, it may also be possible to use thermal sources, where the SWIR radiation is based on the black body radiation from the hot object. Although the thermal and lamp based sources are broadband and have low intensity fluctuations, it may be difficult to achieve a high signal-to-noise ratio due to the low power levels. Also, the lamp based sources tend to be energy inefficient.

In another embodiment, LED's can be used that have a higher power level in the SWIR wavelength range. LED's also produce an incoherent beam, but the power level can be higher than a lamp and with higher energy efficiency. Also, the LED output may more easily be modulated, and the LED provides the option of continuous wave or pulsed mode of operation. LED's are solid state components that emit a wavelength band that is of moderate width, typically between about 20 nm to 40 nm. There are also so-called super-luminescent LEDs that may even emit over a much wider wavelength range. In another embodiment, a wide band light source may be constructed by combining different LEDs that emit in different wavelength bands, some of which could preferably overlap in spectrum. One advantage of LEDs as well as other solid state components is the compact size that they may be packaged into.

In yet another embodiment, various types of laser diodes may be used in the SWIR wavelength range. Just as LEDs may be higher in power but narrower in wavelength emission than lamps and thermal sources, the LDs may be yet higher in power but yet narrower in wavelength emission than LEDs. Different kinds of LDs may be used, including Fabry-Perot LDs, distributed feedback (DFB) LDs, distributed Bragg reflector (DBR) LDs. Since the LDs have relatively narrow wavelength range (typically under 10 nm), in one embodiment a plurality of LDs may be used that are at different wavelengths in the SWIR. The various LDs may be spatially multiplexed, polarization multiplexed, wavelength multiplexed, or a combination of these multiplexing methods. Also, the LDs may be fiber pig-tailed or have one or more lenses on the output to collimate or focus the light. Another advantage of LDs is that they may be packaged compactly and may have a spatially coherent beam output. Moreover, tunable LDs that can tune over a range of wavelengths are also available. The tuning may be done by varying the temperature, or electrical current may be used in particular structures such as distributed Bragg reflector (DBR) LDs, for example. In another embodiment, external cavity LDs may be used that have a tuning element, such as a fiber grating or a bulk grating, in the external cavity.

In another embodiment, super-luminescent laser diodes may provide higher power as well as broad bandwidth. An SLD is typically an edge emitting semiconductor light source based on super-luminescence (e.g., this could be amplified spontaneous emission). SLDs combine the higher power and brightness of LDs with the low coherence of conventional LEDs, and the emission band for SLD's may be 5 to 100 nm wide, preferably in the 60 to 100 nm range. Although currently SLDs are commercially available in the wavelength range of approximately 400 nm to 1700 nm, SLDs could and may in the future be made to cover a broader region of the SWIR.

In yet another embodiment, high power LDs for either direct excitation or to pump fiber lasers and SC light sources may be constructed using one or more laser diode bar stacks. FIG. **7** shows an example of a block diagram **700** or building blocks for constructing the high power LDs. In this embodiment, one or more diode bar stacks **701** may be used, where the diode bar stack may be an array of several single emitter LDs. Since the fast axis (e.g., vertical direction) may be nearly diffraction limited while the slow-axis (e.g., horizontal axis) may be far from diffraction limited, different collimators **702** may be used for the two axes.

Then, the brightness may be increased by spatially combining the beams from multiple stacks **703**. The combiner may include spatial interleaving, it may include wavelength multiplexing, or it may involve a combination of the two. Different spatial interleaving schemes may be used, such as using an array of prisms or mirrors with spacers to bend one array of beams into the beam path of the other. In another embodiment, segmented mirrors with alternate high-reflection and anti-reflection coatings may be used. Moreover, the brightness may be increased by polarization beam combining **704** the two orthogonal polarizations, such as by using a polarization beam splitter. In a particular embodiment, the output may then be focused or coupled into a large diameter core fiber. As an example, typical dimensions for the large diameter core fiber range from diameters of approximately 100 microns to 400 microns or more. Alternatively or in addition, a custom beam shaping module **705** may be used, depending on the particular application. For example, the output of the high power LD may be used directly **706**, or it may be fiber coupled **707** to combine, integrate, or transport the high power LD energy. These high power LDs may grow in importance because the LD powers can rapidly scale up. For example, instead of the power being limited by the power available from a single emitter, the power may increase in multiples depending on the number of diodes multiplexed and the size of the large diameter fiber. Although FIG. **7** is shown as one embodiment, some or all of the elements may be used in a high power LD, or additional elements may also be used.

As described in greater detail in commonly owned US Pat. App. Pub. 2014/0188094, in some instances, it may be desirable to create multiple locations of focused light. For example, the speed of the treatment for varicose veins may be increased by causing thermal coagulation or occlusion at multiple locations. Multiple collimated or focused light beams may be created in one assembly. In such embodiments, optionally a surface cooling apparatus may be used, where a cooling fluid may be flowed either touching or in close proximity to the skin. Also, in this particular embodiment a cylindrical assembly may optionally be used, where the cylindrical length may be several millimeters in length and defined by a clamp or mount placed on or near the leg. In one embodiment, a window and/or lenslet array is also shown on the cylindrical surface for permitting the light to be incident on the skin and varicose vein at multiple spots. The lenslet array may comprise circular, spherical or cylindrical lenses, depending on the type of spots desired. As before, one advantage of placing the lenslet array in close proximity to the skin and varicose vein may be that a high NA lens may be used. Also, the input from the lens and/or mirror assembly to the lenslet array may be single large beam, or a plurality of smaller beams. In one embodiment, a plurality of spots may be created by the lenslet array to cause a plurality of locations of thermal coagulation in the varicose vein. Any number of spots may be used and are intended to be covered by this disclosure.

In a non-limiting example, a plurality of spots may be used, or what might be called a fractionated beam. The fractionated laser beam may be added to the laser delivery assembly or delivery head in a number of ways. In one embodiment, a screen-like spatial filter may be placed in the pathway of the beam to be delivered to the biological tissue.

The screen-like spatial filter can have opaque regions to block the light and holes or transparent regions, through which the laser beam may pass to the tissue sample. The ratio of opaque to transparent regions may be varied, depending on the application of the laser. In another embodiment, a lenslet array can be used at or near the output interface where the light emerges. In yet another embodiment, at least a part of the delivery fiber from the infrared laser system to the delivery head may be a bundle of fibers, which may comprise a plurality of fiber cores surrounded by cladding regions. The fiber cores can then correspond to the exposed regions, and the cladding areas can approximate the opaque areas not to be exposed to the laser light. As an example, a bundle of fibers may be excited by at least a part of the laser system output, and then the fiber bundle can be fused together and perhaps pulled down to a desired diameter to expose to the tissue sample near the delivery head. In yet another embodiment, a photonic crystal fiber may be used to create the fractionated laser beam. In one non-limiting example, the photonic crystal fiber can be coupled to at least a part of the laser system output at one end, and the other end can be coupled to the delivery head. In a further example, the fractionated laser beam may be generated by a heavily multi-mode fiber, where the speckle pattern at the output may create the high intensity and low intensity spatial pattern at the output. Although several exemplary techniques are provided for creating a fractionated laser beam, other techniques that can be compatible with optical fibers are also intended to be included by this disclosure.

Although the output from a fiber laser may be from a single or multi-mode fiber, different spatial spot sizes or spatial profiles may be beneficial for different applications. For example, in some instances it may be desirable to have a series of spots or a fractionated beam with a grid of spots. In one embodiment, a bundle of fibers or a light pipe with a plurality of guiding cores may be used. In another embodiment, one or more fiber cores may be followed by a lenslet array to create a plurality of collimated or focused beams. In yet another embodiment, a delivery light pipe may be followed by a grid-like structure to divide up the beam into a plurality of spots. These are specific examples of beam shaping, and other apparatuses and methods may also be used and are consistent with this disclosure.

SWIR Super-continuum Lasers

Each of the light sources described above have particular strengths, but they also may have limitations. For example, there is typically a trade-off between wavelength range and power output. Also, sources such as lamps, thermal sources, and LEDs produce incoherent beams that may be difficult to focus to a small area and may have difficulty propagating for long distances. An alternative source that may overcome some of these limitations is an SC light source. Some of the advantages of the SC source may include high power and intensity, wide bandwidth, spatially coherent beam that can propagate nearly transform limited over long distances, and easy compatibility with fiber delivery.

Supercontinuum lasers may combine the broadband attributes of lamps with the spatial coherence and high brightness of lasers. By exploiting a modulational instability initiated supercontinuum (SC) mechanism, an all-fiber-integrated SC laser with no moving parts may be built using commercial-off-the-shelf (COTS) components. Moreover, the fiber laser architecture may be a platform where SC in the visible, near-infrared/SWIR, or mid-IR can be generated by appropriate selection of the amplifier technology and the SC generation fiber. But until recently, SC lasers were used primarily in laboratory settings since typically large, table-top, mode-locked lasers were used to pump nonlinear media such as optical fibers to generate SC light. However, those large pump lasers may now be replaced with diode lasers and fiber amplifiers that gained maturity in the telecommunications industry.

In one embodiment, an all-fiber-integrated, high-powered SC light source **800** may be elegant for its simplicity (FIG. **8**). The light may be first generated from a seed laser diode **801**. For example, the seed LD **801** may be a distributed feedback (DFB) laser diode with a wavelength near 1542 or 1550 nm, with approximately 0.5-2.0 ns pulsed output, and with a pulse repetition rate between about one kilohertz to about 100 MHz or more. The output from the seed laser diode may then be amplified in a multiple-stage fiber amplifier **802** comprising one or more gain fiber segments. In one embodiment, the first stage pre-amplifier **803** may be designed for optimal noise performance. For example, the pre-amplifier **803** may be a standard erbium-doped fiber amplifier or an erbium/ytterbium doped cladding pumped fiber amplifier. Between amplifier stages **803** and **806**, it may be advantageous to use band-pass filters **804** to block amplified spontaneous emission and isolators **805** to prevent spurious reflections. Then, the power amplifier stage **806** may use a cladding-pumped fiber amplifier that may be optimized to minimize nonlinear distortion. The power amplifier fiber **806** may also be an erbium-doped fiber amplifier, if only low or moderate power levels are to be generated.

The SC generation **807** may occur in the relatively short lengths of fiber that follow the pump laser. The SC fiber length may range from around a few millimeters to 100 m or more. In one embodiment, the SC generation may occur in a first fiber **808** where the modulational-instability initiated pulse break-up occurs primarily, followed by a second fiber **809** where the SC generation and spectral broadening occurs primarily.

In one embodiment, one or two meters of standard single-mode fiber (SMF) after the power amplifier stage may be followed by several meters of SC generation fiber. For this example, in the SMF the peak power may be several kilowatts and the pump light may fall in the anomalous group-velocity dispersion regime—often called the soliton regime. For high peak powers in the anomalous dispersion regime, the nanosecond pulses may be unstable due to a phenomenon known as modulational instability, which is basically parametric amplification in which the fiber nonlinearity helps to phase match the pulses. As a consequence, the nanosecond pump pulses may be broken into many shorter pulses as the modulational instability tries to form soliton pulses from the quasi-continuous-wave background. Although the laser diode and amplification process starts with approximately nanosecond-long pulses, modulational instability in the short length of SMF fiber may form approximately 0.5 ps to several-picosecond-long pulses with high intensity. Thus, the few meters of SMF fiber may result in an output similar to that produced by mode-locked lasers, except in a much simpler and cost-effective manner.

The short pulses created through modulational instability may then be coupled into a nonlinear fiber for SC generation. The nonlinear mechanisms leading to broadband SC may include four-wave mixing or self-phase modulation along with the optical Raman effect. Since the Raman effect is self-phase-matched and shifts light to longer wavelengths by emission of optical photons, the SC may spread to longer wavelengths very efficiently. The short-wavelength edge

may arise from four-wave mixing, and often times the short wavelength edge may be limited by increasing group-velocity dispersion in the fiber. In many instances, if the particular fiber used has sufficient peak power and SC fiber length, the SC generation process may fill the long-wavelength edge up to the transmission window.

Mature fiber amplifiers for the power amplifier stage **806** include ytterbium-doped fibers (near 1060 nm), erbium-doped fibers (near 1550 nm), erbium/ytterbium-doped fibers (near 1550 nm), or thulium-doped fibers (near 2000 nm). In various embodiments, candidates for SC fiber **809** include fused silica fibers (for generating SC between 0.8-2.7 μm), mid-IR fibers such as fluorides, chalcogenides, or tellurites (for generating SC out to 4.5 μm or longer), photonic crystal fibers (for generating SC between 0.4 and 1.7 μm), or combinations of these fibers. Therefore, by selecting the appropriate fiber-amplifier doping for **806** and nonlinear fiber **809**, SC may be generated in the visible, near-IR/SWIR, or mid-IR wavelength region.

The configuration **800** of FIG. **8** is just one particular example, and other configurations can be used and are intended to be covered by this disclosure. For example, further gain stages may be used, and different types of lossy elements or fiber taps may be used between the amplifier stages. In another embodiment, the SC generation may occur partially in the amplifier fiber and in the pig-tails from the pump combiner or other elements. In yet another embodiment, polarization maintaining fibers may be used, and a polarizer may also be used to enhance the polarization contrast between amplifier stages. Also, not discussed in detail are many accessories that may accompany this set-up, such as driver electronics, pump laser diodes, safety shut-offs, and thermal management and packaging.

In one embodiment, one example of the SC laser that operates in the SWIR is illustrated in FIG. **9**. This SWIR SC source **900** produces an output of up to approximately 5 W over a spectral range of about 1.5 to 2.4 microns, and this particular laser is made out of polarization maintaining components. The seed laser **901** is a distributed feedback (DFB) laser operating near 1542 nm producing approximately 0.5 nsec pulses at an about 8 MHz repetition rate. The pre-amplifier **902** is forward pumped and uses about 2 m length of erbium/ytterbium cladding pumped fiber **903** (often also called dual-core fiber) with an inner core diameter of 12 microns and outer core diameter of 130 microns. The pre-amplifier gain fiber **903** is pumped using a 10 W laser diode near 940 nm **905** that is coupled in using a fiber combiner **904**.

In this particular 5 W unit, the mid-stage between amplifier stages **902** and **906** comprises an isolator **907**, a band-pass filter **908**, a polarizer **909** and a fiber tap **910**. The power amplifier **906** uses an approximately 4 m length of the 12/130 micron erbium/ytterbium doped fiber **911** that is counter-propagating pumped using one or more 30 W laser diodes near 940 nm **912** coupled in through a combiner **913**. An approximately 1-2 meter length of the combiner pig-tail helps to initiate the SC process, and then a length of PM-1550 fiber **915** (polarization maintaining, single-mode, fused silica fiber optimized for 1550 nm) is spliced **914** to the combiner output.

If an output fiber of about 10 m in length is used, then the resulting output spectrum **1000** is shown in FIG. **10**. The details of the output spectrum **1000** depend on the peak power into the fiber, the fiber length, and properties of the fiber such as length and core size, as well as the zero dispersion wavelength and the dispersion properties. For example, if a shorter length of fiber is used, then the spectrum actually reaches to longer wavelengths (e.g., a 2 m length of SC fiber broadens the spectrum to about 2500 nm). Also, if extra-dry fibers are used with less O—H content, then the wavelength edge may also reach to a longer wavelength. To generate more spectra toward the shorter wavelengths, the pump wavelength (in this case ~1542 nm) should be close to the zero dispersion wavelength in the fiber. For example, by using a dispersion shifted fiber or so-called non-zero dispersion shifted fiber, the short wavelength edge may shift to shorter wavelengths.

In one particular embodiment, the SWIR-SC light source of FIG. **9** with output spectrum in FIG. **10** was used in preliminary experiments for examining the reflectance from different dental samples. A schematic of the experimental set-up **1100** for measuring the diffuse reflectance spectroscopy is illustrated in FIG. **11**A. The SC source **1101** in this embodiment was based on the design of FIG. **9** and delivered approximately 1.6 W of light over the wavelength range from about 1500-2400 nm. The output beam **1102** was collimated, and then passed through a chopper **1103** (for lock-in detection at the receiver after the spectrometer **1106**) and an aperture **1104** for localizing the beam on the tooth location. Different teeth **1105** with different lesions and caries were placed in front of the aperture **1104**, and the scattered light was passed through a spectrometer **1106** and collected on a detector, whose signal was sent to a receiver. The tooth samples **1105** were mounted in clay or putty for standing upright. Different types of teeth could be used, including molars, premolars, canine and incisor teeth.

FIG. **11**B shows exemplary reflectance spectra **1150** from a sound enamel region **1151** (e.g., without dental caries), an enamel lesion region **1152**, and a dentine lesion region **1153** of various teeth. The spectra are normalized to have equal value near 2050 nm. In this particular embodiment, the slope from the sound enamel **1151** is steepest between about 1500 and 1950 nm, with a lesser slope in the presence of an enamel lesion **1152**. When there is a sample with dentine lesion **1153**, more features appear in the spectrum from the presence of water absorption lines from water that collects in the dentine. For this experiment, the spectra **1151**, **1152**, and **1153** are flatter in the wavelength region between about 1950 nm and 2350 nm. These are preliminary results, but they show the benefit of using broadband sources such as the SWIR-SC source for diagnosing dental caries. Although the explanation behind the different spectra **1150** of FIG. **11**B may not be understood as yet, it is clear that the spectra **1151**, **1152** and **1153** are distinguishable. Therefore, the broadband reflectance may be used for detection of dental caries and analyzing the region of the caries. Although diffuse reflectance has been used in this experiment, other signals, such as transmission, reflectance or a combination, may also be used and are covered by this disclosure.

Although one particular example of a 5 W SWIR-SC has been described, different components, different fibers, and different configurations may also be used consistent with this disclosure. For instance, another embodiment of the similar configuration **900** in FIG. **9** may be used to generate high powered SC between approximately 1060 and 1800 nm. For this embodiment, the seed laser **901** may be a distributed feedback laser diode of about 1064 nm, the pre-amplifier gain fiber **903** may be a ytterbium-doped fiber amplifier with 10/125 microns dimensions, and the pump laser **905** may be a 10 W laser diode near 915 nm. A mode field adapter may be including in the mid-stage, in addition to the isolator **907**, band pass filter **908**, polarizer **909** and tap **910**. The gain fiber **911** in the power amplifier may be an about 20 m length of ytterbium-doped fiber with 25/400

microns dimension. The pump **912** for the power amplifier may be up to six pump diodes providing 30 W each near 915 nm. For this much pump power, the output power in the SC may be as high as 50 W or more.

In an alternate embodiment, it may be desirous to generate high power SWIR SC over 1.4-1.8 microns and separately 2-2.5 microns (the window between 1.8 and 2 microns may be less important due to the strong water and atmospheric absorption). For example, the SC source of FIG. **12**A can lead to bandwidths ranging from about 1400 nm to 1800 nm or broader, while the SC source of FIG. **12**B can lead to bandwidths ranging from about 1900 nm to 2500 nm or broader. Since these wavelength ranges are shorter than about 2500 nm, the SC fiber can be based on fused silica fiber. Exemplary SC fibers include standard single-mode fiber (SMF), high-nonlinearity fiber, high-NA fiber, dispersion shifted fiber, dispersion compensating fiber, and photonic crystal fibers. Non-fused-silica fibers can also be used for SC generation, including chalcogenides, fluorides, ZBLAN, tellurites, and germanium oxide fibers.

In one embodiment, FIG. **12**A illustrates a block diagram for an SC source **1200** capable of generating light between approximately 1400 nm and 1800 nm or broader. As an example, a pump fiber laser similar to FIG. **9** can be used as the input to a SC fiber **1209**. The seed laser diode **1201** can comprise a DFB laser that generates, for example, several milliwatts of power around 1542 nm or 1553 nm. The fiber pre-amplifier **1202** can comprise an erbium-doped fiber amplifier or an erbium/ytterbium doped double clad fiber. In this example, a mid-stage amplifier **1203** can be used, which can comprise an erbium/ytterbium doped double-clad fiber. A bandpass filter **1205** and isolator **1206** may be used between the pre-amplifier **1202** and mid-stage amplifier **1203**. The power amplifier stage **1204** can comprise a larger core size erbium/ytterbium doped double-clad fiber, and another bandpass filter **1207** and isolator **1208** can be used before the power amplifier **1204**. The output of the power amplifier can be coupled to the SC fiber **1209** to generate the SC output **1210**. This is just one exemplary configuration for an SC source, and other configurations or elements may be used consistent with this disclosure.

In yet another embodiment, FIG. **12**B illustrates a block diagram for an SC source **1250** capable of generating light between approximately 1900 and 2500 nm or broader. As an example, the seed laser diode **1251** can comprise a DFB or DBR laser that generates, for example, several milliwatts of power around 1542 nm or 1553 nm. The fiber pre-amplifier **1252** can comprise an erbium-doped fiber amplifier or an erbium/ytterbium doped double-clad fiber. In this example, a mid-stage amplifier **1253** can be used, which can comprise an erbium/ytterbium doped double-clad fiber. A bandpass filter **1255** and isolator **1256** may be used between the pre-amplifier **1252** and mid-stage amplifier **1253**. The power amplifier stage **1254** can comprise a thulium doped double-clad fiber, and another isolator **1257** can be used before the power amplifier **1254**. Note that the output of the mid-stage amplifier **1253** can be approximately near 1542 nm, while the thulium-doped fiber amplifier **1254** can amplify wavelengths longer than approximately 1900 nm and out to about 2100 nm. Therefore, for this configuration wavelength shifting may be required between **1253** and **1254**. In one embodiment, the wavelength shifting can be accomplished using a length of standard single-mode fiber **1258**, which can have a length between approximately 5 and 50 meters, for example. The output of the power amplifier **1254** can be coupled to the SC fiber **1259** to generate the SC output **1260**. This is just one exemplary configuration for an SC source, and other configurations or elements can be used consistent with this disclosure. For example, the various amplifier stages can comprise different amplifier types, such as erbium doped fibers, ytterbium doped fibers, erbium/ytterbium co-doped fibers and thulium doped fibers.

FIG. **12**C illustrates a reflection-spectroscopy based stand-off detection system having an SC laser source. The set-up **1270** for the reflection-spectroscopy-based stand-off detection system includes an SC source **1271**. First, the diverging SC output is collimated to a 1 cm diameter beam using a 25 mm focal length, 90 degrees off-axis, gold coated, parabolic mirror **1272**. To reduce the effects of chromatic aberration, refractive optics are avoided in the setup. All focusing and collimation is done using metallic mirrors that have almost constant reflectivity and focal length over the entire SC output spectrum. The sample **1274** is kept at a distance from the collimating mirror **1272**, which provides a total round trip path length of twice the distance before reaching the collection optics **1275**. A 12 cm diameter silver coated concave mirror **1275** with a 75 cm focal length is kept 20 cm to the side of the collimation mirror **1272**. The mirror **1275** is used to collect a fraction of the diffusely reflected light from the sample, and focus it into the input slit of a monochromator **1276**. Thus, the beam is incident normally on the sample **1274**, but detected at a reflection angle of $\tan^{-1}(0.2/5)$ or about 2.3 degrees. Appropriate long wavelength pass filters mounted in a motorized rotating filter wheel are placed in the beam path before the input slit **1276** to avoid contribution from higher wavelength orders from the grating (300 grooves/mm, 2 μm blaze). The output slit width is set to 2 mm corresponding to a spectral resolution of 10.8 nm, and the light is detected by a 2 mm×2 mm liquid nitrogen cooled (77K) indium antimonide (InSb) detector **1277**. The detected output is amplified using a trans-impedance pre-amplifier **1277** with a gain of about 105 V/A and connected to a lock-in amplifier **1278** setup for high sensitivity detection. The chopper frequency is 400 Hz, and the lock-in time constant is set to 100 ms corresponding to a noise bandwidth of about 1 Hz. These are exemplary elements and parameter values, but other or different optical elements may be used consistent with this disclosure.

While the above detection systems could be categorized as single path detection systems, it may be advantageous in some cases to use multi-path detection systems. In one embodiment, a detection system from a Fourier transform infrared spectrometer, FTIR, may be used. The received light may be incident on a particular configuration of mirrors, called a Michelson interferometer, that allows some wavelengths to pass through but blocks others due to wave interference. The beam may be modified for each new data point by moving one of the mirrors, which changes the set of wavelengths that pass through. This collected data is called an interferogram. The interferogram is then processed, typically on a computing system, using an algorithm called the Fourier transform. One advantageous feature of FTIR is that it may simultaneously collect spectral data in a wide spectral range.

Another advantage of using the near-infrared or SWIR is that most drug packaging materials are at least partially transparent in this wavelength range, so that drug compositions may be detected and identified through the packaging non-destructively. As an example, SWIR light could be used to see through plastics, since the signature for plastics can be subtracted off and there are large wavelength windows where the plastics are transparent. Because of the hydrocarbon bonds, there are absorption features near 1.7 microns and 2.2-2.5 microns. In general, the absorption bands in the

near infrared are due to overtones and combination bands for various functional group vibrations, including signals from C—H, O—H, C=O, N—H, —COOH, and aromatic C—H groups. It may be difficult to assign an absorption band to a specific functional group due to overlapping of several combinations and overtones. However, with advancements in computational power and chemometrics or multivariate analysis methods, complex systems may be better analyzed. In one embodiment, using software analysis tools the absorption spectrum may be converted to its second derivative equivalent. The spectral differences may permit a fast, accurate, non-destructive and reliable identification of materials. Although particular derivatives are discussed, other mathematical manipulations may be used in the analysis, and these other techniques are also intended to be covered by this disclosure.

Described herein are just some examples of the beneficial use of near-infrared or SWIR lasers for spectroscopy, active remote sensing or hyper-spectral imaging. However, many other spectroscopy and identification procedures can use the near-infrared or SWIR light consistent with this disclosure and are intended to be covered by the disclosure. As one example, the fiber-based super-continuum lasers may have a pulsed output with pulse durations of approximately 0.5-2 nsec and pulse repetition rates of several Megahertz. Therefore, the near-infrared or SWIR spectroscopy, active remote sensing or hyper-spectral imaging applications may also be combined with LIDAR-type applications. Namely, the distance or time axis can be added to the information based on time-of-flight measurements. For this type of information to be used, the detection system would also have to be time-gated to be able to measure the time difference between the pulses sent and the pulses received. By calculating the round-trip time for the signal, the distance of the object may be judged. In another embodiment, GPS (global positioning system) information may be added, so the near-infrared or SWIR spectroscopy, active remote sensing or hyper-spectral imagery would also have a location tag on the data. Moreover, the near-infrared or SWIR spectroscopy, active remote sensing or hyper-spectral imaging information could also be combined with two-dimensional or three-dimensional images to provide a physical picture as well as a chemical composition identification of the materials. These are just some modifications of the near-infrared or SWIR spectroscopy, active remote sensing or hyper-spectral imaging system described in this disclosure, but other techniques may also be added or combinations of these techniques may be added, and these are also intended to be covered by this disclosure.

In yet another example of multi-beam detection systems, a dual-beam set-up **1280** such as in FIG. **12**D may be used to subtract out (or at least minimize the adverse effects of) light source fluctuations. In one embodiment, the output from an SC source **1281** may be collimated using a CaF2 lens **1282** and then focused into the entrance slit of the monochromator **1283**. At the exit slit, light at the selected wavelength is collimated again and may be passed through a polarizer **1284** before being incident on a calcium fluoride beam splitter **1285**. After passing through the beam splitter **1285**, the light is split into a sample **1286** and reference **1287** arm to enable ratiometric detection that may cancel out effects of intensity fluctuations in the SC source **1281**. The light in the sample arm **1286** passes through the sample of interest and is then focused onto a HgCdTe detector **1288** connected to a pre-amp. A chopper **1282** and lock-in amplifier **1290** setup enable low noise detection of the sample arm signal. The light in the reference arm **1287** passes through an empty container (cuvette, gas cell etc.) of the same kind as used in the sample arm. A substantially identical detector **1289**, pre-amp and lock-in amplifier **1290** is used for detection of the reference arm signal. The signal may then be analyzed using a computer system **1291**. This is one particular example of a method to remove fluctuations from the light source, but other components may be added and other configurations may be used, and these are also intended to be covered by this disclosure.

Although particular examples of detection systems have been described, combinations of these systems or other systems may also be used, and these are also within the scope of this disclosure. As one example, environmental fluctuations (such as turbulence or winds) may lead to fluctuations in the beam for active remote sensing or hyper-spectral imaging. A configuration such as FIG. **12**D may be able to remove the effect of environmental fluctuations. Yet another technique may be to "wobble" the light beam after the light source using a vibrating mirror. The motion may lead to the beam moving enough to wash out spatial fluctuations within the beam waist at the sample or detection system. If the vibrating mirror is scanned faster than the integration time of the detectors, then the spatial fluctuations in the beam may be integrated out. Alternately, some sort of synchronous detection system may be used, where the detection is synchronized to the vibrating frequency.

By use of an active illuminator, a number of advantages may be achieved, such as higher signal-to-noise ratios. For example, one way to improve the signal-to-noise ratio would be to use modulation and lock-in techniques. In one embodiment, the light source may be modulated, and then the detection system would be synchronized with the light source. In a particular embodiment, the techniques from lock-in detection may be used, where narrow band filtering around the modulation frequency may be used to reject noise outside the modulation frequency. In an alternate embodiment, change detection schemes may be used, where the detection system captures the signal with the light source on and with the light source off. Again, for this system the light source may be modulated. Then, the signal with and without the light source is differenced. This may enable the sun light changes to be subtracted out. In addition, change detection may help to identify objects that change in the field of view. In the following some exemplary detection systems are described.

In one embodiment, a SWIR camera or infrared camera system may be used to capture the images. The camera may include one or more lenses on the input, which may be adjustable. The focal plane assemblies may be made from mercury cadmium telluride material (HgCdTe), and the detectors may also include thermo-electric coolers. Alternately, the image sensors may be made from indium gallium arsenide (InGaAs), and CMOS transistors may be connected to each pixel of the InGaAs photodiode array. The camera may interface wirelessly or with a cable (e.g., USB, Ethernet cable, or fiber optics cable) to a computer or tablet or smart phone, where the images may be captured and processed. These are a few examples of infrared cameras, but other SWIR or infrared cameras may be used and are intended to be covered by this disclosure.

In another embodiment, an imaging spectrometer may be used to detect the light received from the sample. For example, FIG. **14**A shows a schematic diagram **1400** of the basic elements of an imaging spectrometer. The input light **1401** from the sample may first be directed by a scanning mirror and/or other optics **1402**. An optical dispersing element **1403**, such as a grating or prism, in the spectrometer

may split the light into many narrow, adjacent wavelength bands, which may then be passed through imaging optics **1404** onto one or more detectors or detector arrays **1405**. Some sensors may use multiple detector arrays to measure hundreds of narrow wavelength bands.

An example of a typical imaging spectrometer **1450** used in hyper-spectral imaging systems is illustrated in FIG. **14**B. In this particular embodiment, the input light may be directed first by a tunable mirror **1451**. A front lens **1452** may be placed before the entrance slit **1453** and the collector lens **1454**. In this embodiment, the dispersing element is a holographic grating with a prism **1455**, which separates the different wavelength bands. Then, a camera lens **1456** may be used to image the wavelengths onto a detector or camera **1457**.

FIGS. **14**A and **14**B provide particular examples, but some of the elements may not be used, or other elements may be added, and these are also intended to be covered by this disclosure. For instance, a scanning spectrometer may be used before the detector, where a grating or dispersive element is scanned to vary the wavelength being measured by the detector. In yet another embodiment, filters may be used before one or more detectors to select the wavelengths or wavelength bands to be measured. This may be particularly useful if only a few bands or wavelengths are to be measured. The filters may be dielectric filters, Fabry-Perot filters, absorption or reflection filters, fiber gratings, or any other wavelength selective filter. In one embodiment, a wavelength division multiplexer, WDM, may be used followed by one or more detectors or detector arrays. One example of a planar wavelength division multiplexer may be a waveguide grating router or an arrayed waveguide grating. The WDM may be fiber coupled, and detectors may be placed directly at the output or the detectors may be coupled through fibers to the WDM. Some of these components may also be combined with the configurations in FIGS. **14**A and **14**B.

One advantage of the SC lasers illustrated is that they may use all-fiber components, so that the SC laser can be all-fiber, monolithically integrated with no moving parts. The all-integrated configuration can consequently be robust and reliable.

The Figures provide examples of SC light sources that may advantageously be used for SWIR light generation in various medical and dental diagnostic and therapeutic applications. However, many other versions of the SC light sources may also be made that are intended to also be covered by this disclosure. For example, the SC generation fiber could be pumped by a mode-locked laser, a gain-switched semiconductor laser, an optically pumped semiconductor laser, a solid state laser, other fiber lasers, or a combination of these types of lasers. Also, rather than using a fiber for SC generation, either a liquid or a gas cell might be used as the nonlinear medium in which the spectrum is to be broadened.

Even within the all-fiber versions illustrated such as in FIG. **9**, different configurations could be used consistent with the disclosure. In an alternate embodiment, it may be desirous to have a lower cost version of the SWIR SC laser of FIG. **9**. One way to lower the cost could be to use a single stage of optical amplification, rather than two stages, which may be feasible if lower output power is required or the gain fiber is optimized. For example, the pre-amplifier stage **902** might be removed, along with at least some of the mid-stage elements. In yet another embodiment, the gain fiber could be double passed to emulate a two stage amplifier. In this example, the pre-amplifier stage **902** might be removed, and perhaps also some of the mid-stage elements. A mirror or fiber grating reflector could be placed after the power amplifier stage **906** that may preferentially reflect light near the wavelength of the seed laser **901**. If the mirror or fiber grating reflector can transmit the pump light near 940 nm, then this could also be used instead of the pump combiner **913** to bring in the pump light **912**. The SC fiber **915** could be placed between the seed laser **901** and the power amplifier stage **906** (SC is only generated after the second pass through the amplifier, since the power level may be sufficiently high at that time). In addition, an output coupler may be placed between the seed laser diode **901** and the SC fiber, which now may be in front of the power amplifier **906**. In a particular embodiment, the output coupler could be a power coupler or divider, a dichroic coupler (e.g., passing seed laser wavelength but outputting the SC wavelengths), or a wavelength division multiplexer coupler. This is just one further example, but a myriad of other combinations of components and architectures could also be used for SC light sources to generate SWIR light that are intended to be covered by this disclosure.

One definition of process analytical technology, PAT, is "a system for designing, analyzing and controlling manufacturing through timely evaluations (i.e., during processing) of significant quality and performance attributes of raw and in-process materials and processes, with the goal of ensuring final product quality." Near-infrared or SWIR spectroscopy may have applications in the PAT of the pharmaceutical industry by providing, for example, quantitative analysis of multiple components in a sample and in pack quantification of drugs in formulation, as well as quality of a drug and quality control of complex excipients used in formulation. The PAT process may benefit from near-infrared or SWIR spectroscopy for some steps, such as: raw material identification, active pharmaceutical ingredient applications, drying, granulation, blend uniformity and content uniformity. Some of the strengths of near-infrared or SWIR spectroscopy include: radiation has good penetration properties, and, thus, minimal sample preparation may be required; measurement results may be obtained rapidly, and simultaneous measurements may be obtained for several parameters; non-destructive methods with little or no chemical waste; and organic chemicals that comprise most pharmaceutical products have unique spectra in the near-infrared and SWIR ranges, for example.

One goal of the manufacturing process and PAT may be the concept of a "smart" manufacturing process, which may be a system or manufacturing operation responding to analytical data generated in real-time. Such a system may also have an in-built "artificial intelligence" as decisions may be made whether to continue a manufacturing operation. For example, with respect to the raw materials, integration of the quality measurement into smart manufacturing processes could be used to improve manufacturing operations by ensuring that the correct materials of the appropriate quality are used in the manufacture. Similarly, a smart blender would be under software control and would respond to the real-time spectral data collected.

FIG. **15** illustrates what might be an eventual flow-chart **1500** of a smart manufacturing process. The manufacturing process **1501** may have as input the process feed **1502** and result in a process output **1503**. A process controller **1504** may at least partially control the manufacturing process **1501**, and the controller **1504** may receive inputs from the closed loop control (process parameters) **1505** as well as the on-line monitoring of process parameters **1506**. The feedback loops in the process could refine the manufacturing

process **1501** and improve the quality of the process output **1503**. These are particular embodiments of the use of near-infrared or SWIR spectroscopy in the PAT of the pharmaceutical industry, but other variations, combinations, and methods may also be used and are intended to be covered by this disclosure.

The discussion thus far has centered on use of near-infrared or SWIR spectroscopy in applications such as identification of counterfeit drugs, detection of illicit drugs, and pharmaceutical process control. Although drugs and pharmaceuticals are one example, many other fields and applications may also benefit from the use of near infrared or SWIR spectroscopy, and these may also be implemented without departing from the scope of this disclosure. As just another example, near-infrared or SWIR spectroscopy may also be used as an analytic tool for food quality and safety control. Applications in food safety and quality assessment include contaminant detection, defect identification, constituent analysis, and quality evaluation. The techniques described in this disclosure are particularly valuable when non-destructive testing is desired at stand-off or remote distances.

Wireless Link to the Cloud

The non-invasive dental caries measurement device may also benefit from communicating the data output to the "cloud" (e.g., data servers and processors in the web remotely connected) via wireless means. The non-invasive devices may be part of a series of biosensors applied to the patient, and collectively these devices form what might be called a body area network or a personal area network. The biosensors and non-invasive devices may communicate to a smart phone, tablet, personal data assistant, computer and/or other microprocessor-based device, which may in turn wirelessly or over wire and/or fiber optic transmit some or all of the signal or processed data to the internet or cloud. The cloud or internet may in turn send the data to dentists, doctors or health care providers as well as the patients themselves. Thus, it may be possible to have a panoramic, high-definition, relatively comprehensive view of a patient that doctors and dentists can use to assess and manage disease, and that patients can use to help maintain their health and direct their own care.

In a particular embodiment **1300**, the non-invasive measurement device **1301** may comprise a transmitter **1303** to communicate over a first communication link **1304** in the body area network or personal area network to a receiver in a smart phone, tablet, cell phone, PDA, and/or computer **1305**, for example. For the measurement device **1301**, it may also be advantageous to have a processor **1302** to process some of the measured data, since with processing the amount of data to transmit may be less (hence, more energy efficient). The first communication link **1304** may operate through the use of one of many wireless technologies such as Bluetooth, Zigbee, WiFi, IrDA (infrared data association), wireless USB, or Z-wave, to name a few. Alternatively, the communication link **1304** may occur in the wireless medical band between 2360 MHz and 2390 MHz, which the FCC allocated for medical body area network devices, or in other designated medical device or WMTS bands. These are examples of devices that can be used in the body area network and surroundings, but other devices could also be used and are included in the scope of this disclosure.

The personal device **1305** may store, process, display, and transmit some of the data from the measurement device **1301**. The device **1305** may comprise a receiver, transmitter, display, voice control and speakers, and one or more control buttons or knobs and a touch screen. Examples of the device **1305** include smart phones such as the Apple iPhones® or phones operating on the Android or Microsoft systems. In one embodiment, the device **1305** may have an application, software program, or firmware to receive and process the data from the measurement device **1301**. The device **1305** may then transmit some or all of the data or the processed data over a second communication link **1306** to the internet or "cloud" **1307**. The second communication link **1306** may advantageously comprise at least one segment of a wireless transmission link, which may operate using WiFi or the cellular network. The second communication link **1306** may additionally comprise lengths of fiber optic and/or communication over copper wires or cables.

The internet or cloud **1307** may add value to the measurement device **1301** by providing services that augment the measured data collected. In a particular embodiment, some of the functions performed by the cloud include: (a) receive at least a fraction of the data from the device **1305**; (b) buffer or store the data received; (c) process the data using software stored on the cloud; (d) store the resulting processed data; and (e) transmit some or all of the data either upon request or based on an alarm. As an example, the data or processed data may be transmitted **1308** back to the originator (e.g., patient or user), it may be transmitted **1309** to a health care provider or doctor or dentist, or it may be transmitted **1310** to other designated recipients.

Service providers coupled to the cloud **1307** may provide a number of value-add services. For example, the cloud application may store and process the dental data for future reference or during a visit with the dentist or healthcare provider. If a patient has some sort of medical mishap or emergency, the physician can obtain the history of the dental or physiological parameters over a specified period of time. In another embodiment, alarms, warnings or reminders may be delivered to the user **1308**, the healthcare provider **1309**, or other designated recipients **1310**. These are just some of the features that may be offered, but many others may be possible and are intended to be covered by this disclosure. As an example, the device **1305** may also have a GPS sensor, so the cloud **1307** may be able to provide time, date, and position along with the dental or physiological parameters. Thus, if there is a medical or dental emergency, the cloud **1307** could provide the location of the patient to the dental or healthcare provider **1309** or other designated recipients **1310**. Moreover, the digitized data in the cloud **1307** may help to move toward what is often called "personalized medicine." Based on the dental or physiological parameter data history, medication or medical/dental therapies may be prescribed that are customized to the particular patient. Another advantage for commercial entities may be that by leveraging the advances in wireless connectivity and the widespread use of handheld devices such as smart phones that can wirelessly connect to the cloud, businesses can build a recurring cost business model even using non-invasive measurement devices.

Beyond the above benefits, the cloud application **1307** and application on the device **1305** may also have financial value for companies developing devices **1301** such as a non-invasive blood constituent monitor. In the case of glucose monitors, the companies make the majority of their revenue on the measurement strips. However, with a non-invasive monitor, there is no need for strips, so there is less of an opportunity for recurring costs (e.g., the razor/razor blade model does not work for non-invasive devices). On the other hand, people may be willing to pay a periodic fee for

the value-add services provided on the cloud **1307**. Diabetic patients, for example, would probably be willing to pay a periodic fee for monitoring their glucose levels, storing the history of the glucose levels, and having alarm warnings when the glucose level falls out of range. Similarly, patients taking ketone bodies supplement for treatment of disorders characterized by impaired glucose metabolism (e.g., Alzheimer's, Parkinson's, Huntington's or ALS) may need to monitor their ketone bodies level. These patients would also probably be willing to pay a periodic fee for the value-add services provided on the cloud **1307**. Thus, by leveraging the advances in wireless connectivity and the widespread use of handheld devices such as smart phones that can wirelessly connect to the cloud, businesses can build a recurring cost business model even using non-invasive measurement devices.

In addition, it may be advantageous to use pattern matching algorithms and other software and mathematical methods to identify the blood constituents of interest. In one embodiment, the spectrum may be correlated with a library of known spectra to determine the overlap integrals, and a threshold function may be used to quantify the concentration of different constituents. This is just one way to perform the signal processing, and many other techniques, algorithms, and software may be used and would fall within the scope of this disclosure.

One of the issues in measuring a particular blood constituent is the interfering and overlapping signal from other blood constituents. The selection of the constituent of interest may be improved using a number of techniques. For example, a higher light level or intensity may improve the signal-to-noise ratio for the measurement. Second, mathematical modeling and signal processing methodologies may help to reduce the interference, such as multivariate techniques, multiple linear regression, and factor-based algorithms, for example. For instance, a number of mathematical approaches include multiple linear regression, partial least squares, and principal component regression (PCR). Also, various mathematical derivatives, including the first and second derivatives, may help to accentuate differences between spectra. In addition, by using a wider wavelength range and using more sampling wavelengths may improve the ability to discriminate one signal from another.

Described herein are just some examples of the beneficial use of near-infrared or SWIR lasers for non-invasive measurements of dental caries and early detection of carious regions. However, many other dental or medical procedures can use the near-infrared or SWIR light consistent with this disclosure and are intended to be covered by the disclosure.

Although the present disclosure has been described in several embodiments, a myriad of changes, variations, alterations, transformations, and modifications may be suggested to one skilled in the art, and it is intended that the present disclosure encompass such changes, variations, alterations, transformations, and modifications as falling within the spirit and scope of the appended claims.

While exemplary embodiments are described above, it is not intended that these embodiments describe all possible forms of the disclosure. Rather, the words used in the specification are words of description rather than limitation, and it is understood that various changes may be made without departing from the spirit and scope of the disclosure. Additionally, the features of various implementing embodiments may be combined to form further embodiments of the disclosure. While various embodiments may have been described as providing advantages or being preferred over other embodiments with respect to one or more desired characteristics, as one skilled in the art is aware, one or more characteristics may be compromised to achieve desired system attributes, which depend on the specific application and implementation. These attributes include, but are not limited to: cost, strength, durability, life cycle cost, marketability, appearance, packaging, size, serviceability, weight, manufacturability, ease of assembly, etc. The embodiments described herein that are described as less desirable than other embodiments or prior art implementations with respect to one or more characteristics are not outside the scope of the disclosure and may be desirable for particular applications.

What is claimed is:

1. A measurement system comprising:

a light source comprising a plurality of semiconductor sources that are configured to generate an output optical beam with one or more optical wavelengths, the light source configured to increase signal-to-noise ratio by increasing a light intensity relative to an initial light intensity from at least one of the plurality of semiconductor sources;

a measurement device configured to:

receive a portion of the output optical beam, and

deliver an analysis output beam to a sample;

a receiver configured to:

receive and process at least a portion of the analysis output beam reflected or transmitted from the sample,

generate an output signal representing at least in part a non-invasive measurement on blood contained within the sample,

synchronize to the light source,

capture light while the semiconductor sources are off and convert the captured light into a first signal,

capture light while at least one of the semiconductor sources is on and convert the captured light into a second signal, the captured light including at least a part of the at least a portion of the analysis output beam reflected or transmitted from the sample, and

the measurement system further configured to improve the signal-to-noise ratio by differencing the first signal and the second signal;

a smart phone or tablet comprising a wireless receiver, a wireless transmitter, a display, a microphone, a speaker, one or more buttons or knobs, a microprocessor and a touch screen, the smart phone or tablet configured to:

receive and process at least a portion of the output signal,

store and display the processed output signal, and

transmit at least a portion of the processed output signal over a wireless transmission link; and

a cloud configured to:

receive, over the wireless transmission link, an output status comprising the at least a portion of the processed output signal,

process the received output status to generate processed data, and

store the processed data.

2. The measurement system of claim **1**, wherein the plurality of semiconductor sources comprises at least one of: light emitting diodes (LEDs), laser diodes (LD's), tunable LD's, and super-luminescent laser diodes (SLDs), and wherein the measurement system further comprises a reflective surface to receive and redirect at least some of the at least a portion of the analysis output beam reflected or transmitted from the sample.

3. The measurement system of claim 1, wherein the light source is further configured to increase the light intensity from the plurality of semiconductor sources by spatially coupling the optical output beam from at least two of the plurality of semiconductor sources.

4. The measurement system of claim 1, wherein the receiver comprises a plurality of detectors arranged along a first arc, and wherein the plurality of semiconductor sources are arranged along a second arc.

5. The measurement system of claim 4, wherein the first arc is offset from the second arc.

6. The measurement system of claim 4, wherein the first arc and the second arc are concentric.

7. The measurement system of claim 6, wherein the plurality of semiconductor sources comprises six light emitting diodes, and wherein the receiver comprises six detectors.

8. The measurement system of claim 7, wherein the six detectors are located on the first arc surrounding the six light emitting diodes.

9. The measurement system of claim 8, wherein the measurement system is configured to use artificial intelligence in making decisions;

wherein the measurement system is configured to perform pattern identification or classification, and wherein the measurement system is configured to apply a threshold function to a comparison with a stored data set; and

wherein the measurement system is at least in part configured for selection or identification of an object, and wherein the measurement system is configured to improve a signal-to-noise ratio of the selection or identification by applying regression signal processing methodologies or multivariate techniques.

10. The measurement system of claim 8, wherein the light source is configured to further increase signal-to-noise ratio by increasing a pulse rate of at least one of the plurality of semiconductor sources from an initial non-zero pulse rate.

11. A measurement system comprising:

a wearable measurement device for measuring one or more physiological parameters, including a light source comprising a plurality of semiconductor sources that are configured to generate an output optical beam with one or more optical wavelengths;

the light source configured to increase signal-to-noise ratio by increasing a light intensity relative to an initial light intensity from at least one of the plurality of semiconductor sources;

the wearable measurement device configured to receive a portion of the output optical beam and to deliver an analysis output beam to a sample;

the wearable measurement device further comprising a receiver configured to:

receive and process at least a portion of the analysis output beam reflected or transmitted from the sample,

generate an output signal representing at least in part a non-invasive measurement on blood contained within the sample,

synchronize to the light source,

capture light while the semiconductor sources are off and convert the captured light into a first signal,

capture light while at least one of the semiconductor sources is on and convert the captured light into a second signal, the captured light including at least a part of the at least a portion of the analysis output beam reflected or transmitted from the sample,

wherein the measurement system is further configured to improve the signal-to-noise ratio by differencing the first signal and the second signal;

a smart phone or tablet comprising a wireless receiver, a wireless transmitter, a display, a microphone, a speaker, one or more buttons or knobs, a microprocessor and a touch screen, the smart phone or tablet configured to receive and process at least a portion of the output signal, to store and display the processed output signal, and to transmit a portion of the processed output signal over a wireless transmission link; and

a cloud configured to receive over the wireless transmission link an output status comprising the at least a portion of the processed output signal, to process the received output status to generate processed data and to store the processed data, and wherein the cloud is capable of storing a history of at least a portion of the received output status over a specified period of time.

12. The measurement system of claim 11, wherein the measurement system is configured to use artificial intelligence in making decisions;

wherein the measurement system is configured to perform pattern identification or classification, and wherein the measurement system is configured to apply a threshold function to a comparison with a stored data set; and

wherein the measurement system is at least in part configured for selection or identification of an object, and wherein the measurement system is configured to improve a signal-to-noise ratio of the selection or identification by applying regression signal processing methodologies or multivariate techniques.

13. The measurement system of claim 12, wherein the light source is configured to further increase the signal-to-noise ratio by increasing a pulse rate of at least one of the plurality of semiconductor sources from an initial non-zero pulse rate.

14. The measurement system of claim 11, wherein the plurality of semiconductor sources comprises at least one of: light emitting diodes (LEDs), laser diodes (LD's), tunable LD's, and super-luminescent laser diodes (SLDs), and the measurement system further comprising a reflective surface to receive and redirect at least some of the at least a portion of the analysis output beam reflected or transmitted from the sample.

15. The measurement system of claim 11, wherein the receiver comprises a plurality of detectors arranged along a first arc, and wherein the plurality of semiconductor sources are arranged along a second arc that is offset from the first arc.

16. The measurement system of claim 15, wherein the first arc and the second arc are concentric.

17. The measurement system of claim 16, wherein the plurality of semiconductor sources comprises six light emitting diodes, and wherein the receiver comprises six detectors.

18. The measurement system of claim 17, wherein the six detectors are located on the first arc surrounding the six light emitting diodes.

19. A wearable device for use with a smart phone or tablet, the wearable device comprising:

a measurement device including a light source comprising a plurality of semiconductor sources for measuring one or more physiological parameters, the measurement device configured to:

generate, by modulating at least one of the semiconductor sources having an initial light intensity, an input optical beam having one or more optical wavelengths, and

receive and to deliver a portion of the input optical beam to tissue, wherein the tissue reflects at least a portion of the input optical beam delivered to the tissue;

the measurement device further comprising a receiver configured to:

capture light while the semiconductor sources are off and convert the captured light into a first signal, and

capture light while at least one of the semiconductor sources is on and convert the captured light into a second signal, the captured light including at least a portion of the input optical beam reflected from the tissue;

synchronize to the modulation of the at least one of the semiconductor sources;

the measurement device further configured to improve a signal-to-noise ratio of the input optical beam reflected from the tissue by:

differencing the first signal and the second signal, and

increasing the light intensity relative to the initial light intensity from at least one of the semiconductor sources;

the measurement device further configured to generate an output signal representing at least in part a non-invasive measurement on blood contained within the tissue;

the wearable device configured to communicate with the smart phone or tablet, the smart phone or tablet comprising a wireless receiver, a wireless transmitter, a display, a voice input module, a speaker, and a touch screen; and

the smart phone or tablet configured to:

receive and to process at least a portion of the output signal,

store and display the processed output signal, and

transmit at least a portion of the processed output signal over a wireless transmission link.

20. The wearable device of claim **19**, wherein the light source is configured to further improve the signal-to-noise ratio of the input optical beam reflected from the tissue by increasing a pulse rate of at least one of the plurality of semiconductor sources from an initial non-zero pulse rate.

21. The wearable device of claim **20**, wherein the receiver comprises a plurality of detectors arranged along a first arc, and wherein the plurality of semiconductor sources are arranged along a second arc that is offset from the first arc.

22. The wearable device of claim **21**, wherein the first arc and the second arc are concentric.

23. The wearable device of claim **22**, wherein the plurality of semiconductor sources comprises six light emitting diodes, and wherein the receiver comprises six detectors.

24. The wearable device of claim **23**, wherein the six detectors are located on the first arc surrounding the six light emitting diodes.

25. The wearable device of claim **19**, further comprising a cloud configured to:

receive, over the wireless transmission link, an output status comprising the at least a portion of the processed output signal,

process the output status to generate processed data, and store the processed data, and

wherein the cloud is capable of storing a history of at least a portion of the output status over a specified period of time.

26. The wearable device of claim **19**, wherein the wearable device is configured to use artificial intelligence in making decisions;

wherein the wearable device is configured to perform pattern identification or classification, and wherein the wearable device is configured to apply a threshold function to a comparison with a stored data set; and

wherein the wearable device is at least in part configured for selection or identification of an object, and wherein the wearable device is configured to improve a signal-to-noise ratio of the selection or identification by applying regression signal processing methodologies or multivariate techniques.

27. The wearable device of claim **19**, wherein the measurement device further comprises a reflective surface configured to receive and redirect at least a portion of light reflected from the tissue.

* * * * *